



中央研究院  
天文及天文物理研究所

## Research Highlights

研究成果專刊



**ACADEMIA SINICA**  
**Institute of Astronomy and Astrophysics**



# Contents

**01 • Letter from the Director**

**03 • Introduction**

**07 • Projects**

**37 • Science Highlights**

**61 • Instrumentation Research**

**73 • Education and Public Outreach**



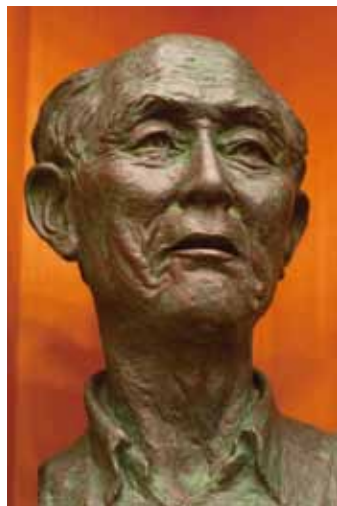
# Letter from the Director

## Letter from the Director

---

Dear Colleagues and Friends:

As proposed by Academician Chia-Chiao Lin and approved by the Academia Sinica with the support of Academy President Ta-You Wu, the Preparatory Office of the Academia Sinica Institute of Astronomy and Astrophysics (ASIAA) was established in 1993. During these intervening years, our researches have become competitive at the frontier, and our staff of young scientists have achieved international recognition for their accomplishments. On June 1, 2010, the ASIAA became a full-fledged institute.



*The busts of Academician Chia-Chiao Lin (left panel) and Academy President Ta-You Wu (right panel) in the auditorium of Astronomy-Mathematics Building, in memory of those who proposed and supported the establishment of ASIAA. (Sculptor: I-Hsiung Chou; Picture Credit: Tony Zou)*





Our Institute's mission has been to engage in research on fundamental astrophysical problems and to gain access to advanced instruments through constructing forefront facilities. One emphasis has been on developing innovative technology that will substantially increase the sensitivity in order to drive the progress in our discipline. We focus our research initiatives and we concentrate our resources in order to work on the most important topics. In this brochure, we report on the current progress and the scientific achievements from the large projects at our Institute. We also present scientific highlights from our research staff members, who are pursuing studies ranging from planet formation to cosmology. Our observational investigations cover all wavelength bands. Our theoretical studies utilize both analytical and numerical methods. Our instrumentation projects are in the radio, optical, and infrared windows. In these past few years, we are also increasing our efforts in education and public outreach. These are also described.

The success of our Institute has been guided by a succession of Directors, starting with Typhoon Lee, Chi Yuan, Kwok-Yung Lo, Sun Kwok, and Paul Ho. We are grateful for the support of past Academy President Yuan-Tseh Lee, and our current Academy President Chi-Huey Wong. The hard work of our scientists, engineers, students, and administrative staff, has earned the achievements of our Institute. As scientists, we are fortunate to be able to study such fundamental problems as the origin of life, the formation of planets and stars, stellar energy and chemical feedback, the mystery of black holes, the evolution and fate of galaxies and of the Universe itself, and the existence of dark matter and dark energy. We are mindful that our work has been supported by public funds from the people of Taiwan. We also thank our friends and collaborators who work with us all around the world. With this brochure, it is our privilege and our responsibility to continue to engage the interest of young people and the general public by sharing our excitement in working on the forefront problems in modern astronomy.

You-Hua Chu 6.15.2015



# ***Introduction***





# Introduction

The Academia Sinica Institute of Astronomy and Astrophysics (ASIAA) is one of the 31 institutes and centers of the Academia Sinica. Our Preparatory Office was established in 1993, and we became a full-fledged Institute in 2010. ASIAA is located in the Astronomy-Mathematics Building (ASMAB) on the campus of the National Taiwan University (NTU). We now have a staff of around 200, including research fellows, research engineers and scientists, postdoctoral fellows, visiting scholars, assistants and supporting personnel.



ASMAB Building



The 2015 ASIAA panel meeting

ASIAA works at the forefronts of astronomical research. We concentrate our efforts in specific directions, building up core groups in instrumentation, experimental astrophysics, and theory.

During the first decade of ASIAA, the focus of our development has been on radio astronomy. Starting with a training effort on millimeter wavelength interferometry with the Berkeley-Illinois-Maryland Association (BIMA), ASIAA soon became a partner in the Submillimeter Array (SMA) in 1996. In 2000, ASIAA led the design and construction of the Array for Microwave Background Anisotropy (AMiBA) together with NTU. In 2005, Taiwan joined the international Atacama Large Millimeter/submillimeter Array (ALMA) project. In 2009, ASIAA began a program in submillimeter wavelength Very Long Baseline Interferometry, to deploy the Greenland Telescope (GLT). These efforts have led to the establishment of the Receiver Laboratory, the Microwave Device Laboratory, and the Superconducting Device Laboratory, at ASIAA.

During the second decade of ASIAA, we also began our development in optical and infrared astronomy. ASIAA has collaborated with National Central University (NCU) and Lawrence Livermore National Laboratory (LLNL) since 1998 on the Taiwan-America Occultation Survey (TAOS) project. This project is being succeeded by the Trans-Neptunian Automated Survey (TAOS II) which is being deployed in 2015.

To engage with larger optical facilities, ASIAA participated in the Canada-France-Hawaii Telescope (CFHT) Widefield Infrared Camera (WIRCam) project in 2000 and the SpectroPolarimètre Infra-Rouge (SPIRou) project in 2009. We also joined the Subaru Telescope Hyper Suprime-Cam (HSC) project in 2008 and the

Prime Focus Spectrograph (PFS) in 2011. These efforts led to the establishment of the Optical/Infrared Laboratory at ASIAA. In 2013, we further established a submicron resolution Secondary Ion Mass Spectrometer (NanoSIMS) facility for studying isotopic compositions in retrieved solar system samples. This serves to connect physical samples on earth with the astrophysics of the Universe.

In the area of astrophysical theory, our Computational Fluid Dynamics/Magnetohydrodynamics (CFD/MHD) group has been developing numerical computation capabilities at ASIAA. This was followed by the establishment of the Theoretical Institute for Advanced Research in Astrophysics (TIARA) in 2004, which provides a coordinated program of research and education. TIARA regularly holds workshops and schools as well as international meetings. In 2012, the CFD/MHD group became the core member of our program on Computational Astrophysics.

The first three major ASIAA telescope projects—SMA, AMiBA, and TAOS—have all been brought into operation. The SMA was dedicated on Mauna Kea in Hawaii in November of 2003. Initial science results from the SMA were published in a special volume of the *Astrophysical Journal* in 2004. The SMA is now in regular science mode, featuring weekly remote operations from Taipei. AMiBA was dedicated with seven elements on Mauna Loa in Hawaii in October of 2006. Science operations started in 2007, and the first seven science papers were published in the *Astrophysical Journal* in 2009. In the same year, the upgrade of AMiBA to the 13-element configuration was completed, improving the speed by about a factor of 60. All four elements of the Taiwan-American Occultation Survey (TAOS) have been operating on top of Lu-Lin Mountain since 2006. Eight years of data have been accumulated, and the first science papers were published in 2008. The system operates in fully automatic mode, with remote monitoring from ASIAA and NCU. In addition, ALMA began Early Science operations in 2011, and the full array was completed in 2014.

In the area of instrument development for large optical telescopes, WIRCam was completed and delivered in 2005, and HSC was completed and delivered in 2012. Our efforts continue on SPIRou and PFS, with delivery in the 2016–2017 time frame.

For on-going telescope projects, TAOS II is being constructed at the San Pedro Martir Observatory in Mexico, and the three telescopes will be delivered in 2015. The GLT is currently being retrofitted for polar operations, and the new ISI Station at the summit of Greenland will be developed. The GLT will work with the SMA and ALMA, to provide interferometry at submillimeter wavelengths with intercontinental baselines. The GLT will also produce science in the unexplored terahertz window. The GLT is scheduled to be shipped to Thule in 2016 and start operations in 2017.

ASIAA aims to collaborate with the university groups in developing astronomical research in Taiwan. Collaboration with NCU has been underway for years through our partnership on the TAOS project. Collaboration with NTU has also been ongoing through our partnership on the AMiBA project. Collaboration with National Tsing Hua University (NTHU) has been ongoing in the fabrication of SIS junctions and on the TIARA project. From 2013, we have also been collaborating with the National Cheng Kung University on the Exploration of energization and Radiation in Geospace (ERG) space mission. In addition, ALMA includes participation from all the major universities in Taiwan.

ASIAA has benefitted by collaborating with various international groups, including the Smithsonian Astrophysical Observatory (SAO) on SMA, TAOS, TAOS II, and GLT; the Australia Telescope National Facility (ATNF) and the Carnegie-Mellon University (CMU) on AMiBA; the National Radio Astronomy Observatory (NRAO) on ALMA and GLT; the Jet Propulsion Laboratory (JPL) on AMiBA and PFS; the CFHT on WIRCam and SPIRou; the University of Pennsylvania (UPenn), LLNL, the Harvard-Smithsonian Center for Astrophysics, and the Yonsei University on TAOS; the Universidad Nacional Autónoma de México (UNAM) on TAOS II; the Nobeyama Radio Observatory (NRO) and the Purple Mountain Observatory (PMO) on SIS junction development; the National Astronomical Observatory of Japan (NAOJ) on ALMA, HSC, PFS, and SIS junctions; the European Southern Observatory (ESO), the Herzberg Institute for Astrophysics (HIA), and the University of Chile on ALMA; the Institute for the Physics and Mathematics of the Universe (IPMU) of the University of Tokyo, the California Institute of Technology/ Jet Propulsion Laboratory (Caltech/JPL), Princeton University, Johns Hopkins University, Laboratoire d'Astrophysique de Marseille (LAM), and National Astrophysical Laboratory (LNA) of Brazil on PFS; Institute of Space and Astronautical Science (ISAS) of the Japan Aerospace Exploration Agency (JAXA) on ERG.

ASIAA is also a founding member of the East Asian Core Observatories Association (EACOA), together with NAOJ, the National Astronomical Observatories, Chinese Academy of Sciences (NAOC), and the Korea Astronomy and Space Science Institute (KASI). The EACOA promotes collaborations in East Asia, especially in the construction of future instruments. In 2014, the East Asia Observatory (EAO) was formed and started to operate the James Clerk Maxwell Telescope (JCMT), the first telescope acquired by EAO and available to the East Asian astronomers for research.

ASIAA will continue to participate in the development of advanced astronomical instrumentation for research by the Taiwan astronomical community. The staff at ASIAA makes use of all the leading astronomical instruments in the world, and we aim to bring this access to the astronomical community in Taiwan.



# *Projects*



## Atacama Large Millimeter/Submillimeter Array

Since 2005 ASIAA has participated in the Atacama Large Millimeter/submillimeter Array (ALMA) project, the largest ground-based astronomical project ever built. The array is located on the Chajnantor plateau in the Atacama Desert in northern Chile, at an elevation of about 5,000 meters (Figure 1). The ALMA observatory was officially inaugurated in Chile on March 11, 2013 (Figure 2). With the last one of the 66 high-precision radio antennas delivered in October 2013, the full array was completed and started normal operation in 2014. Its expected lifetime is at least 50 years.



Figure 1. Upper panel: the ALMA Operations Site (AOS) at 5,000 m, with around 66 antennas operational in 2013. Lower left panel: aerial view of the Operations Support Facilities (OSF) at around 2,900 m. To the right are the three antenna assembly sites belonging to the Japanese, North American, and European partners; in the upper middle section is the operations building, and in the upper right, the road to the Chajnantor Plain. Lower right panel: an aerial view of the technical building at the AOS at 5,000 m. (Picture Credit: ALMA (ESO/NAOJ/NRAO), W. Garnier)



The ALMA project has three major international partners: North America, Europe, and East Asia. The North American and European partners are responsible for the construction of the 12-meter Array (ALMA baseline project), while East Asia is responsible for the construction of the Morita Atacama Compact Array (ACA; ALMA-Japan project). In September 2005, Academia Sinica entered into an agreement with the National Institutes of Natural Sciences (NINS) of Japan to join ALMA through the ALMA-Japan project. In October 2008, the National Science Council (NSC) of Taiwan and the US National Science Foundation (NSF) reached an agreement for collaboration with ALMA-North America.

At its full capability, ALMA will cover a wavelength range from about 0.3 to 10 mm (about 35 GHz to 1 THz in frequency). With baselines up to 16 km, an angular resolution of up to 4 milli-arcsec is achievable for the highest frequencies, yielding images 10 times sharper than the Hubble Space Telescope. ALMA will be tremendously sensitive, and will be more than 10,000 times faster than any existing instrument at millimeter and sub-millimeter bands. With an unprecedented combination of sensitivity, angular resolution, spectral resolution, and imaging fidelity at the shortest radio wavelengths, ALMA is expected to make breakthrough contributions in a variety of areas such as weather patterns on solar system planets, the formation of planets and stars in our Galaxy, gas motions within active galactic nuclei, and the formation of the earliest galaxies at a redshift of  $z \sim 10$ . In particular, ALMA will be a premier tool for capturing never-before seen details of the first stars and galaxies that emerged from the cosmic "dark ages" billions of years ago, and is expected to directly image young planets that are still in the process of developing.

Initial scientific observations (ALMA Cycle 0 Early Science) started on September 30, 2011 with sixteen 12-meter antennas. Although not yet completed at that time, with an over-subscription rate of more than 8, only 112 out of 919 proposals were accepted, demonstrating very stiff international competition for observing time. Taiwanese astronomers succeeded in leading 8 of the 112 accepted projects. For Taiwan, this amounts to an impressive 6% of the worldwide allocated time in Cycle 0. The first ALMA-Taiwan results with Cycle 0 data were published in 2012 (Wang et al. 2012, ApJL, 761, L32). (see Figure 5 of "Extragalactic Studies" in the "Research Highlight" reports)

In the following Cycle 1 proposal call in 2012, a total of 1,133 proposals were submitted of which 196 highest priority programs were selected, and 14 out of 56 Taiwanese proposals were among the highest priority proposals, amounting to 47.2 hours of observation. This leaves Taiwan with a share of about 5.4% of array time for Cycle 1 and an impressive proposal success rate of 25% compared to an over-



Figure 2. Delegation from Taiwan during the ALMA inauguration in March 2013 at the OSF in Chile. Pictured from left to right are Paul Ho (Former Director of ASIAA, Academician of the Academia Sinica), Maw-Kuen Wu (President of the National Dong Hwa University, Former Minister of NSC, Academician of the Academia Sinica), Frank Shu (Former President of National Tsing Hua University, Academician of the Academia Sinica), Chung-Yuan Mou (Former Deputy Minister of NSC), Ho-Chung Chang (Former NSC Office Director, TECRO), Ai-Chia Hsu (Former ALMA Program Director of NSC), Jiin-Shuang Lee (Former NSC Office Director, Oficina Económica y Cultural de Taipei) (Picture Credit: Ai-Chia Hsu)

subscription rate of almost 6. Cycle 1 observations were carried out until June 2014 when Cycle 2 was expected to start. In the Cycle 2 proposal call, Taiwan submitted 73 proposals in December 2013, which reflects an even larger demand of ALMA observing time. Out of the world-wide submitted 1,381 proposals, 353 were selected as highest-priority programs which leave an oversubscription rate of 4. With 21 accepted proposals, Taiwan has further surpassed the previous cycles, doubling the acquired array time to almost 90 hours and improving the success rate to about 29%. In a recent publication, streams of gas falling onto the circumstellar disk surrounding the protostar L1489 IRS were detected for the first time (Figure 3). This observation is shedding light on how circumstellar disks can accrete material from ambient gas, grow and eventually evolve into a proto-planetary system where planets are formed. With ALMA's superb sensitivity, this observation is made possible with an integration time of about 1 hour.

In addition to scientific projects for ALMA, ASIAA is also contributing to the construction of the array and associated engineering efforts. Under collaboration with the Aeronautical Research Laboratory and the Chung Shan Institute of Science and Technology, ASIAA established the East Asia Front-End Integration Center (EA FEIC) in Taichung, Taiwan in 2008 (Figure 4). The EA FEIC is one of three facilities (besides the FEIC in Europe and North America) that integrates the ALMA receiver front-end components, tests the integrated assemblies and ships them out to Chile. The EA FEIC has been extraordinarily successful in delivering twenty-six out of 69 front ends by the end of 2012 (17 under the collaboration with ALMA Japan, 5 under the collaboration with ALMA North America and 4 under the collaboration with ALMA Europe). With the delivery of the last one of the 26 front ends in December 2012 and the shipping and commissioning of one testing line at the OSF in Chile in 2013, Taiwan gained international recognition among the ALMA partners and Taiwan's first major ALMA engineering project was completed.

The expertise gained from the EA FEIC is now being transferred to the new 35–50 GHz Band-1 receiver project which has been selected as the next major initiative for Taiwan and which will be delivered as part of the East-Asian development within ALMA. In 2012, ASIAA founded a Band-1 consortium with the Herzberg Institute of Astrophysics in Canada, the National Radio Astronomy Observatory (NRAO) of the USA, the University of Chile and the National Astronomical Observatory of Japan. Subsequently, the ALMA Development Steering Committee and the ALMA Board approved the development of a Band-1 prototype. The Preliminary Design Review was held at ASIAA in July 2013. Now the detailed receiver cartridge design is ready and intensive system testing is underway in the Band-1 receiver laboratory at ASIAA.

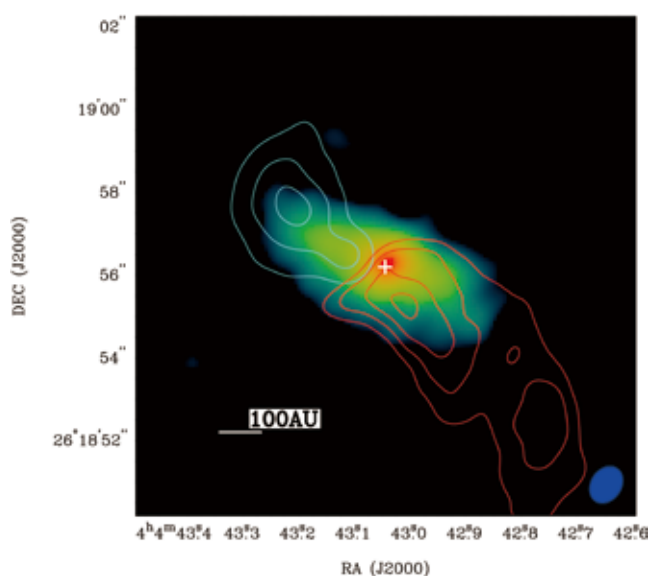


Figure 3. Circumstellar disk and ambient gas surrounding the protostar, L1489 IRS (white cross), from an ALMA cycle-0 observation with an integration time of 74 minutes at a resolution of 1" (blue ellipse at the bottom right corner). The color image shows the 1.3 mm continuum emission. Streams of gas falling onto the disk (blue and red contours) are detected in C<sup>18</sup>O(201) emission, feeding both mass and angular momentum to the disk system. Prior to this observation, the infalling gas motion was not clearly resolved. (Yen et al. 2014, ApJ, 793, 1)



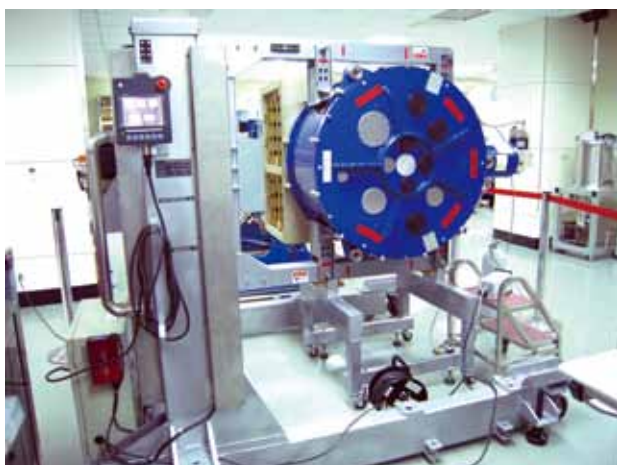


Figure 4. Top left panel: one of the front ends during testing and integration at the EA FEIC in Taichung, Taiwan. Pictured is the tilt table holding the cryogenic dewar (in blue) in which the receiver units are installed and tested. Top right: EA FEIC team delivering the first front end to Chile in 2008. EA FEIC staff members celebrating the delivery of the last receiver front-end system for our ALMA-Japan partner (lower left) and the very last front-end for Europe in 2012 (lower right). (Picture Credit: ASIAA/ARL EA FEIC)

In collaboration with NRAO, the Taiwan team also delivered two custom-designed Front-End Service Vehicles (FESV) which transport and service ALMA's front ends. The two Taiwan-made FESVs, named Mei-hua (梅花) after the national flower of Taiwan and Lan-que (藍鵲) after the Formosan blue magpie, arrived in Chile in August and December 2011 (Figure 5). Together with on-island industry and NRAO, ASIAA also delivered 5 nutating secondary subreflectors. This nutating subreflector is used to remove atmospheric noise, requiring large chopping ranges up to 18 arcmin at frequencies up to 10 Hz. It further requires very accurate pointing of 1.3 arcseconds and very short settling times of within 10 ms, posing new technical challenges for such a system. Recent successful site acceptance tests in Chile in October 2013 concluded this project (Figure 5). ALMA-Taiwan also delivered an engineering model of an Alternative Laser Synthesizer (ALS) for side-by-side comparison with the ALMA baseline local oscillator system. ALMA-Taiwan established a Taiwan ALMA Regional Center (ARC) at the ASIAA, serving as the prime interface for the Taiwanese user community organizing regular workshops and tutorials, and coordinating with the ARCs in Japan and in North America. The ALMA Band-10 receiver development was successful in providing an alternative source of Band-10 junctions for NAOJ. Finally, the prototype Vertex ALMA 12 m telescope was procured in 2012 by a team led by ASIAA with the goal of developing a site in Greenland (see "the Greenland Telescope (GLT) and Submillimeter VLBI" report) in the coming years (Figure 5).

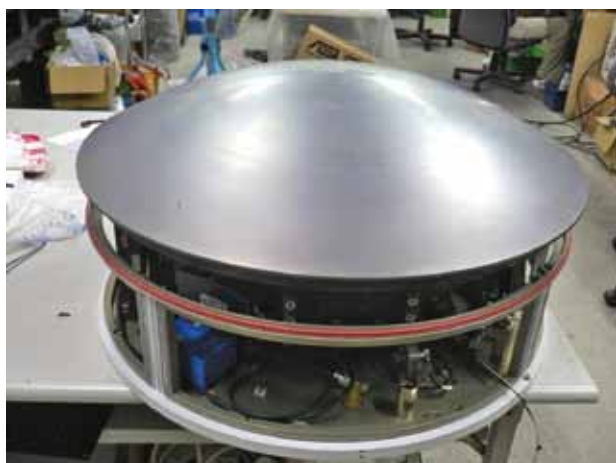


Figure 5. Completed and ongoing ALMA-Taiwan projects. Top row: nutating subreflector in the laboratory at ASIAA and during installation for site-acceptance testing in 2013. Part of the antenna primary mirror is visible on the top right panel. Middle row: the alternative laser synthesizer and one of the FESVs at the AOS at 5,000 m. Bottom row: a CASA-ASIAA imaging workshop held at National Taiwan Normal University and the procured NA 12 m Vertex prototype antenna at the JVLA site in Socorro, New Mexico. (Picture Credits: top row- Pierre Martin-Cocher; middle row- Derek Kubo (left) and Carlos Padilla (right); Bottom row- ASIAA/UCAT (left) and Shu-Hao Chang (right))



# The Yuan-Tseh Lee Array for Microwave Background Anisotropy

The Yuan-Tseh Lee Array for Microwave Background Anisotropy (AMiBA) is a forefront instrument for research in the field of cosmology. It is an interferometer operating at a 3 mm wavelength to study arcminute-scale fluctuations in the cosmic microwave background (CMB) radiation. In addition to the primordial fluctuations, AMiBA can also detect perturbations to the CMB photons by galaxy clusters along the line of sight. The perturbations happen when hot electrons in a deep gravitational potential scatter and transfer energy to the cold CMB photons. Such perturbation, called the Sunyaev-Zel'dovich effect (SZE), is directly related to the density and temperature of the hot gas, which traces the underlying dark matter distribution. The SZE is also complementary to information derived from X-ray, gravitational lensing, and kinematic observations of galaxy clusters.

AMiBA is situated on the slope of Mauna Loa at an elevation of 3,400 meters, on the Big Island of Hawaii. The telescope was built and operated in two phases. The first phase consisted of seven 0.6-meter antennas, with scientific observations from 2007–2008 (Figure 1). The second phase includes the expansion of the array to thirteen 1.2-meter antennas, which provides more collecting area and an angular resolution that better matches galaxy clusters at higher redshifts. Although the surface brightness of the SZE is redshift-independent, the apparent size of the cluster determines the total flux that can be received. Therefore matching the angular resolution



Figure 1. The first phase of AMiBA consisted of seven 0.6 m antennas close-packed in the center of the 6 m platform, offering a field-of-view of 23' and a resolution of 6'. Scientific observations were carried out from 2007–2008.



Figure 2. The second phase of AMiBA consisting of thirteen 1.2 m antennas was completed at the end of 2009. The 13-element array, with improved resolution and sensitivity, can effectively detect clusters that are much further away from us. Scientific operations resumed in 2011. The background shows another volcanic peak, Mauna Kea.

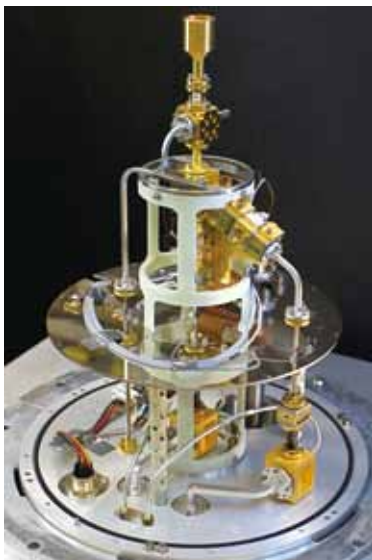


Figure 3. The AMiBA receiver with the vacuum chamber removed (Chen et al. 2009, ApJ, 694, 1664). The diameter of the chamber is about 30 cm. The detectors are cooled to 20 K by a closed-cycle cryocooler during operation.

to cluster size reduces the beam dilution effect and enhances the cluster's detectability. The expanded array (Figure 2) has been in operation since June 2011.

As the first major international astronomical project led by Taiwan, the AMiBA is also the first and only CMB telescope for Asia. It has established experimental cosmology as a viable field in Taiwan. This project also produced a team capable of leading, designing, and building frontier instruments. Young students, engineers, and faculty, have been trained, cultivated, and mentored for Taiwan.

AMiBA is designed, constructed, and operated by ASIAA, in collaboration with the Electronic Engineering and Physics Departments of the National Taiwan University, and the Australia Telescope National Facility (ATNF). Additional contributions were also provided by Carnegie Mellon University (CMU), the National Radio Astronomy Observatory (NRAO), and the Jet Propulsion Laboratory (JPL). The construction of AMiBA includes a novel hexapod mount, a carbon fiber platform, carbon fiber reflectors, low-noise receivers, a broadband correlator, sensitive and stable electronics, a retractable cover, site infrastructures, and software development. Figure 3 shows the AMiBA receiver. In October 2006 the 7-element system was dedicated to the then President of Academia Sinica Yuan-Tseh Lee for his continued support of the project (Figure 4).



Figure 4. AMiBA was dedicated in October 2006. The two panels show the gathering of team members and the Academy President Yuan-Tseh Lee at the dedication ceremony.

In April 2007, the first SZE signal was detected with the 7-element AMiBA towards the galaxy cluster Abell 2142 at a redshift of  $z = 0.091$ , followed by successful SZE detections towards five more clusters ranging from  $z = 0.18$  to  $0.32$ . In this phase, six galaxy clusters in the redshift range of 0.09 to 0.32 were detected. The cleaned images of the clusters are shown in Figure 5, and the main results were published in 2009. The primary efforts were in the areas of calibration and data reduction, identifying and flagging of bad data, removal of systematic errors, elimination of foreground contamination from



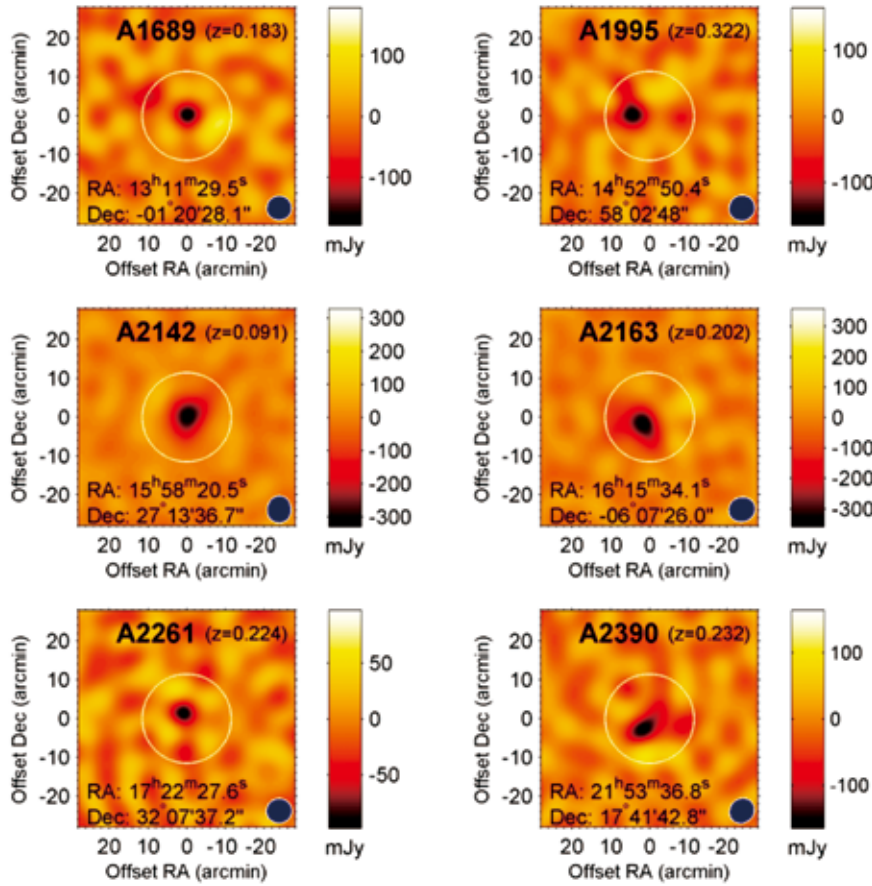


Figure 5. Six galaxy clusters observed by AMiBA at 3 mm wavelength. Compared to the surrounding region, the center of the cluster is dimmer due to the SZ effect (Wu et al. 2009, ApJ, 694, 1619).

local environment, converting output from the lag correlator into data points, and compensation for poor sampling or dirty beam pattern. Much effort was devoted to verifying the quality of the data. This involved analysis of the noise characteristics of the data, evaluating the contamination from CMB structures, and compensating for expected point sources in the field of view (Ho et al. 2009, ApJ, 694, 1610; Wu et al. 2009, ApJ, 694, 1619; Lin et al. 2009, ApJ, 694, 1629; Nishioka et al. 2009, ApJ, 694, 1637; Liu et al. 2010, ApJ, 720, 608).

While the SZE is suitable for probing the extent of hot gas, the weak gravitational lensing (WL) effect is ideal for measuring the large-scale distribution of dark matter. Comparison of the two data sets can reveal how the gas mass fraction varies with the cluster radius, which can constrain the formation mechanism of the galaxy clusters. WL data were obtained for four of the clusters detected by AMiBA. The averaged result from the comparison of SZ and WL data is shown in Figure 6.

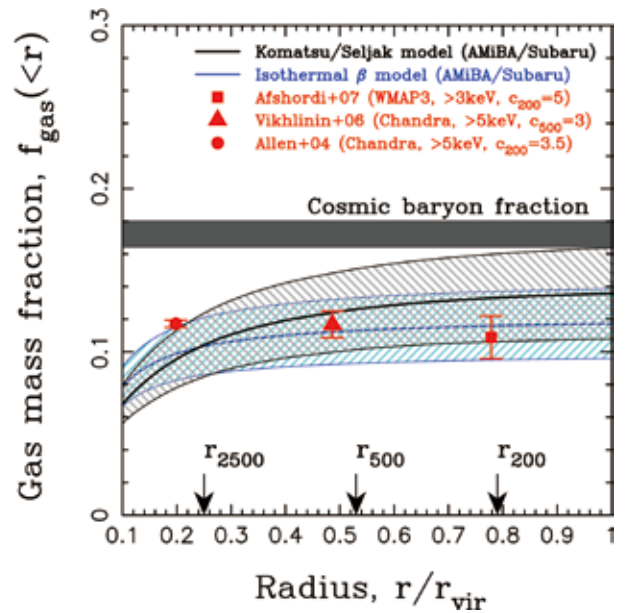


Figure 6. Combined with weak lensing measurements from the Subaru telescope, the AMiBA SZE data can be used to derive the gas mass fraction (Umetsu et al. 2009, ApJ, 694, 1643). The results here are shown as a function of clustercentric radius scaled to the virial radius ( $r_{vir}$ ) (Umetsu et al. 2009, ApJ, 694, 1643).

Of our sample, the cluster Abell 2142 is of particular interest since this is our brightest, most-nearby (hence resolvable) SZE cluster at  $z = 0.09$ , known as a merging cluster. Our AMiBA SZE map shows an elliptical structure extending in the northwest (NW)-southeast (SE) direction, similar to the weak lensing (dark matter) distribution (Figure 7). The extent of almost 20 arcmin in length from NW to SE is an example where sampling with the small antennas of 0.6-meter can be important for providing sensitivity to large-scale structures.

Other scientific impacts include the comparison of SZE with X-ray data in order to derive cluster angular diameter distances and the Hubble constant, cluster scaling relations, and studies of cluster gas properties. These early science experiments served to demonstrate the potential and performance of AMiBA (Huang et al. 2010, ApJ, 716, 758; Liao et al. 2010, ApJ, 713, 584; Molnar et al. 2010, ApJ, 723, 1272).

The 13-element 1.2 m antennas expansion was completed in June 2009, and was followed by periods of intense re-commissioning to meet the more stringent requirements. The new array is shown to be 8 times more sensitive for point sources, increasing the observation speed by a factor of 60. Science observations of the 13-element AMiBA, started in June 2011, provide smaller-scale information for the six clusters previously observed with the 7-element AMiBA. Combining both the large- and small-scale AMiBA data sets enable a precise constraint on the size and concentration of the hot gas distribution within these clusters. AMiBA will also be used to observe 24 clusters of the CLASH (Cluster Lensing And Supernova survey with the Hubble Space Telescope) sample (PI: Marc Postman), which is a multi-wavelength study oriented to understand the complex cluster structure covering optical strong lensing, weak lensing, spectroscopy, X-ray, and SZE. Some examples of the SZE maps obtained by the 13-element AMiBA are shown in Figure 8.

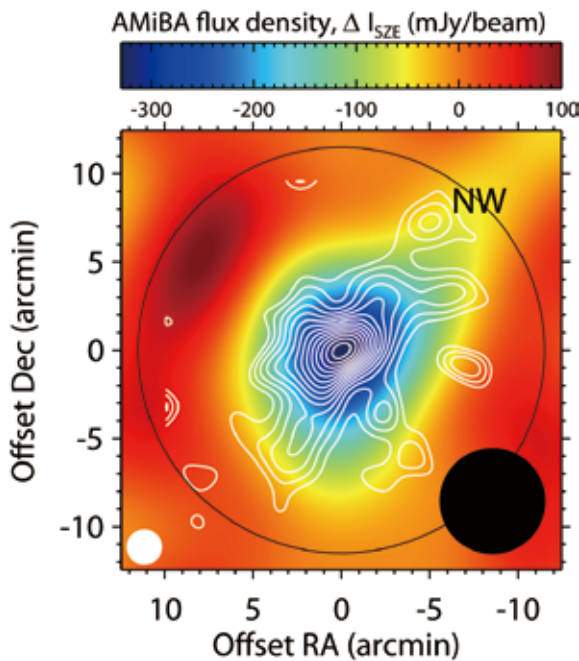


Figure 7. The Subaru weak lensing mass map (white contour) is overlaid on top of the AMiBA SZE measurement (color map) for the cluster Abell 2142. The open and filled black circles represent the field of view and resolution of AMiBA respectively. The filled white circle represents the resolution of the weak lensing data. This map shows that hot gas as seen in both SZE and the dark matter, traces an elongated distribution in the NW-SE direction (Ho et al. 2009, ApJ, 694, 1610).

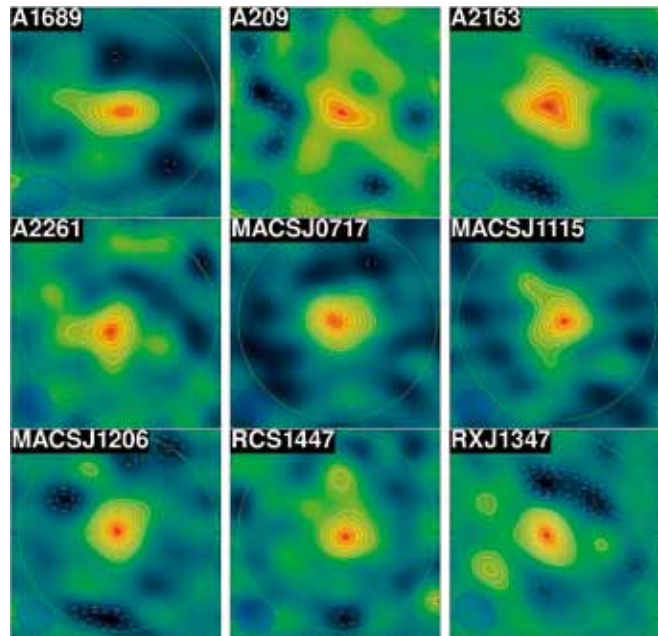


Figure 8. SZE maps and associated detection significance contours for nine clusters observed with the 13-element AMiBA. The contours start at  $\pm 3\text{-}\sigma$  and are separated by  $1\text{-}\sigma$ . The large open circle in each plot represents the FWHM of the primary beam, and the shaded ellipse at the bottom left corner denotes the synthesized beam. Size of map is  $12' \times 12'$  for each cluster. (Picture Credit: Hiroaki Nishioka & Kai-Yang Lin)



# Canada France Hawaii Telescope (CFHT) Collaboration



Figure 1. Left panel: the WIRCam was completed and installed on the CFHT in 2005. Right panel: Orion nebula image taken by WIRCam. (Picture Credit: Shiang-Yu Wang (left) & Chi-Hung Yen (right))

The optical and infrared instrumentation program of ASIAA started with the development of the Wide Field Infrared Camara (WIRCam) for the 3.6-meter Canada-France-Hawaii Telescope (CFHT). The WIRCam project officially started in late 2001. This camera has four  $2048 \times 2048$  HAWAII-2RG HgCdTe detector arrays, with a  $20'$  field of view, and  $0.3''$  pixel resolution. The camera optics are cooled to liquid nitrogen temperatures to suppress the infrared background. With the on-chip guiding capability of the IR array, the camera provides a 50 Hz tip-tilt correction and micro-dithering observations. In 2005, the WIRCam was installed and commissioned on CFHT (Figure 1). The camera has been fully functional for scientific observations since then without any major failure. The limiting magnitude in Ks band for a 10 sigma detection in an 1 hour exposure under  $0.7$  arcsecond seeing is about 23.1 in AB magnitude.

In this project, ASIAA staff was heavily involved in the development of the array control electronics and the real time image analysis. Participation also included system definition and final integration of the camera. Furthermore, we contributed a major effort in upgrading the official data pipeline. With the delivery of WIRCam, ASIAA continues its instrumentation collaboration with CFHT on the development of the CCD curvature wavefront sensor "FlyEyes" (Figure 2). The main goal of this project is to evaluate and characterize the MIT CCID-35 detector as a suitable replacement for the avalanche photo diode modules (APDs) in the existing curvature wavefront sensor. ASIAA mainly contributed to the hardware interface definition, detector controller system software design, CCD characterization, and AO system simulation.



Figure 2. Image of a mag 8.1 star with AO off and on with FlyEyes (Picture Credit: Shiang-Yu Wang)

For science activities, Taiwanese astronomers share about 15 nights of CFHT observations every year since 2004. Up to now, hundreds of hours of the Taiwan CFHT time has been spent observing various scientific targets using three major CFHT instruments: WIRCam, MegaCam (an optical square degree imager), and EsPADOnS (an Echelle SpectroPolarimetric Device for the Observation of Stars). The research fields include the solar system, star formation, galaxies, large scale structure, and cosmological studies. In particular, the studies of high redshift galaxies and large scale structures are actively carried out at ASIAA.

For high redshift studies, ultra-deep WIRCam images at J- and H-band were obtained for the  $28' \times 28'$  area of the Extended Great Observatories Origins Deep Survey-North field (Extended GOODS-N). The photometric data obtained with WIRCam were combined with existing deep ground-based and space-based data in the optical, infrared, and radio wave bands, and used to study the stellar mass and star formation rate at  $z > 2$ , far-infrared-radio correlation at high-redshifts, and candidates at  $z > 7$ . Several papers have been published resulted from this WIRCAM GOODS-N program, including the study of the clustering properties of  $z \sim 2$  galaxies (Lin et al. 2012, ApJ, 756, 71).

A similar survey project was also carried out in the Extended Chandra Deep Field-South (ECDF-S). The Taiwan ECDF-S Near-Infrared Survey (TENIS, Hsieh et al. 2012, ApJS, 203, 23) covered the  $30' \times 30'$  area of the ECDF-S with WIRCam at J and with a 5-sigma point source sensitivity of 25.5 mag in AB. The first scientific result of TENIS reporting galaxy candidates at  $z > 7$  (Figure 3) has been published (Hsieh et al. 2012, ApJ, 749, 88). The images and catalogs obtained by the TENIS project have also been released to the public.

For large scale and galaxy cluster studies, Taiwanese astronomers have joined several international collaboration projects for large surveys such as “WIRCam SDSS Equatorial Region survey (WISER)” and “The second Red-sequence Cluster Survey (RCS2)”.

WISER is part of the VISTA-CFHT Stripe 82 survey (VICS82), which is an international collaboration project (including Canada, Taiwan, Brazil, and France) to obtain near-infrared data (WIRCam J and Ks)



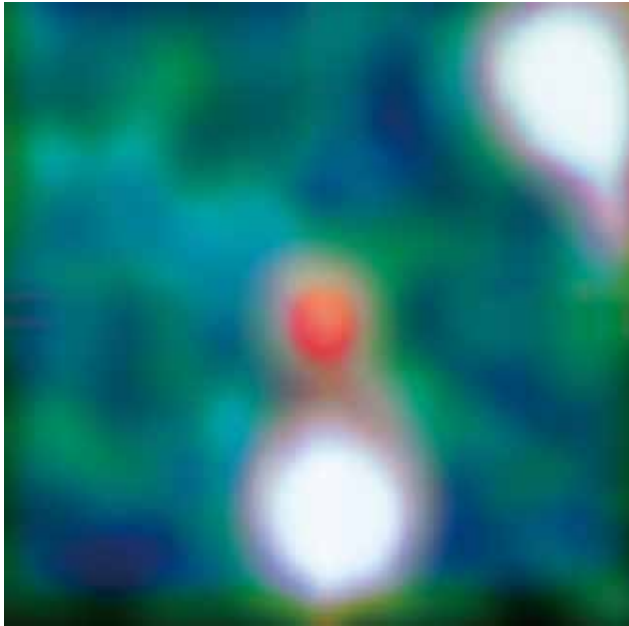


Figure 3. Galaxy candidate at  $z \sim 7.8$  found by the TENIS team (Picture Credit: Bau-Ching Hsieh)

covering 140 square degrees of the Sloan Digital Sky Survey (SDSS) equatorial Stripe 82. The near-infrared data obtained with WISER improve the photometric redshift quality and reduce the scatter of the stellar mass estimates for galaxies out to  $z \sim 1$ .

RCS2 is a multi-band imaging survey covering nearly 1,000 square degrees carried out using the MegaCam instrument. The RCS2 collaboration comprises an international team of over 20 members from Canada, USA, Taiwan, and Chile. It is designed to search for clusters of galaxies over a redshift range between 0.1 and 1.0. The project uses the red-sequence of cluster early-type galaxies to identify clusters. The survey comprises three-filter imaging ( $g'$ ,  $r'$ , and  $z'$ ), with additional  $i'$ -band imaging via a data-exchange with the Canada-France High- $z$  Quasar Survey. Dozens of papers have been published using the RCS2 data.

Besides the large survey programs, the CFHT has been used to observe Gamma Ray Burst (GRB) events. In addition, EsPADOnS was used very frequently for stellar studies such as long-term monitoring observations of active T-Tauri stars and a possible nearby Sagittarius tidal structure.

In conclusion, this collaboration enhances the communications between astronomers in Taiwan and those all over the world. The participation in large programs with other CFHT users provides the opportunity for us to access large CFHT databases and to work with experts in the world. Moreover, students in Taiwan are able to access a world-class telescope, which is important for the development of the next generation of astronomers in Taiwan.

## The Greenland Telescope (GLT) and Submillimeter VLBI

Very Long Baseline Interferometry (VLBI) is a technique to pursue the highest angular resolution. The angular resolution of interferometry is proportional to  $\lambda/D$ , where  $\lambda$  is the observing wavelength and  $D$  is the length of the baseline between two telescopes. Thus, observations at shorter wavelengths and/or longer baselines are essential to attain a higher angular resolution. By the combination of submillimeter wavelengths and intercontinental baselines, submillimeter (submm) VLBI will achieve a resolution of several tens of micro arcseconds (1 micro arcsecond = 1/[3.6 billion] degree), the equivalent of the apparent size of a 1 NTD coin (2 cm) on the moon seen from Taipei 101.

With such high angular resolution, a supermassive black hole (SMBH) is expected to be observed as a silhouette against luminous materials (such as an accretion disk and/or jet) near the event horizon. Such a “shadow” image will provide a direct probe for the existence of the black hole. Furthermore, the image of the immediate vicinity of a SMBH will provide a new window for studying General Relativity in the strong field regime. The size and shape of the shadow image will provide a determination of the mass and spin parameters of the SMBH.

Our main target is the SMBH in the galaxy M87. With a distance of 16 Mpc (52 million light years) and a mass of about  $6.6 \times 10^9 M_{\odot}$  (6.6 billion times heavier than the Sun), its apparent shadow size is about a few tens of micro arcseconds (Figure 1), only surpassed by the SMBH Sgr A\* in our own Galaxy. Furthermore, unlike the latter, M87 exhibits a prominent jet launched in the vicinity of the SMBH. Thus, this imaging project will allow an investigation of the launching mechanisms of the ultra-relativistic jets and the accretion process onto the SMBH. Imaging the jet and accretion disk will also reveal the connection between the innermost part of the jet and the accretion disk around the SMBH.

Submm VLBI observations are conducted via international collaborations. ASIAA is planning to play a leading role in the observations by proposing a new submm VLBI array consisting of the Submillimeter Array (SMA) in Hawaii, the Atacama Large Millimeter/submillimeter Array (ALMA) in Chile, and a new telescope at an excellent site. All these telescopes are either partly or fully operated by ASIAA. The new telescope is a prototype ALMA telescope, 12 meters in diameter, designed for mm and submm wavelengths (0.3 to 10 mm, or 30 to 950 GHz, Figure 2). In July 2010, the US National Science Foundation (NSF) announced a call for expression of interests for this telescope. ASIAA was awarded the telescope in April 2011, under collaboration with the Harvard-Smithsonian Center for Astrophysics (CfA), MIT Haystack Observatory, and the National Radio Astronomy Observatory (NRAO).

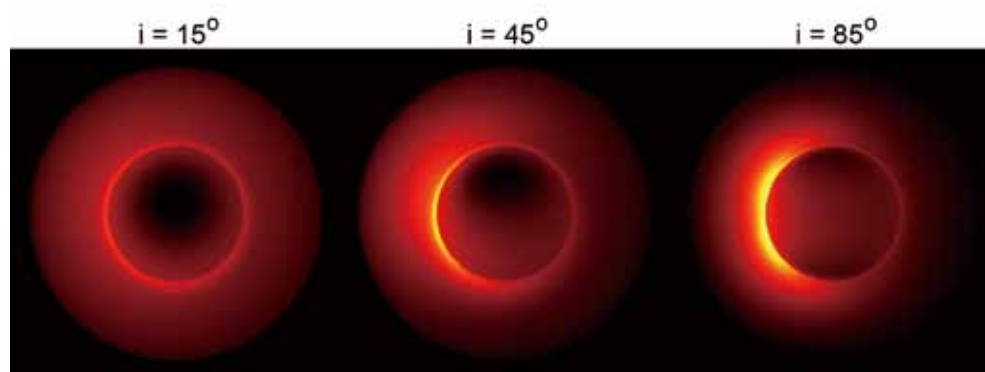


Figure 1. Image simulation of black hole shadow ("silhouette") images based on a possible accretion flow model for M87, shown for three cases of the disk inclination angle  $15^\circ$  (most probable according to the observed jet direction),  $45^\circ$ , and  $85^\circ$ . It is expected that this shadow can be observed in future submm VLBI observation. (Picture Credit: Hung-Yi Pu)





Figure 2. The ALMA-NA prototype telescope at Socorro, New Mexico (Picture Credit: Inoue Makoto)



Figure 3. Radiometer in the Greenland summit (Picture Credit: Pierre Martin-Cocher)



Figure 4. ASIAA Cluster for VLBI DiFX correlator (Picture Credit: Juan Carlos Algaba Marcos)

We have examined possible sites for the new submm telescope. Our main requirements are (1) excellent observing conditions to perform high quality observations at submm and even shorter wavelengths, and (2) location providing long baselines with the other key stations (e.g., SMA, ALMA). Based upon the precipitable water vapor (PWV) data measured by the NASA satellites Aqua and Terra/MODIS, the summit in Greenland was selected as the best candidate. For further evaluation, site testing has started at the summit station in Greenland from 2011 by installing a radiometer to measure the atmospheric transparency at 225 GHz (Figure 3). Current data indicate the median value of the measured opacity is 0.06 in the winter season between August 2011 and June 2013.

The telescope has been tested for functionality at the Jansky Very Large Array (JVLA) site in Socorro, NM, USA, and disassembled for retrofitting to allow operations at temperatures down to  $-50^{\circ}\text{C}$ . First assembly, testing for cold environment and commissioning observations are expected to occur at Thule, Greenland, in 2016. Subsequently, it will be moved to its final location at the Greenland summit as the Greenland Telescope (GLT). The project is currently working with the NSF Office of Polar Research Programs for logistics in Greenland.

The incorporation of the ALMA antennas will be the key in the submm VLBI network, as this will increase the sensitivity by a factor of ten due to the large increase in the collecting area. To optimize ALMA for this kind of observations it is essential to keep all its antennas in-phase for a single perfectly aligned telescope. This task is non trivial and ASIAA has a very active participation in an international collaboration aimed towards the ALMA phase-up project. This project has passed two external reviews and has been accepted by the ALMA administration. Commissioning will start in 2015.

As VLBI observations will be performed with an intercontinental array of various telescopes, data from different sites have to be correlated afterwards. ASIAA has acquired a CPU cluster and started the project to build and run a DiFX (A Distributed FX-style software correlator: Figure 4), which is easy to maintain and upgrade and will be able to handle the massive data rate from submm VLBI observations.

# The SAO/ASIAA Submillimeter Array



Figure 1. The SMA, built at the top of Mauna Kea at an elevation of 4,000 meters in Hawaii (Picture Credit: Sergio Martin)

The Submillimeter Array (SMA) project has been carried out by the ASIAA in collaboration with the Smithsonian Astrophysical Observatory (SAO) since 1996. The array was dedicated on Mauna Kea, Hawaii in November 2003 by the Academia Sinica President Yuan-Tseh Lee and Smithsonian Institution Secretary Larry Small. The SMA is a radio interferometer consisting of eight 6-meter antennas (Figure 1), with two of them (including the associated electronics and receiver systems) delivered by ASIAA under close collaborations with university groups and industry in Taiwan (Figure 2). It is now operating at three frequency bands at 230, 345, and 400 GHz. The array can be arranged into configurations with baselines as long as 509 meters, allowing observation of submillimeter emission from warm, dense gas and dust at unprecedentedly high resolutions of up to 0.1 arcsecond. Each element can observe up to a 4 GHz bandwidth, which has recently been enhanced to 8 GHz. The digital correlator backend provides thousands of spectral channels to each receiver. Polarization measurements with the SMA have been particularly useful in studying the structure of magnetic fields. The research fields include the Solar system, star and planet forming regions, evolved stars, and galaxies at nearby and cosmological distances.



As a partner of the SMA project, ASIAA contributes towards the maintenance and operation of the array on Mauna Kea. ASIAA has a small local staff residing in Hilo, Hawaii. In addition, the scientific and engineering staff visits the site regularly, and conducts remote operation from Taipei.

Figure 2. The SMA antenna built in Taiwan (Picture Credit: Ming-Tang Chen)



The SMA has been playing an important role in studying extragalactic objects. One of our targets is the closest giant elliptical galaxy, Centaurus A (NGC 5128). The most prominent feature of this galaxy is the dust lane (clearly seen in the left panel of Figure 3), which is likely to be the remnant of a small galaxy that fell into Centaurus A about 300 million years ago. The molecular gas distribution traced by the CO(2–1) (green color in the right panel of Figure 3) almost coexists with the dust emission (red color in the right panel of Figure 3). However, the CO image newly reveals spiral arm features, which extend from the circumnuclear gas at a radius of 200 pc to at least 1 kpc. The spiral arms in Centaurus A provides evidence that spiral-like features can develop within ellipticals if enough cold gas exists. The formation of these spiral arms is closely related to the formation of the dust lane. The formation of spiral arms might have happened rather quickly, on a time scale of less than 100 million years.

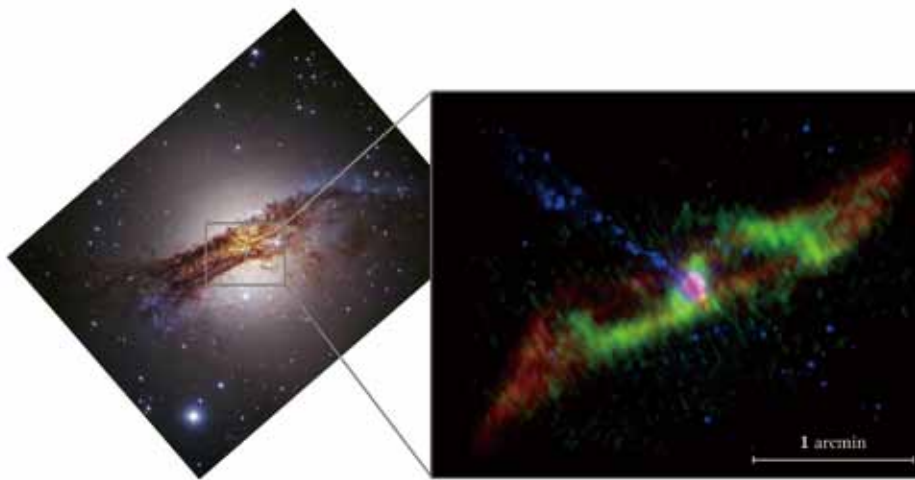


Figure 3. Left: Optical image of Centaurus A (ESO/IDA/Danish 1.5 m R-1. Gendler, J.-E. Ovaldsen, & S. Guisard, ESO). The prominent dust lane is clearly visible. Right: Molecular gas CO( $J = 2-1$ ) observed with the SMA (green), PAH and dust emission at 8 micron observed with Spitzer (red; Quillen et al. 2006), and the high energy jet observed with the Chandra X-ray observatory (blue) (Espada et al. 2012, ApJ, 756, L10).

The SMA is a very powerful tool for studying the site of star formation. Thanks to the capability of the wide-field imaging, the SMA allows the study of the structure of star-forming molecular clouds. The SMA successfully imaged the thermal dust emission at 0.85 mm from a  $0.9 \times 0.3$  pc area of Orion Molecular Cloud-3 (OMC-3), which is located to the north of Orion nebula M42 (Figure 4). The SMA image reveals that the filamentary cloud consists of a chain of clumps with a semi-regular interval of 0.035 pc. In the Orion molecular cloud, similar quasi-periodical structures have been observed at different size scales; fragmentation scales of the giant molecular cloud ( $\approx 35$  pc), large-scale clumps ( $\approx 1.3$  pc), and small-scale clumps ( $\approx 0.3$  pc). The observed quasi-periodical structures from large to small scale imply that the Orion molecular cloud fragments hierarchically and forms stars.

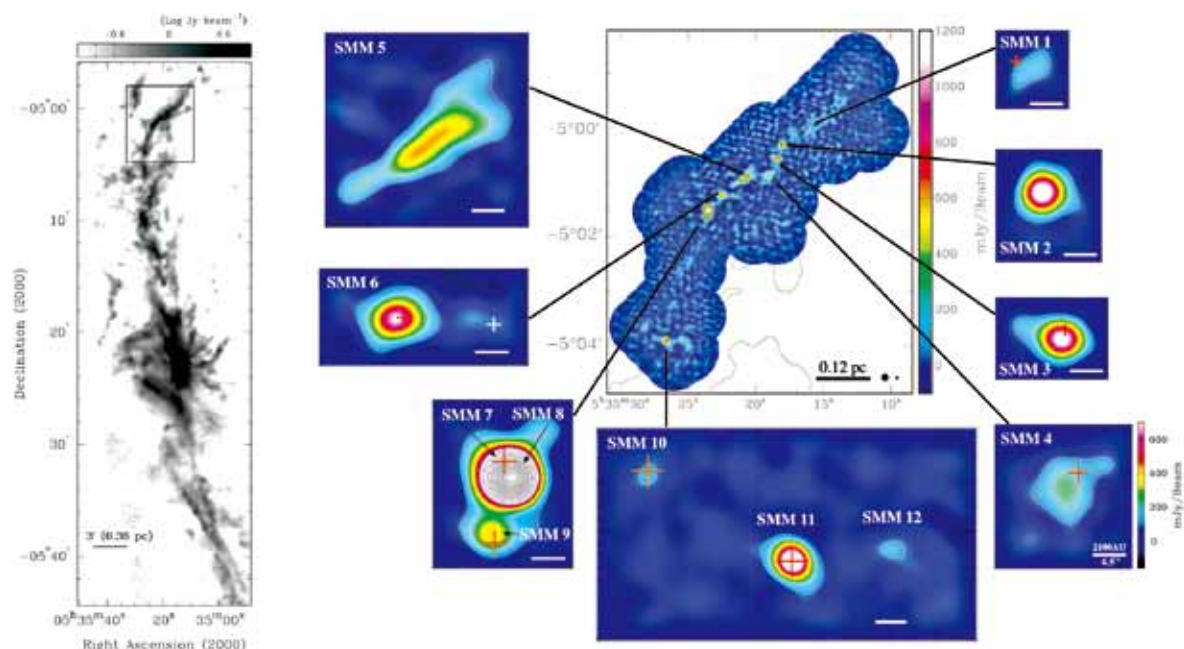


Figure 4. Left: Filamentary structure observed in the Orion Molecular Cloud obtained in 850  $\mu\text{m}$  continuum emission taken with the JCMT/SCUBA (Johnstone & Bally 1999). Right: SMA 850  $\mu\text{m}$  continuum image (color) obtained with 85-pointing mosaic observations overlaid with the 850  $\mu\text{m}$  continuum image taken with the JCMT/SCUBA (black contours) (Takahashi et al. 2013, ApJ, 763, 57).

The SMA is also powerful in studying dying stars. When they die, they expel material from their outer layers to space, producing outflowing spherically symmetric winds. Surprisingly, when most of the material in the outer layers is expelled, highly collimated structures suddenly appear around some of the dying stars, such as in CRL 618. An unprecedentedly high angular resolution CO image obtained with the SMA has revealed multiple fast molecular outflows with two different dynamical ages oriented along different optical lobes seen in the HST image (Figure 5). The SMA results imply two episodes of bullet ejections in different directions; one producing the fast molecular outflows near the central star, and the other producing fast molecular outflows near the tips of the extended optical lobes. One possibility to launch these bullets is the magneto-rotational explosion of the stellar envelope.

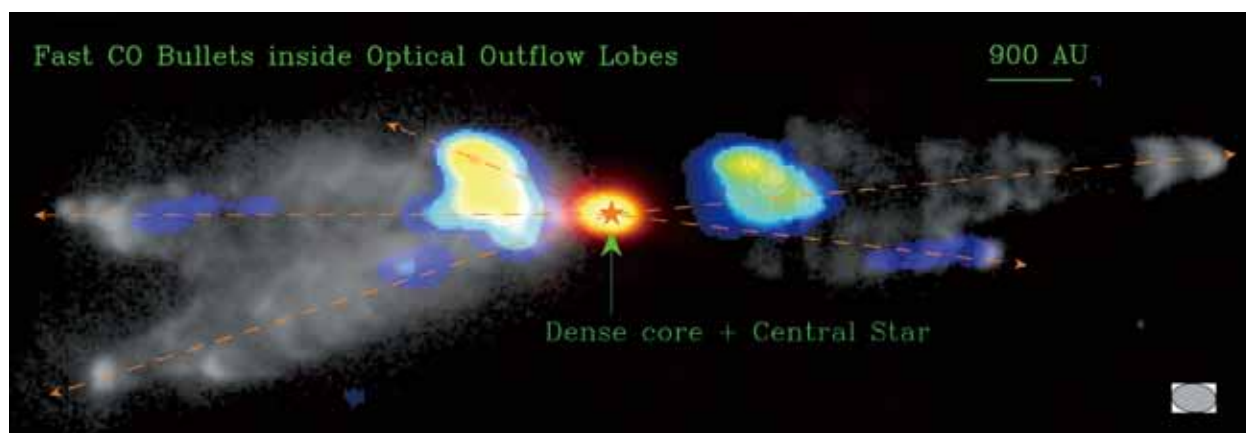


Figure 5. Gray image is the HST image in H $\alpha$ , showing multiple optical outflow lobes expanding away from the central star. Color image shows the fast CO bullets inside the lobes, detected with the SMA. The yellow image shows a dense core encompassing the star (Lee et al. 2013, ApJ, 777, 37).



## Subaru Telescope Collaboration



Figure 1. Left: the FES running with HSC installed. The two long boxes attached to the center black cylinder is the FES. Right: HSC during the observation. (Picture Credit: NAOJ)

In order to access larger aperture telescopes, ASIAA started to work with the Subaru telescope in 2008 based on its experience with Canada-France-Hawaii Telescope (CFHT). ASIAA contributes to the wide-field camera at optical wavelengths known as Hyper Suprime-Cam (HSC). HSC is the new camera for Subaru telescope which provides a 1.5 degree FOV with superb efficiency and image quality at the red end of the visible region. HSC is a collaboration between the National Astronomical Observatory of Japan (NAOJ), Princeton University and ASIAA. Combined with the 8.2 m aperture, HSC is the most powerful imaging camera in the world. The camera delivers a superior performance as compared with Suprime Cam, with a 10 times larger FOV. With the newly developed fully depleted CCDs, HSC is expected to provide 40% higher overall throughput in the  $z'$  band and provide reasonable efficiency in the Y band.

The challenge of developing HSC was to overcome the space and weight limit allowed at the prime focus of the Subaru telescope. In the development of HSC, NAOJ managed the project and developed the CCD integration, camera dewar and electronic system. Mitsubishi Electronics and Canon were responsible for the mechanical and optical system. ASIAA was responsible for the delivery of the filter exchanger system (FES), testing system of the wide field correctors (WFC) with Canon, and the testing of a few CCD chips. The FES (Figure 1) was developed in collaboration with the Aeronautical Systems Research Division (ASRD) of the Chung-shan Institute of Science and Technology (CSIST). Due to space limitation, the FES of HSC is designed to be a robotic system attached outside of the camera body. FES delivers the filters over a distance of 1.5 m to the optical axis with a precision of 50  $\mu\text{m}$ . Six filters can be installed at one time for the HSC observations. This project further enhanced our instrumental capabilities and provided a unique opportunity to work with the new generation CCDs. The HSC has captured the first light in August 2012, and demonstrated its superb image quality over the entire field of view (Figure 2). The scientific operation of the HSC including a large-scale survey with 300 nights has started in the 2014A semester.

To complement the capability of HSC, the Institute for the Physics and Mathematics of the Universe (IPMU) of the University of Tokyo decided to develop a multi-object spectrograph for the prime focus of Subaru telescope in late 2010. The design of Prime Focus Spectrometer (PFS) is based on the Wide Field Multi-Object Spectrograph project (WFMOS) proposed to the Gemini telescope. PFS will have 2,392

adjustable fibers within a 1.5 degree field. Each fiber guides the light of a target to four identical spectrometers which generate spectra from 400–1,300 nm with a resolution of about 4,000. The PFS team is led by IPMU in collaboration with the California Institute of Technology (Caltech)/Jet Propulsion Laboratory (JPL), Laboratoire d'Astrophysique de Marseille (LAM), National Astrophysical Laboratory (LNA) of Brazil, Princeton University, Johns Hopkins University, and ASIAA.

The PFS and HSC share the same wide field corrector. The Prime Focus Instrument (PFI, Figure 3), optical fibers, spectrometers, and metrology camera are the major components for

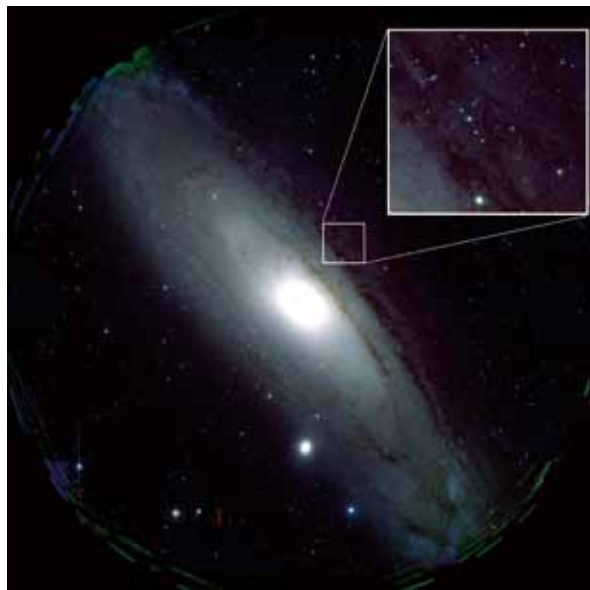


Figure 2. The first color image (M31) of HSC. (Picture Credit: NAOJ)

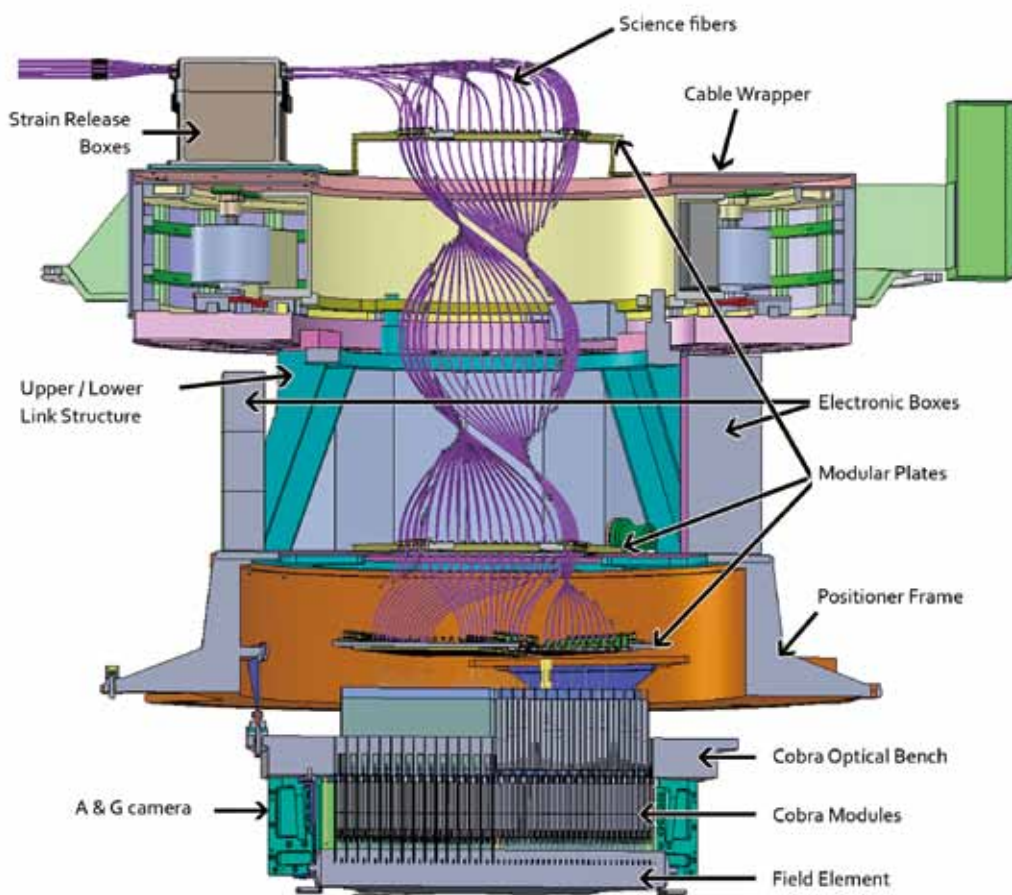


Figure 3. The Prime focus instrument of PFS (Picture Credit: Shiang-Yu Wang)



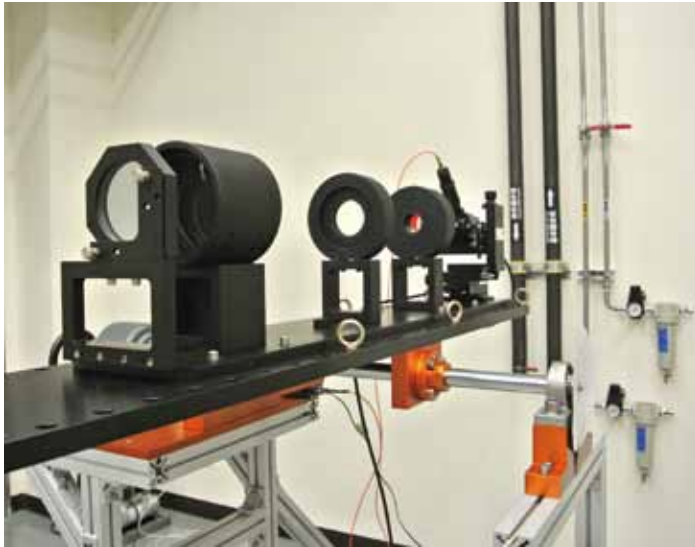


Figure 4. The metrology camera optics under tests in ASIAA (Picture Credit: Shiang-Yu Wang)

the PFS. The major challenge of PFS is to configure the fibers to match the targets within 0.1" error in 2 minutes. During the WFMOS development, JPL has been working to develop miniature motors. Each fiber will be driven by the two stage rotary piezoelectric motors. The fiber can be moved to any location within the 9 mm working area of the motor without an absolute encoder. A dedicated metrology camera is designed to provide precise location information for the fibers. Caltech/JPL will be responsible for delivering the fiber positioners while ASIAA will be responsible for the metrology camera and the PFI mechanical structure. LNA will provide the fibers connecting the prime focus with the spectrometers located outside of the observing floor. LAM will develop the spectrometers while Princeton University and John Hopkins University will deliver the cameras for them. The project passed the preliminary design review in February 2013. The optics for the metrology camera (Figure 4) are being tested, and the completion of this camera is planned in 2014 with the delivery of the PFI structure in the summer of 2015. The whole PFS is projected to see the first light in 2016, and open for science observations in 2017.

The PFS will be open to Subaru users, and it will also be used to conduct a large survey planned by the development team. The PFS survey will be focused on the following major topics: cosmology BAO study with galaxy surveys, Galactic archaeology, studies of galaxy evolution with high redshift galaxies, and AGN studies including its evolution and dust-enshrouded population. Taiwanese astronomers are working with scientists from other partners for the design of the survey.

## The Transneptunian Automated Occultation Survey (TAOS II)

TAOS II is a collaboration between ASIAA, the Universidad Nacional Autónoma de México (UNAM), the Harvard-Smithsonian Center for Astrophysics (CfA), National Central University (NCU), and Yonsei University in South Korea. The survey aims to detect occultations of distant stars by small (0.5 to 30 km diameter) Kuiper Belt Objects (KBOs). This survey presents several challenges, in particular due to the fact that such events have a very short duration, typically less than 0.2 seconds. It is further complicated by the fact that the sizes of the objects searched for lie in the Fresnel regime, and the events thus show significant diffraction effects (see Figure 1).



Figure 1. Left panel: An occultation event occurs when a KBO passes between the telescope and a distant star. Right panel: Shadow of a KBO projected onto the surface of the Earth. Note the significant diffraction effects. The image is 10 km on a side. (Picture Credit: ASIAA)

The estimated KBO occultation rate is extremely low and highly uncertain. Predicted rates range from 0.0001 to 0.01 events per year per star. Given that we expect to make more than 100 billion photometric measurements per year on a single telescope, special care must be taken to minimize the rate of false positive events. Therefore, coincident detection of any event on multiple telescopes is essential.

TAOS II will be sensitive to distant objects up to 1,000 AU, which is beyond the reach of any telescope using direct detection of reflected sunlight. The discovery of Sedna implies the existence of a hitherto unknown population of objects beyond 100 AU, which are too distant to be perturbed by any known planets at their present positions.

The TAOS II survey infrastructure is currently under development, with an expected start of scientific observations in late 2016. The goal of TAOS II is to measure the brightnesses of 10,000 stars simultaneously with three telescopes at a readout cadence of 20 Hz. The collaboration will install three 1.3 m F/4 telescopes at San Pedro Mártir (SPM) Observatory in Baja California, México, and equip each telescope with a custom camera, each consisting of an array of 10 fast readout CMOS chips. The new CMOS sensors will allow the readout of sub-apertures around individual stars, making the 20 Hz readout cadence possible. (This high readout speed is not possible using conventional CCD imagers.)

TAOS II held its official groundbreaking ceremony at SPM on 2 May 2013 (the left panel of Figure 2). The observatory is located at longitude 115°27'49" E., latitude 31° 02'39" N., and is at an altitude of 2,830 meters (the right panel of Figure 2). SPM, run by our partner UNAM, has excellent observing





Figure 2. Left panel: TAOS II groundbreaking ceremony at San Pedro Mártir Observatory (May 2, 2013). Pictured from left to right are Carlos Aramburo (Dean of Sciences UNAM), William Lee (Director of the Instituto de Astronomía at the UNAM), Paul Ho (Former Director of ASIAA), and Charles Alcock (Director of the CfA). Right panel: diagram of the layout of the three TAOS II telescopes. The control room is shown on the right, and the existing 2.1 m telescope at SPM is seen in the background. (Picture Credit: ASIAA)

characteristics. The weather is good, with more than 250 clear nights per year. The nominal seeing is 0.6 arcsecond, and the sky is very dark ( $V = 21.5 \text{ mag/arcsecond}^2$ ,  $R = 20.7 \text{ mag/arcsecond}^2$ ). The state of Baja California has recently enacted a light pollution ordinance, so the sky should remain dark for the foreseeable future.

All necessary permits for TAOS II installation at SPM have now been obtained, and the site development was started in September, 2013. Road work and electrical infrastructure has been completed in 2014, and pouring of the foundations for the three telescope enclosures are done by mid-2015. The enclosures will be constructed during the summer of 2015, after which the telescopes will be installed. Each enclosure will be topped by a 7.4 m diameter dome, fabricated by Ash Manufacturing.

TAOS II is in the process of procuring three telescopes from DFM Engineering. Each of the three identical telescopes has a 1.3 meter diameter primary mirror and a Cassegrain focus (Figure 3). The wide field telescopes are F/4, and image a 2.3 square degree field onto a circle of 154 mm diameter at the focal plane. The optical quality of the telescopes is such that 80% of the enclosed energy of a star will fall within a circle of 0.8" on axis, and 1.0" at the edge of the field. TAOS II has accepted all three telescopes in November of 2013, and the telescopes will be delivered to SPM in the summer of 2015.



Figure 3. The three TAOS II telescopes under construction in the factory at DFM engineering. (Picture Credit: ASIAA)

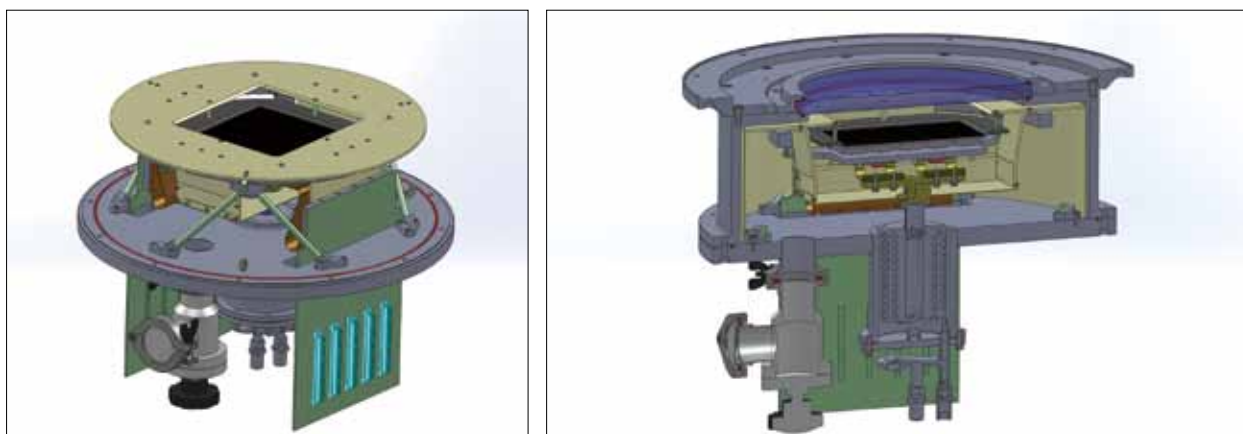


Figure 4. Left panel: Illustration of the TAOS II camera design. Right panel: Cross section of the TAOS II camera design.

The prototypes of TAOS II cameras are now under manufacturing (Figure 4). The cameras need to be capable of high-speed readout on a large number of stars. To read out a typical astronomical-grade CCD imager at our target cadence of 20 Hz is difficult, if not impossible, to achieve without introducing an unacceptable level of noise into the readout electronics. The TAOS II has thus opted to construct its cameras using CMOS imagers. CMOS imagers have built-in readout electronics in each pixel, allowing random access to any individual pixel at any time (with some constraints). Thus, one can read out only those pixels in sub-apertures around the individual stars targeted by the survey, while ignoring the rest of the field. One can thus reduce both the pixel readout rate and the data volume by 99%, while still reading out image data for over 10,000 stars at 20 Hz.

CMOS imagers have historically been of limited use in astronomy due to two drawbacks. First, the readout electronics on the pixels are on the photo-collecting surface of the imagers. The area of a pixel containing the readout transistors is not photosensitive. Thus, these imagers collect much less light than a CCD. Second, the read noise on a CMOS imager is typically five to ten times as high as that on a CCD imager. However, back-illuminated CMOS imagers are now available, and the collecting surfaces of such devices are fully photosensitive. CMOS imagers are now nearly as sensitive as CCD imagers. Second, recent developments implementing correlated double sampling onboard the devices have helped reduce the read noise to levels near those achieved using CCDs. The TAOS II collaboration has opted to use custom CMOS devices, each with an array of with  $1,920 \times 4,608$  16 micron pixels ( $31 \times 74$  mm), which will be produced by the company e2v. The contract was approved by Academia Sinica on August 7, 2012. Each camera will comprise a  $2 \times 5$  array of these custom devices to cover the 154 mm viewable field. The first engineering device has been delivered in 2014, and all of the devices will be delivered in the summer of 2016. After installation, these cameras are expected to be the very first low-noise, back-illuminated CMOS imaging cameras used in astronomy.





Figure 5. Left panel: One of the TAOS 0.5 m telescopes in its enclosure. Right panel: The four TAOS telescopes on top of Lu-Lin Mountain. (Picture Credit: Sun-Kun King (left) and Matthew Lehner (right))

TAOS II is a successor to the TAOS I project (the Taiwanese-American Occultation Survey), which is a collaboration between ASIAA, the CfA, NCU, and Yonsei University. TAOS I operates four 50-cm robotic telescopes at Lu-Lin Observatory in central Taiwan (Figure 5). Each telescope is equipped with a  $2k \times 2k$  CCD camera, with which we read out with a cadence of 5 Hz. Depending on the field, 500 to 1,000 stars are monitored simultaneously with all four telescopes to search for coincidental flux variations consistent with occultations by KBOs.

We began the survey using only three telescopes in February 2005, and four telescope operations commenced in August 2008. To date TAOS I has collected over 20 billion three-telescope photometric measurements and more than 5 billion multi-telescope measurements with all four telescopes. The system operates in a fully automatic mode, with remote monitoring from ASIAA and NCU.

The team has analyzed all of the three-telescope data through September 2011. No candidate events were found, and TAOS I has placed the strongest upper limits on the size distribution of objects with  $0.7 \text{ km} < D < 28 \text{ km}$  that have been published to date (Zhang et al. 2013, AJ, 146, 14). TAOS II will be more than 100 times as sensitive as TAOS I, allowing the survey to probe all of the predicted parameter space at the small end of the KBO size distribution.

# Theoretical Institute for Advanced Research in Astrophysics

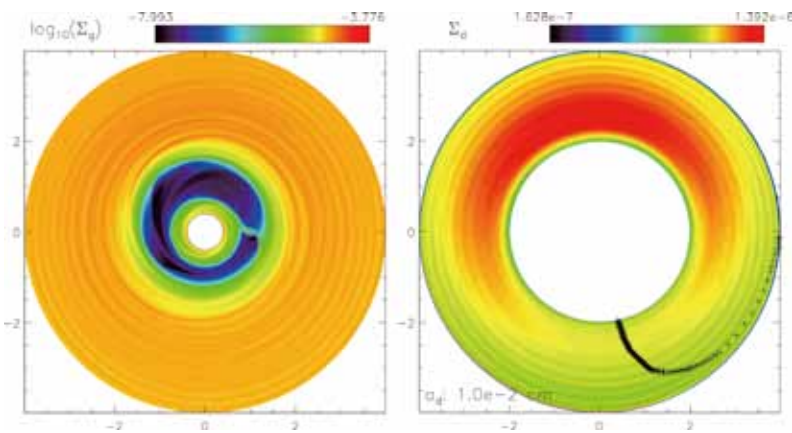


Figure 1. Numerical model for the asymmetric distribution of gas (left panel) and dust (right panel) column density maps of a face-on protoplanetary disk. A massive giant planet (0.5% of the mass of the central star) revolves about the central star on a circular orbit. The dust density map is only shown for the outer part of the disk where the disk is eccentric and the black crosses indicate the location of the disk pericenter. (Hsieh & Gu 2012, *ApJ*, 760, 119)

The Theoretical Institute for Advanced Research in Astrophysics (TIARA) was established in 2004 to provide an integrated world-class program of research and education in theoretical astrophysics. The institute aims to coordinate efforts of researchers and the training of future theoretical astrophysicists throughout Taiwan and Asia. It serves as an international center of excellence where forefront research can be integrated into the graduate education at Taiwan's universities and academic institutions. Its research and computational facilities are located at the Academia Sinica Institute of Astronomy and Astrophysics in Taipei. Currently, seven research fellows, two adjunct fellows, three visiting research fellows, and five post-doctoral research fellows are affiliated with TIARA.

TIARA's mission involves the investigation of the astrophysical processes associated with the formation of structure in the universe. Current research activities span star and planet formation, evolved stars, galactic structure and dynamics, accretion phenomena, and high energy astrophysics including compact objects. The problems lie at the forefront and are computationally challenging, intrinsically three dimensional and characterized by a wide range of length and time scales. In order to attack these problems, which require significant computational memory and long evolutionary timescales, TIARA provides access to computational resources using many processors on computational clusters and visualization servers.

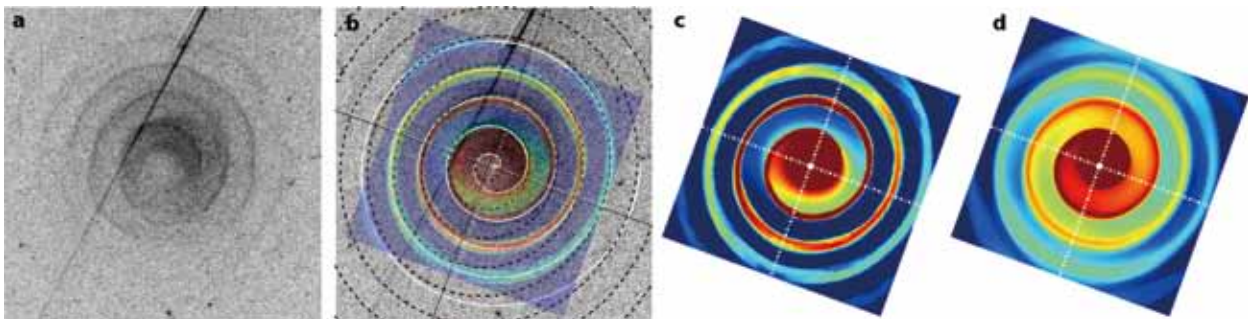


Figure 2. Model comparison with an observed pinwheel spiral pattern in the circumstellar envelope of the asymptotic giant branch star AFGL 3068. The panels correspond to (a) HST image from Maun & Huggins (2006), (b) the observed image with an overlay of the hydrodynamical model, (c) density distribution from a numerical hydrodynamical model, and (d) column density distribution from the model. (Kim & Taam 2012, *ApJL*, 759, 22)

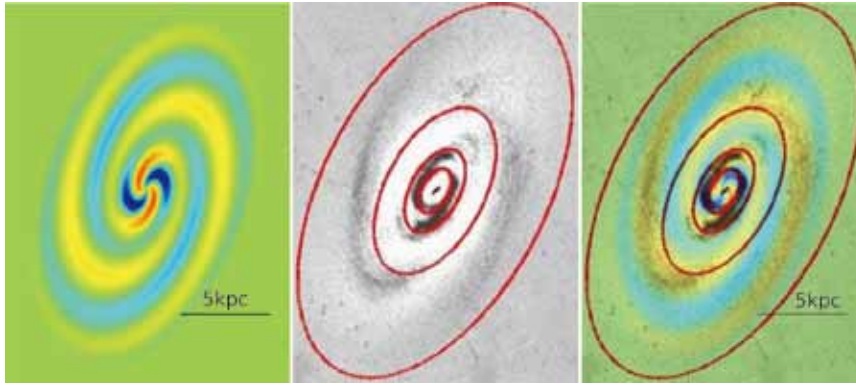


Figure 3. Stellar density wave of the spiral galaxy M81. Left panel: theoretical density distribution for a spiral mode. Middle panel: IRAC 3.6 micron map of the non-axisymmetric density distribution. Right panel: comparison of observation with the theoretical model. (Picture Credit: Hsiang-Hsu Wang)

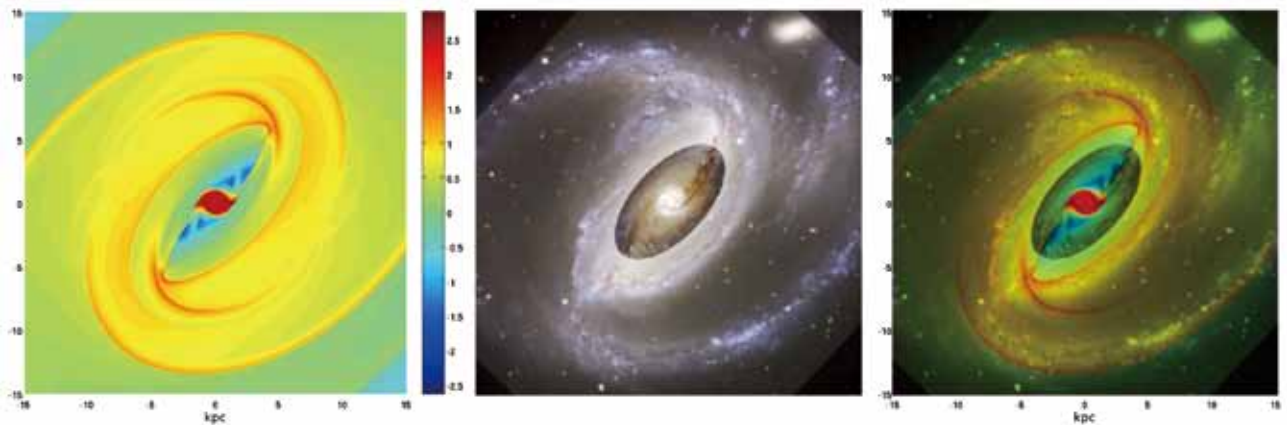


Figure 4. A comparison between the numerical simulation result and the observations of NGC 1097. Left: projected surface density distribution of the numerical simulation. Middle: optical VLT image of NGC 1097, exhibiting a bright nucleus associated with an AGN and a nuclear starburst ring. Two straight dust lanes nearly connect to the bar in the central region and to the two main spirals in the outer region. Right: superposition of the simulated and observed images, revealing that the morphology is reproduced in both their shape and location. (Lin et al. 2013, ApJ, 771, 8)

These research activities are carried out, in part, under the Computational Astrophysics (CompAS) and Chemistry, Hydrodynamics, and Astrophysics of Modeling Molecular Lines subprojects (CHARMS). A number of the research projects under TIARA have been highlighted in the research sections elsewhere. A few examples include giant planet perturbations on gas and dust in protoplanetary disks (Figure 1), nature of arcs and spirals in outflowing circumstellar envelopes of asymptotic giant branch stars (Figure 2), and the modeling of stellar spiral and gaseous arms in galaxies (Figures 3, 4).

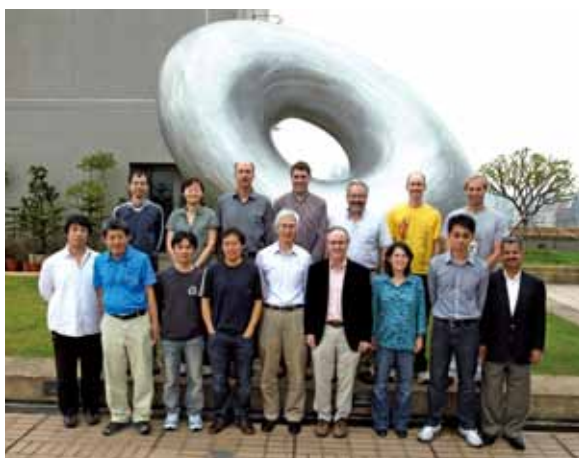


Figure 5. "The First Hundred Million Years of the Solar System" workshop in November 2013 (Picture Credit: Tony Zou)

To provide scientists with current developments in these rapidly changing fields and to inform the international community of the developments in Taiwan, TIARA runs an active visitors program (hosting over 20 scientists on a short term basis each year) and organizes and hosts a vigorous series of topical workshops on especially timely areas. TIARA has hosted workshops focusing on special topics in star formation, high energy astrophysics and compact objects, and cosmology. Of particular interest are workshop topics promoting interactions across different communities as exemplified in recent workshops on Star Formation and its Environment in the Center of Galaxies (involving the star formation and extragalactic groups) and the First Hundred



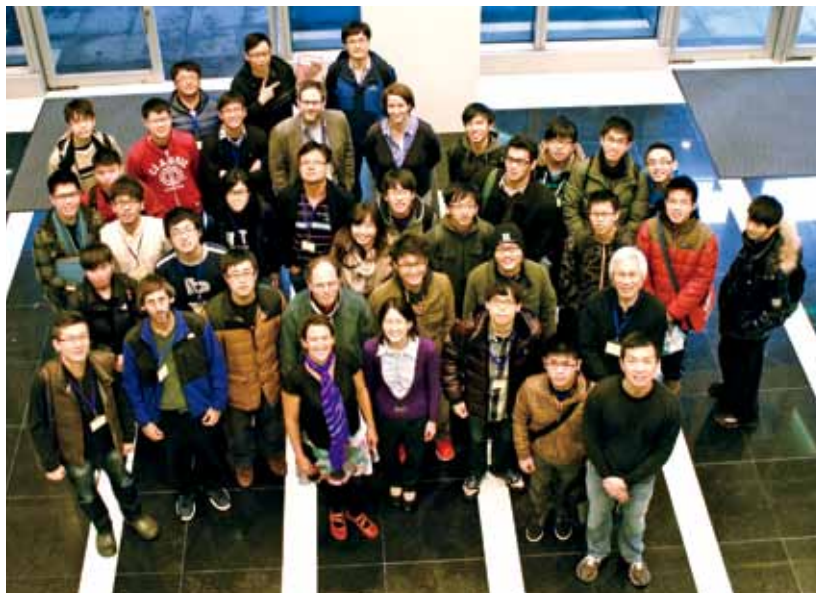


Figure 6. TIARA Winter School on Cosmology in February 2014 (Picture Credit: Shu-Hao Chang)

Million Years of the Solar System (involving the planet, stellar, and meteoritic groups, see Figure 5) held in the last two years. Depending on the scale of the workshop, the number of participants range from ten to twenty international experts and domestic researchers at the universities and ASIAA from Taiwan. These workshops have been highly successful in facilitating the exchange of scientific ideas and numerous papers have been produced which acknowledge the activities hosted by TIARA.

TIARA is also playing a major role in improving the graduate education of students at universities throughout Asia by holding schools on special topics in Taiwan. The schools are geared towards college and university students as well as to young postdoctoral researchers who wish to deepen their knowledge or branch out into a new area. These schools offer intensive, in depth courses over a one-week period to allow a complete pedagogical approach starting from fundamental theory to advanced applications in confronting current observational facts. Many successful schools have been held in the past, both in the winter and summer since TIARA's inception. For example, the 2014 winter school was held in cosmology (Figure 6) and the 2013 summer school on astrobiology (Figure 7). These schools last for one week with lectures delivered by invited speakers from throughout the world. Students from East Asian regions outside of Taiwan including China, Japan, Korea, Malaysia, and Philippines as well as from Europe have participated.

In the future, plans are underway to develop collaborative and cooperative programs with potential partner universities and institutes in China and with the University of California in the United States.

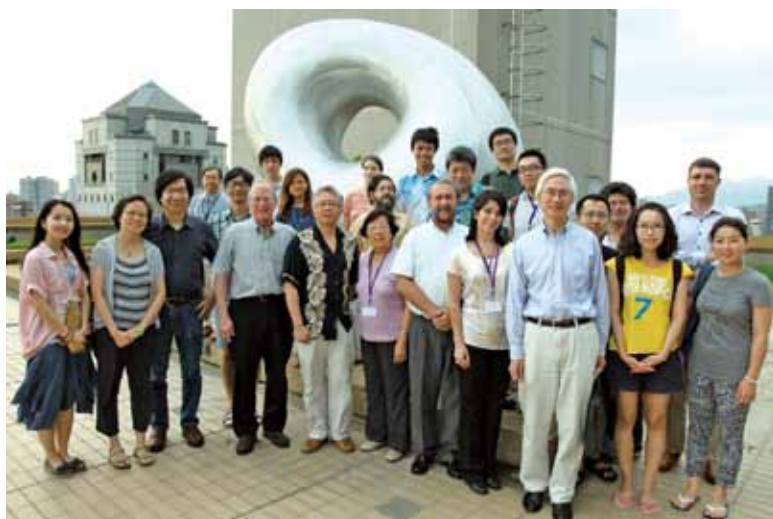


Figure 7. TIARA 2013 Summer School on Astrobiology (Picture Credit: Sam Tseng)

# The NanoSIMS Project



Figure 1. Left panel: instrument room. NanoSIMS sits on an anti-vibration platform. Right panel: control room. The control console is at the center of this picture. The instrument is located next door. This is to ensure the maximum stability of NanoSIMS.

NanoSIMS, a Secondary Ion Mass Spectrometer (SIMS) featuring submicron (tens to hundreds of nm) spatial resolution, was purchased in December 2011 and installed in Academia Sinica in July 2013. Since its debut in academia in 1998, NanoSIMS has been proven to be an extremely powerful tool in a wide range of research fields, including astrophysics and cosmochemistry, geochemistry, cellular biology and material science. Researchers in ASIAA is applying this instrument to the study of meteorites, in hopes of better understanding the origin and evolution of the Solar System as well as the chemical history of the Galaxy. NanoSIMS is also made available to colleagues from other Academia Sinica research institutes including, but not limited to, Institute of Earth Sciences (IES), Research Center for Environmental Changes (RCEC), and Genomic Research Center (GRC).

Given the submicron spatial resolution of NanoSIMS, this instrument is housed in a specially designed laboratory, where ground vibrations from the surroundings are reduced to a level 10 times better than the required lab condition (Figure 1). To maximize the stability of NanoSIMS, the operation console is separated from the instrument, and the instrument room is well air-conditioned to minimize thermal disturbances. The on-site acceptance test results have demonstrated the effectiveness of such floor and AC designs.

One important research topic performed with NanoSIMS in ASIAA is the study of isotopic compositions of the oldest Solar System solids, namely Ca-Al-rich Inclusions (CAIs). These inclusions, with absolute radiometric ages of 4.568 billion years, formed at the very beginning of the Solar System history and therefore witnessed to the earliest evolution of the Solar System. CAIs are known to have preserved fossil records of some short-lived radionuclides (half-life < 3 Myr). Such radioactivities could have

originated from a specific stellar source (supernova, asymptotic giant branch star, or Wolf-Rayet star) and/or have been produced by nuclear reactions between nebular dust and solar energetic charged particles. If the initial abundances and distributions of, and the relationships amongst, different short-lived radionuclides in the solar nebula can be quantitatively constrained, a clearer picture regarding the Solar System formation can be obtained.

The chemical evolution history of the Galaxy can also be studied with NanoSIMS through the isotopic analysis of “true stardust” or “presolar grains”. These dust particles are condensates in the outflows of evolved stars so that they sample material directly produced by stellar nucleosynthesis. Some presolar grains survived their interstellar passage and destructive processes in the early Solar System, and then were incorporated into meteorite parent bodies. In the laboratory, these grains can be identified by their extremely anomalous isotopic compositions (far different from the average solar ratios) in many elements, such as C, N, O and Si, and then can be analyzed for other isotopic systems. One topic that has been of interest to ASIAA researchers is the residence time of presolar grains in the interstellar medium. This problem can be constrained by analyzing the isotopic compositions of purely spallogenic elements, such as Li-Be-B, in the presolar grains. These elements are destroyed by stellar nucleosynthesis, therefore, any Li-Be-B seen in presolar grains must be due to spallation by Galactic Cosmic Rays (GCRs) when grains resided in the interstellar medium. Therefore, combined with theoretical modeling, the results of Li-Be-B measurements will not only provide the residence time of stardust in the interstellar medium, but also constrain the paleo-flux and compositions of GCRs.

Other potential research projects from other fields include, but are not limited to, U-Pb isotopic systematics and Ti concentrations in terrestrial zircons ( $\text{ZrSiO}_4$ ), Li isotope diffusion as geospeedometer, O isotopic compositions of otolith as a tracer for fish migration history and S isotopic compositions of aerosols. At this moment, ASIAA researchers along with colleagues from IES are developing analytical techniques necessary for high quality isotope measurements of natural material. The instrument will become available to other interested colleagues once the protocols are developed.



# ***Science Highlights***

Letter from the Director

Introduction

Projects

Science Highlights

Instrumentation Research

Education and Public Outreach

# Extragalactic Studies

## Clustering Properties of $z \sim 2$ Star-Forming Galaxies

It is widely known that the star formation activities of galaxies are closely related to the galaxy environment, often referred as the “star formation rate (SFR)-density” relation, at least out to  $z \sim 1$ . To explore this relationship to even greater redshift, the halo masses of  $z \sim 2$  galaxies, selected using the B-z and z-K colors, were measured as a function of their specific star formation rate (SSFR, defined as the SFR normalized by the stellar mass) by using a galaxy clustering technique. The most interesting result from this work is that the clustering strength, i.e., the hosting halo mass, reaches a minimum for galaxies with  $\text{SSFR} \sim 2 \times 10^{-9} \text{ yr}^{-1}$ . This is illustrated in Figure 1. For galaxies with SSFR smaller than this critical point, the hosting halo mass increases, implying that the environmental quenching effect has taken place as early as  $z \sim 2$ . On the other hand, for galaxies with SSFR above the threshold, the hosting halo mass also increases, suggesting that some mechanism operating in denser environments may also boost the star formation activity of galaxies.

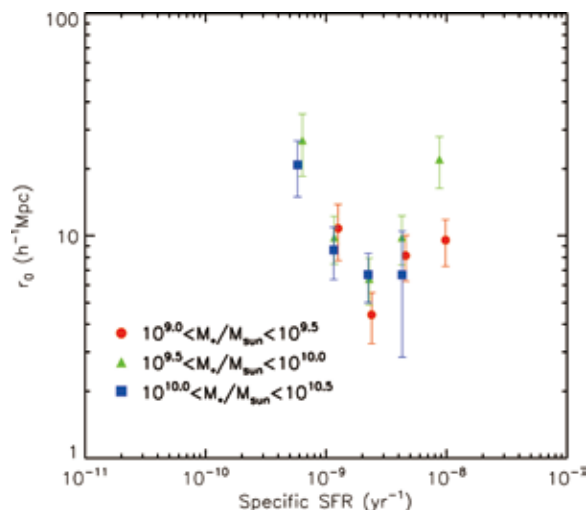


Figure 1. Clustering strength vs. specific star formation rate of  $z \sim 2$  star forming galaxies (Lin et al. 2012, ApJ, 756, 71)

## Taiwan ECDF-S Near-Infrared Survey (TENIS)

TENIS is a deep near-infrared imaging survey of the Extended Chandra Deep Field-South (ECDF-S). The primary goal of TENIS is to select robust galaxy candidates at  $z > 7$  in the ECDF-S. TENIS provides J (1.2 micron) and Ks (2.1 micron) data (limiting magnitude reaching 25.5 AB) for an area of  $0.5 \times 0.5 \text{ deg}^2$  (Figure 2), obtained with the Wide Field Infrared Camera (WIRCam) on the 4-m Canada-France-Hawaii Telescope (CFHT) on Mauna Kea. These are the deepest near-infrared images to cover the entire ECDF-S, and are as deep as the Spitzer Space Telescope images at longer wavelengths. Over 60 thousand objects are detected in the TENIS J+K image, and are valuable for studying Galactic objects and distant galaxies. The images and catalogs have been publicly released to the astronomical community (Hsieh et al. 2012, ApJS, 203, 23).



Figure 2. The center of the TENIS field. In this color picture, blue is the Hubble Space Telescope z-band image, green is our TENIS J-band image, and red is TENIS Ks-band image. The square is the famous Hubble Ultra Deep Field. The total area covered by our TENIS survey is roughly 12 times larger than what is shown here.

## Dual Molecular Outflows revealed by ALMA in a Merging Galaxy

A galaxy sometimes collide with another galaxy and the two eventually merge. For each galaxy, the tidal perturbation from the other galaxy is often large enough to induce a stellar bar that funnels a large amount of interstellar gas to the galactic center. The large influx of gas to each nucleus causes a burst of star formation (or ‘starburst’) there or fuels a supermassive black hole in the nucleus, letting it shine as an active galactic nucleus (AGN). These are the reasons why the most luminous galaxies in the local universe are predominantly merging galaxies. Details of this luminous merger phase of galaxy evolution are, however, still actively studied. One of the large remaining issues is the feedback from the luminous nuclei to the funneled gas. How does it happen? How strong is it?

We used the Atacama Large Millimeter/submillimeter Array (ALMA) to observe molecular gas in the most luminous galaxy in the local universe ( $z < 0.01$ ,  $D < 40$  Mpc). It is the merging galaxy NGC 3256, having two galaxy nuclei prior to coalescence at a separation of 850 pc (3000 light years). The left side of the figure is an optical-light image of the merger taken with the Hubble Space Telescope. We observed the central region with ALMA, and imaged the complex distribution of molecular gas more clearly than ever (upper-left image in the 860 $\mu$ m J=3-2 transition of carbon monoxide, CO). The two nuclei are marked with + signs.

A surprise was that each of the two merger nuclei was found to drive an outflow of molecular gas (lower-left panels.) The most blue-shifted (via Doppler-shift) and most red-shifted gas are symmetrically located around the S nucleus. The same pattern can be seen around the N nucleus although its redshifted lobe is blended with that from the S nucleus. We knew from our previous SMA observations that the merger has a molecular outflow (Sakamoto et al. 2006). But the new ALMA observations revealed for the first time that there are dual outflows, one from each nucleus (Sakamoto et al. 2014). Each nucleus drives an outflow at a rate of  $\sim 50$   $M_{\odot}$ /yr. This is comparable to the rate at which star formation consumes molecular gas in the merger.

The molecular outflow from the S nucleus is more intriguing in that it is well collimated like a jet, that the gas outflow velocity probably exceeds 2000 km/s, and that the outflow appears to accelerate out to about 300 pc (1000 light years) from the nucleus. What is driving this unusual molecular jet? A hidden AGN in the S nucleus was suggested in Sakamoto et al. (2014). Indeed, our recent careful analysis of optical, infrared, and X-ray data found that the S nucleus does host a low-luminosity AGN (Ohya et al. 2015). Our research continues on this ideal target to study merger-induced activities and their feedback.

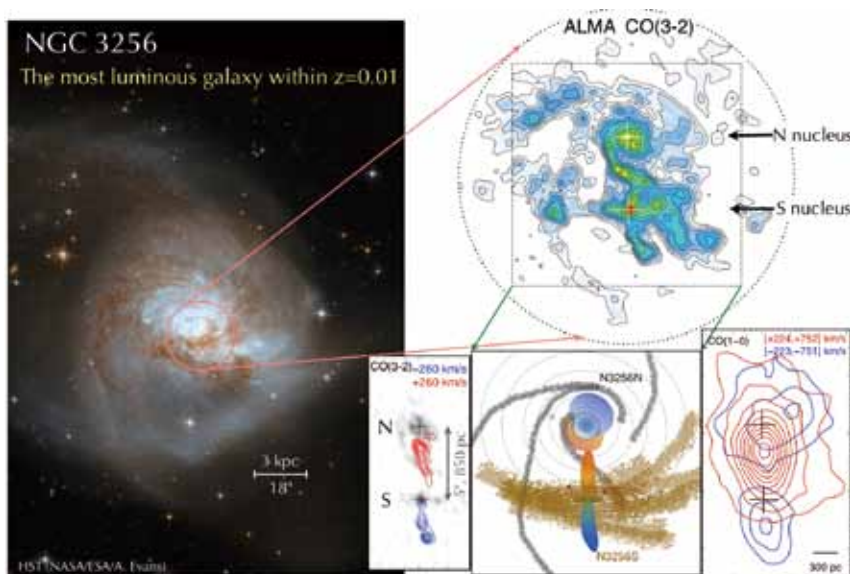


Figure 3. NGC 3256, a merging galaxy and the most luminous galaxy in the local universe. (Left) Optical image taken with the Hubble Space Telescope. We observed the center of this merger with ALMA. (Right-top) ALMA image of submillimeter-wave molecular line emission, revealing gas concentrations at the two nuclei and disturbed gas spirals around them. (Right-bottom) Evidence of dual molecular outflows, one each from each nucleus. Approaching and receding gas are shown in blue and red. The central panel illustrates the two bipolar molecular outflows from the two galaxy nuclei.



## Tracing the Stellar Mass Growth of Most Massive Galaxies

The most massive member in galaxy clusters (the brightest cluster galaxy, or BCG) represents a unique class of galaxies. They are ultraluminous and huge in spatial extent. They are believed to form via galactic mergers, and their evolution may be well connected to the formation history of the host clusters. It is thus imperative to understand in detail how these amazing beasts come into existence. Observationally, it remains challenging to measure how their stellar mass increases with time, however, and different observational approaches have led to opposite conclusions regarding whether their evolution is in accord with the predictions from leading galaxy formation theories in the  $\Lambda$ CDM structure formation paradigm.

The astronomers in ASIAA have recently developed a method to trace the stellar mass growth of BCGs that is believed to offer a better way of comparison with theoretical predictions. Although the evolution of any single cluster cannot be followed in time, by utilizing large samples of clusters, one can statistically identify high redshift clusters that could be the progenitors of a given set of low redshift clusters. We are thus able to “connect” BCGs observed at different cosmic epochs, and the study of their mass growth becomes more straightforward. The Spitzer and WISE data have suggested that galaxy formation models in general do fairly well in describing the mass growth history of BCGs from redshift  $z = 1.5$  to about 0.5; below that epoch, however, there is a hint of divergent behaviors (Figure 4). While the model BCGs continue to grow at the same pace, the observed ones appear to stop growing. This finding will help theorists fine tune their model, especially the treatment of dynamical friction for galaxy evolution within clusters (Lin et al. 2013, ApJ, 771, 61).

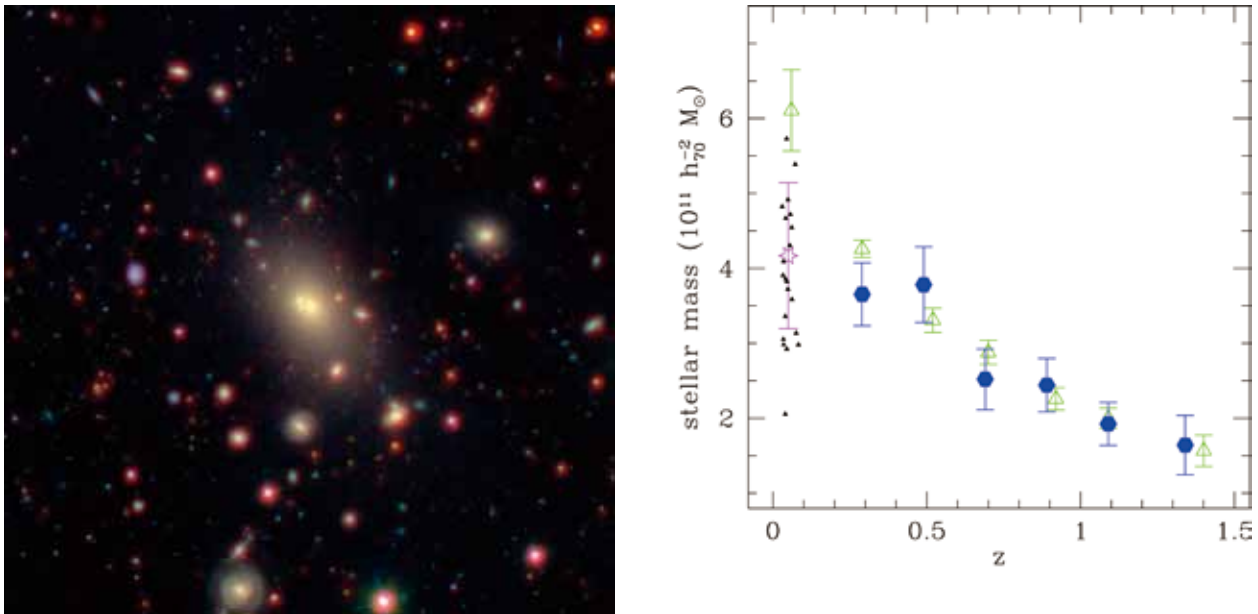
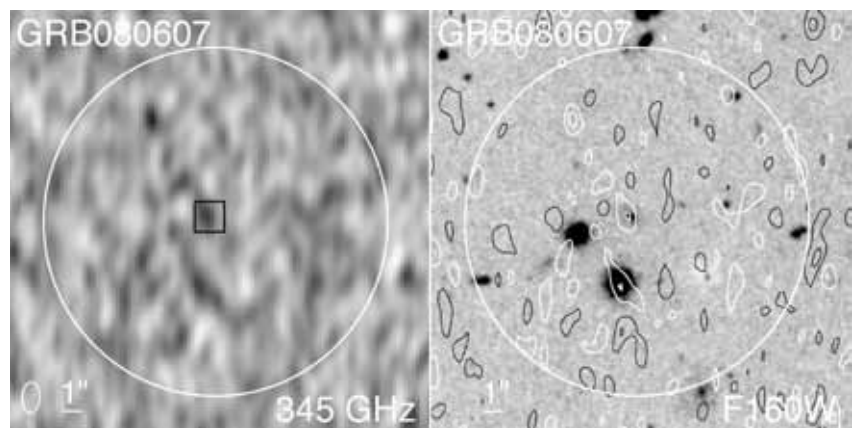


Figure 4. The left panel is a picture of a galaxy cluster observed by the WISE and Spitzer Space Telescopes. The bright galaxy at the center is the BCG. The right panel shows the mass growth of BCGs. The green triangles represent predictions of the stellar mass growth of BCGs by a highly successful galaxy formation model (Guo et al. 2011), which are found to agree fairly well with the Spitzer and WISE infrared observations for a large sample of BCGs (blue points and the pink star), down to  $z \sim 0.5$  or so. Below that redshift, there is some hint of different behavior between the model and data, in the sense that the model BCGs continue to grow, while the observed ones slow down their growth considerably.

## ALMA Detection of a Gamma-Ray Burst Host Galaxy

Long duration gamma-ray bursts (GRB) are believed to originate in the death of massive stars, and therefore are expected to trace star formation in distant galaxies. In order to establish the link between GRB host galaxies and the cosmic star formation history, it is crucial to measure the star formation rate (SFR) of GRB host galaxies. By far, most of the measurements of the SFR of GRB host galaxies come from rest-frame UV observations, where the effect of dust extinction may produce significant bias. Using ALMA in Cycle 0, astronomers in ASIAA carried out deep 345 GHz dust continuum imaging of two high-redshift GRB host galaxies, and successfully detected the dust emission from the host galaxy of GRB 080607, which is at a high redshift of  $z = 3.036$  (Figure 5). The ALMA detection shows that it is not an extremely dusty galaxy (cf. ultraluminous infrared galaxies) and it only has a moderate SFR of  $40\text{--}80\text{ M}_{\odot}\text{ yr}^{-1}$ . GRB 080607 is classified as a “dark burst” meaning that the GRB afterglow shows large dust extinction. The new ALMA result suggests that the large extinction of the afterglow is confined along a particularly dusty sight line, but not representative of the global properties of the host galaxy. Our result also suggests that high-redshift GRB host galaxies may correspond to the typical star-forming galaxies that produce the bulk of the cosmic far-infrared background.

Figure 5. ALMA (left) and Hubble Space Telescope (HST, right) images of the host galaxy of the gamma-ray burst GRB 080607. In the HST panel, white contours of 345 GHz flux are overlaid. In the ALMA panel, the black box indicates the optical position of the host galaxy, which was detected by ALMA at 345 GHz. The ALMA observations show that the host galaxy is a normal star forming galaxy, rather than an ultraluminous infrared galaxy. (Wang et al. 2012, ApJL, 761, L32)



## Star Formation

Stars including our Sun are basic building blocks of the Universe and it is important to understand where and how they come to be. It is believed that stars are formed inside dusty cocoons called “molecular cloud cores” by means of gravitational collapse. The details of the process, however, are complicated by the presence of magnetic fields and angular momentum. Astronomers in ASIAA aim to advance our understanding of star formation by detailed observational and theoretical studies of nearby star-forming regions in our Galaxy.

### Magnetic Fields Measurements

In order to determine the role of magnetic fields in star formation, it is necessary to measure the field strength. Commonly used observational techniques provide either only one single averaged field strength for an entire star forming region, or only isolated values (e.g. Zeeman observations). As reported in Koch et al. (2012), dust polarization observations from the Submillimeter Array (SMA) at radio frequencies around 345 GHz are used for position-dependent estimates of the field strength. Dust particles couple to the field, which is why coherent polarized emission can be detected. From the polarized emission the orientation of the magnetic field is derived. Their method uses these field orientations in combination with changes (gradients) in dust densities. The geometry of these morphological features is linked to magneto-hydrodynamics equations, so that the field strength can be calculated. In this way, the field strength at every location where polarization is detected can be derived for the first time. Applied to the SMA observation of the W51 e2 core, an increase in field strength from about 1 mG in the outer parts to about 10 mG in the center is found (Figure 1). Additionally, their method yields a model-independent force ratio, which quantifies how effectively the field tension force withstands gravity. For W51 e2, they find that the field increases the collapse time by a factor of about 10, making the effect of the magnetic field a promising mechanism to explain observed low star formation efficiencies. (Koch, Tang, & Ho 2012, ApJ, 747, 79)

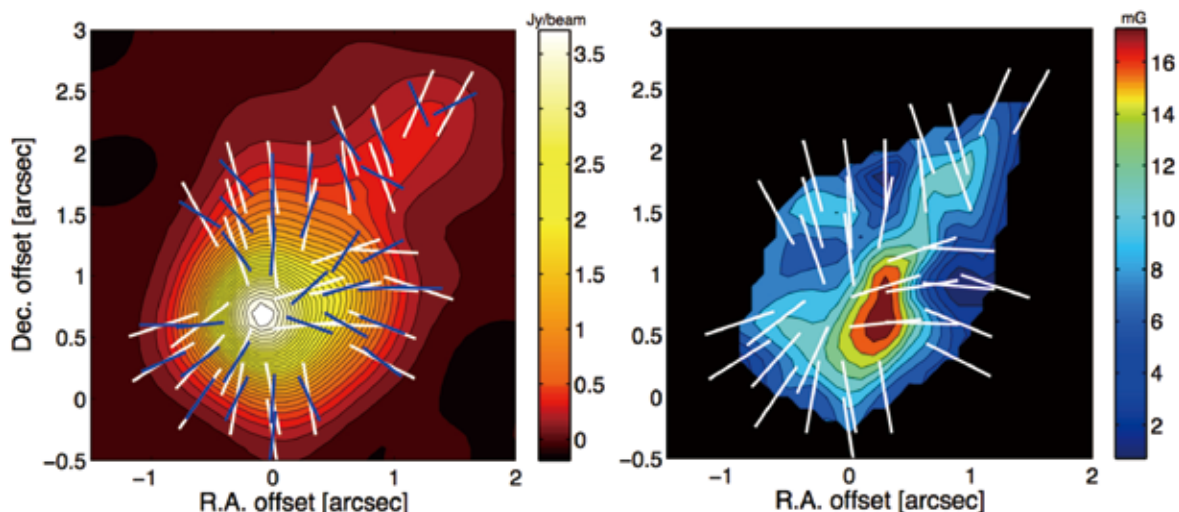


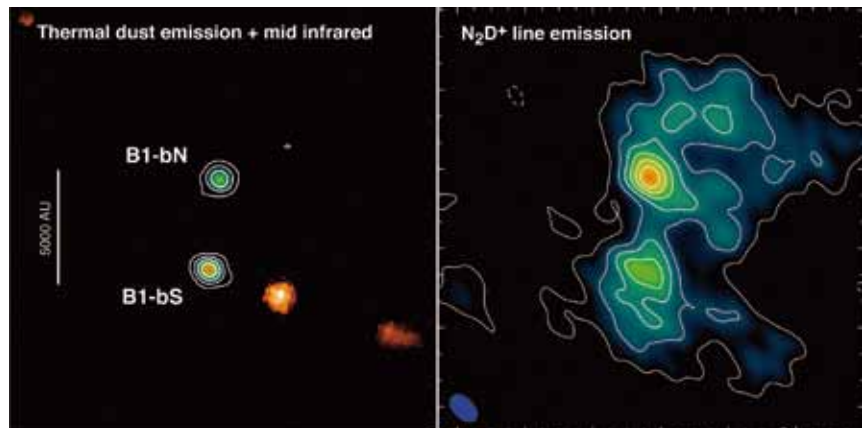
Figure 1. Left panel: SMA dust continuum observation at 345 GHz of the star-forming core W51 e2. The color-wedge indicates the dust emission intensity. The measured magnetic field morphology (white segments) shows that gravity is bending the field lines almost radially and pulling them toward the core center. Overlaid in blue are the intensity gradients of the dust emission. The correlation between field and intensity gradient orientations is used to derive the field strength. Right panel: resulting field strength map for W51 e2. An increase in field strength toward the center is apparent. (Picture Credit: Ya-Wen Tang)



## Earliest Stage of Star Formation

A dense molecular cloud core, Barnard 1b (B1-b), in the Perseus molecular cloud complex harbors two submillimeter sources. These two sources, labeled B1-bN and B1-bS, are clearly seen in the thermal dust emission at 1.1 mm observed with the SMA, but not seen in the mid-infrared image observed by the Spitzer Space Telescope (see the left panel of Figure 2). This indicates that these two sources are very cold and observable only at wavelengths longer than the far-infrared. Both B1-bN and B1-bS are colder and fainter than most of the known protostellar sources, suggesting that they are in the very early stage of protostellar evolution. The two sources are also bright in line emission from the  $\text{N}_2\text{D}^+$  molecule, which is a deuterated species of the  $\text{N}_2\text{H}^+$  molecule (the right panel of Figure 2). It is found that the  $\text{N}_2\text{D}^+/\text{N}_2\text{H}^+$  ratio in these two sources is extremely high,  $\sim 0.2$ , which is 4 orders of magnitude larger than the D/H ratio of  $10^{-5}$  in interstellar space. Such a high  $\text{N}_2\text{D}^+/\text{N}_2\text{H}^+$  ratio is also typical in the earliest stage of protostellar evolution. The physical and chemical properties suggest that B1-bN and B1-bS are promising candidates for the "first hydrostatic cores" to be formed at the beginning of the star formation process. (Huang & Hirano 2013, ApJ, 766, 131)

Figure 2. Two submillimeter sources in the B1-b molecular cloud core. Left panel: thermal dust emission at 1.1 mm observed with the SMA (white contours) on top of the mid-IR image taken with the Spitzer Space Telescope (color image). Right panel:  $\text{N}_2\text{D}^+$  emission line observed with the SMA and the Submillimeter Telescope of Arizona Radio Observatory (SMT).



## Disk and Jet Systems

HH 212 is a very young star-forming region, with the central forming star (protostar) being about 36 thousand years old and having a mass of about 0.2 solar mass. It is in Orion at a distance of about 1300 light-years away. We mapped it with ALMA and found that the core material there does not fall directly onto the protostar, but through first a flattened tenuous structure called a "pseudo-disk" and then a dense Keplerian rotating disk (the left panel of Figure 3). This result is consistent with the current collapse model of a magnetized rotating core (the right panel of Figure 3), where the formation of the pseudo-disk (brown) and Keplerian disk (dark brown) are due to a combined effect of the magnetic fields and angular momentum. An accretion shock is formed at the interface between the pseudo-disk and Keplerian disk, turning the pseudo-disk into the Keplerian disk. Interestingly, the protostar also ejects mass into the interstellar medium in the form of a highly collimated and supersonic bipolar jet (the left panel of Figure 3). The jet seems to carry away excess angular momentum from the innermost part of the Keplerian disk, allowing the disk material to fall onto the protostar.

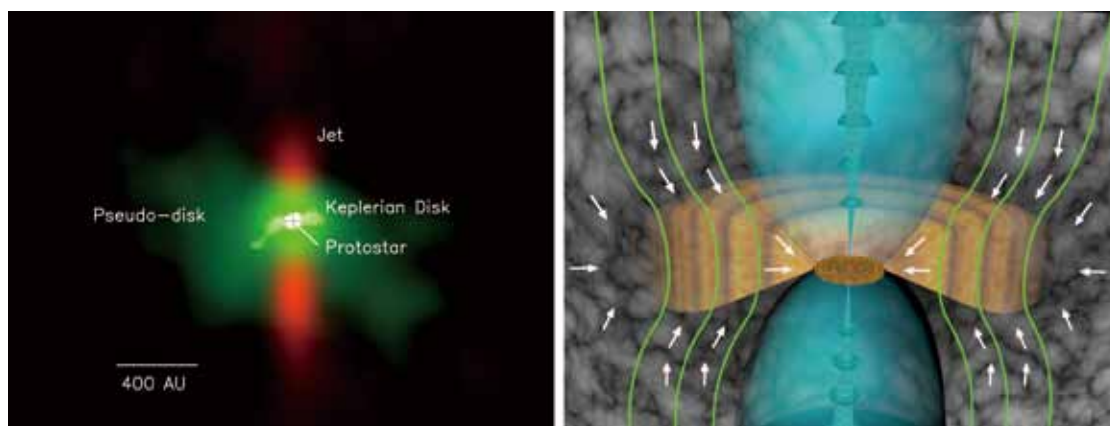


Figure 3: Left panel: ALMA composite image of HH 212, showing a pseudo-disk (green) and a Keplerian disk (bright green) in dust continuum, and a bipolar jet in  $\text{HCO}^+$  gas (red). (Lee et al. 2014) Right panel: An artist's conception showing the pseudo-disk (brown), Keplerian rotating disk (dark brown), and bipolar jet in a collapsing model of a magnetized rotating core. Green lines are magnetic fields. Arrows indicate gas motion. Credit: Change Tsai (ASIAA).

## ALMA Observation of Gas Spirals as a Nursery of Binary Stars

More than half of stars with a mass similar to that of the Sun are known to be binaries (Raghavan et al. 2010). It is thus crucial to unveil the physical mechanism of binary formation observationally to obtain more comprehensive understanding of star formation. We have observed the protostellar binary L1551 NE with ALMA in dust-continuum emission at a 0.9-mm wavelength, a tracer of the distribution of interstellar materials, and carbon monoxide molecular emission, which can be used to study gas motion with the Doppler Effect. The 0.9-mm ALMA image shown in Figure 4 (the left panel) exhibits a component associated with each binary star (the two central components), and a disk surrounding both stars, a circumbinary disk, with a radius of 300 AU. The circumbinary disk consists of a southern U-shaped feature and northern emission protrusions pointing to the northwest and the northeast.

To understand these features around the protostellar binary, we conducted a supercomputer numerical simulation of binary formation in L1551 NE (the right panel of Figure 4). The observed southern U-shaped feature and northern emission protrusions are reproduced with a pair of spiral arms stemming from each star. We also investigated the gas motion as seen in the ALMA observation of carbon monoxide molecular emission, and identified faster rotating motions in the spiral arms and slower rotating motions in the inter-arm regions. The inter-arm regions also exhibit an infalling gas motion toward the central binary stars, namely, the ongoing feeding process of the materials to the binary. These gas motions are consistent with those predicted by our numerical simulation, and our ALMA observation has unveiled the ongoing process of the growth of the binary stars (Takakuwa et al. 2014).

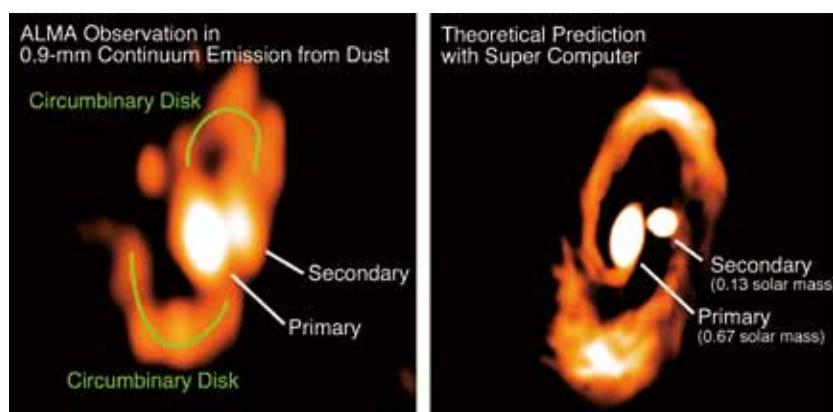


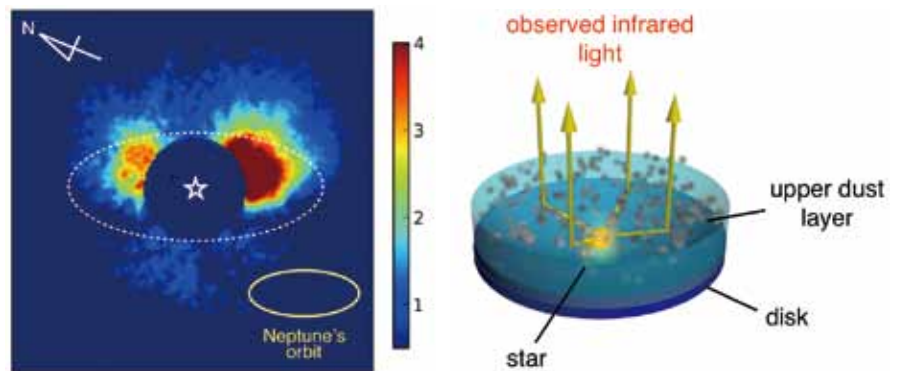
Figure 4. 0.9-mm dust-continuum image of the protostellar binary L1551 NE observed with ALMA (left), and that predicted from our supercomputer numerical simulation (right). Green curves in the left panel traces the observed structures of the circumbinary disk.

## Proto-Planetary Disks

Near the end of star formation, circumstellar disks evolve to proto-planetary disks where planets are formed. Planet formation, an exciting and active area for astronomical research, has long fascinated many scientists. From the Strategic Explorations of Exoplanets and Disks with the Subaru (SEEDS) project, Takami et al. (2013) unprecedentedly found a layer of dust almost transparent in the near infrared sitting above the protoplanetary disk around RY Tau (the left panel of Figure 5). This finding, achieved by comparing observations and simulations, has brought significant insights to planet evolution theories.

The star is about 460 light years away from Earth in the constellation Taurus and is about half a million years old. The dust layer could be a remnant of the dust that fell onto the star and the disk during earlier stages of planet formation (see the right panel of Figure 5). It may act as a special blanket to warm the interior of the disk for baby planets born therein. This may affect the number, size, and composition of the planets born in this system. Therefore, this may be one of the key features for understanding how a variety of exoplanetary systems exist. (Takami et al. 2013, ApJ, 772, 145)

Figure 5. Left panel: an image in the near infrared ( $1.65\ \mu\text{m}$ ) around RY Tau, observed using the HiCIAO coronagraph of the Subaru Telescope. This type of observation is preferred for faint emissions associated with scattered light around planet-forming disks, as there is less light from the much brighter star. A coronagraphic mask in the telescope optics blocks the central star, with its position marked at the center. A white ellipse shows the position of the midplane of the disk. Scattered light observed in the near infrared is offset to the top of the image compared with the disk. Right panel: schematic view of the observed infrared light. The light from the star is scattered in the upper dust layer, which leads to the offset of the observed light from the midplane.



## Complex Molecules in Protoplanetary Disks

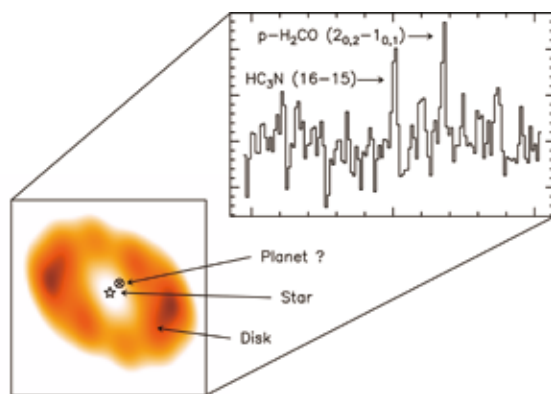


Figure 6. Top: the spectra of  $\text{HC}_3\text{N}$  and  $\text{H}_2\text{CO}$  towards LkCa15 in the  $3.5''$  beam of the IRAM interferometer. Bottom: the  $0.5''$  image of the  $1.3\ \text{mm}$  thermal dust emission from the circumstellar disk of LkCa15. (Picture Credit: Vincent Piétu)

Protoplanetary disks are the birthplaces of planets, and a study of their structure and content will shed light on the origin of planets. Using the IRAM facilities (30 m telescope and Plateau de Bure Interferometer), Chapillon et al. (2012) detected for the first time the molecule of cyanoacetylene ( $\text{HC}_3\text{N}$ ) in the disks around Sun-like stars, e.g., LkCa15 and GO Tau. Here LkCa15 already shows a cavity in the disk (the bottom panel of Figure 6) that could be attributed to the presence of a Jupiter-like planet recently detected in the infrared.  $\text{HC}_3\text{N}$  is so far the heaviest and most complex molecule detected in protoplanetary



disks. It is the simplest form of cyanopolyne, and it is one of the elementary building blocks leading to the formation of organic molecules, and, perhaps, to the emergence of life. Disk chemistry models show that  $\text{HC}_3\text{N}$  is mainly formed on the grain surface in the cold regions near the disk mid-plane. In such cold regions, the "simple" molecules like CO and  $\text{H}_2\text{O}$  are frozen onto the ice mantle of the grains. These molecules can react in the mantle to form more complex species. The newly formed molecule can then be released in the gas-phase, thanks to desorption mechanisms (induced by ultraviolet radiation or cosmic rays). The observation of  $\text{HC}_3\text{N}$  in the planet forming regions is thus an important first step toward an understanding of the origin of molecular complexity, and thus life, on Earth and on exoplanets. (Chapillon et al. 2012, ApJ, 756, 58)

## Formation of Massive Stars in Extreme Environment

The molecular gas in the central 10 pc area around the Galactic supermassive black hole has a high temperature. In addition, the molecular gas structures in this region are subject to strong levels of turbulence, strong magnetic fields, and strong tidal forces, which are all adverse to the self-gravitational collapse to form stars. How high-mass stars form in such an extreme environment has been one of the most intriguing issues in astrophysics. Liu et al. (2013) combined the 157 fields mosaic observations of the Submillimeter Array and the archival James Clerk Maxwell Telescope 15 m telescope observations to yield the first interferometric 0.86 mm dust continuum image for this region, with an unprecedented high angular resolution and large field of view (Figure 7). The dust continuum emission at this wavelength is the most promising tracer of the molecular gas mass. From this image, candidates of gas reservoirs were identified for feeding the young high-mass stars. They found these localized gas structures might be extreme cases of highly pressurized cores, which is in contrast to the virialized self-gravitating cores in normal star-forming regions. (Liu et al. 2013, ApJ, 770, 44)

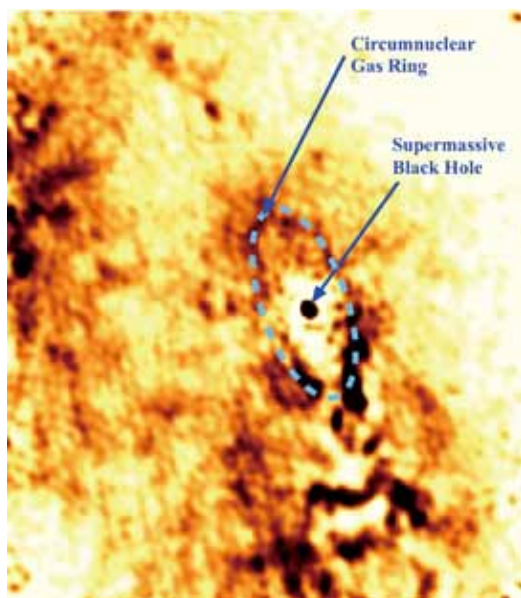


Figure 7. Dust distribution around the Galactic center, as observed in 0.86 mm continuum with the SMA and the JCMT.

# The Interstellar and Circumstellar Medium (ICSM)

The Interstellar and Circumstellar Medium group at ASIAA uses state of the art observing facilities to study the life cycle of matter in our own Milky Way and external galaxies. Group members work on star formation, stars and stellar ejecta, and the interstellar medium itself, probing all the steps in the life cycle of baryonic matter in the Universe. Of particular interest are the Small and Large Magellanic Clouds. These nearby irregular galaxies offer a bird's eye view of an entire galaxy, but also allow for sufficient detail to study individual galaxy components. Moreover, their relatively unpolluted interstellar composition makes them excellent analogs for galaxies at the peak of star formation in the history of the Universe.

## Evolution of Dust Abundance in Galaxies

The properties of interstellar dust in galaxies depend on the physical conditions, and can vary from one galaxy to the next. The evolution of dust abundance relative to the total gas content was calculated in theoretical models (see Kuo & Hirashita 2012, MNRAS, 432, 637). Two cases, without and with small ( $< 0.1 \mu\text{m}$ ) dust grains were examined. Without small grains (i.e. only with large grains), the dust abundance increases rapidly in the later phase (the blue line of Figure 1). This model cannot explain the observationally acceptable range (blue box) for the distant quasars. With small grains, the rapid increase of the dust abundance occurs earlier.

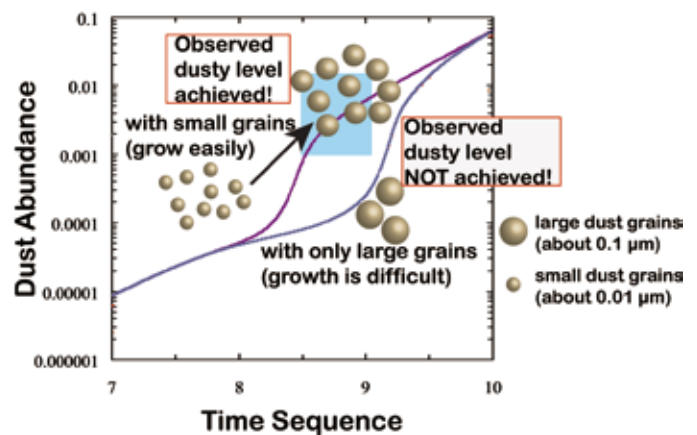


Figure 1. The evolution of dust abundance relative to the total gas. The horizontal axis shows the time sequence (precisely, the oxygen abundance  $12 + \log(\text{O}/\text{H})$ ). The vertical axis shows the dust abundance (dust-to-gas ratio). The purple and blue curves show the model with and without small grains, respectively. (Picture Credit: Hiroyuki Hirashita)

## Molecular Hydrogen, PAH, and Ionized Line Emission from the Interstellar Environments in the Large Magellanic Cloud

Massive stars end their lives in an explosive fashion, in the form of a supernova, leaving behind a supernova remnant (SNR) in the form of a cloud of gas and dust. N49 in the Large Magellanic Cloud (LMC) is such a SNR. The emission in three important tracers of the physical conditions peaks in the eastern region (Figure 2), although the emission peaks do not align perfectly. UV radiation can ionize gas in the SNR, which is traced by the Bra emission map, while the  $\text{H}_2$  map shows the location of UV-illuminated molecular hydrogen. The polycyclic aromatic hydrocarbons (PAHs) are complex pre-biotic molecules that are ubiquitous in the interstellar medium, and also require UV illumination to be observable, but are far more robust than hydrogen molecules. Both the  $\text{H}_2$  and PAH emission exceed the Bra boundary, at the northeastern part of the region, which is at the center of an interacting molecular cloud. The two clumps of the PAH emission in the south (white crosses) could be seen at the coincident positions in the  $\text{H}_2$  map. Thus, the PAH emission can be associated with either the ionic gas or the molecular gas. Although PAHs can survive a slow shock, detectable PAH emission may not arise due to the lack of UV radiation in certain conditions. For PAHs to exist and radiate in SNRs, an ambient dense medium and a sufficient heating source around the medium are most likely required. (Seok, Koo, & Onaka 2012, ApJ, 744, 160)

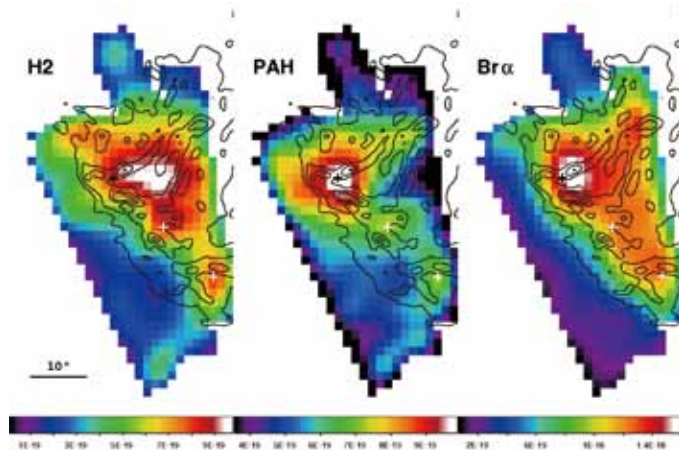


Figure 2.  $H_2$  1-0  $O(3)$ , PAH, and  $Br\alpha$  line maps of N49 by using the AKARI / IRC spectra. For comparison, contours (black) are taken from an  $H\alpha$  image of the HST / WFPC2 (Bilikova et al. 2007). The black cross marks the peak of the PAH emission at  $(\alpha 2000, \delta 2000) = (05h26m05.s14, -66d05' 03'')$ . The white crosses denote two clumps seen in the PAH line map. The scale bar represents  $10''$  or 2.4 pc at 50 kpc. The color bars are given in units of  $W m^{-2} arcsec^{-2}$ . North is up and east is to the left.

## The Dust Input from Evolved Stars to the Interstellar Medium of the Magellanic Clouds

Post-main sequence stars drive the evolution of the interstellar medium in galaxies, as they eject the products of nucleosynthesis processes, in the form of gas, or condensed into micron-sized dust grains. The SAGE survey of the Magellanic Clouds allows for a complete census of the dust production by these evolved stars, as it mapped both the Large and Small Magellanic Clouds in the infrared using the Spitzer and Herschel Space Telescopes. At infrared wavelengths the dusty eject from evolved stars are readily observed by their thermal radiation. Figure 3 presents the cumulative evolved-star dust production rate for the LMC, obtained by measuring the dust production rate for tens of thousands of evolved stars using pre-computed models, which allow for distinguishing the chemistry

(O-rich or C-rich) at the same time (Srinivasan et al. 2011). The figure shows that O-rich sources contribute most of the dust at low dust production rates, while the highly evolved, extremely dusty population is found to predominantly contain carbon stars. This means that there is 2.5 times as much carbon dust as silicate (oxygen-rich) dust being ejected into the interstellar medium of the LMC. A similar study for the Small Magellanic Cloud is in progress (Srinivasan et al. 2014).

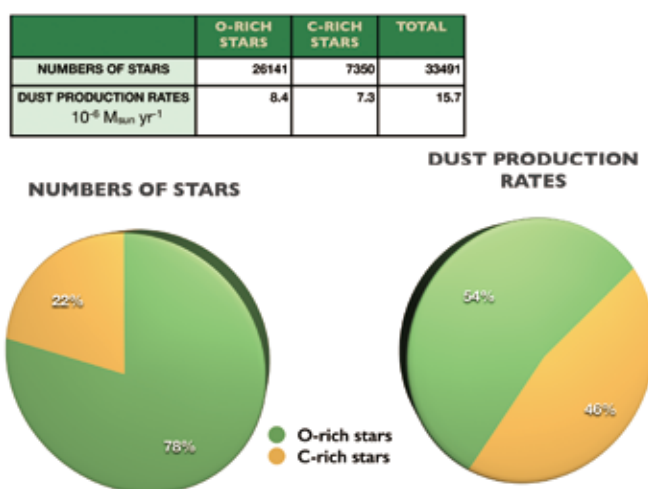


Figure 3. The cumulative dust production rate from the entire population of red supergiant (RSG) and asymptotic giant branch (AGB) stars in the LMC. (Picture Credit: Sundar Srinivasan)

## Clumpiness and Transient Clumps in Starless Cores

Star formation occurs in dense molecular cores. High-angular resolution observations of LDN 673 show that these cores can be clumpier at smaller scales, and that some of these clumps can also be unbound or transient. The dust continuum in LDN 673 shows four condensations (see Figure 4), three of them centrally peaked, coinciding with previously identified SCUBA sub-millimeter sources (Visser et al. 2002), but it does not recover all the clumps detected with the BIMA telescope (Morata et al. 2003, 2005).

The white crosses in the figure indicate the positions of what we had identified as clump and inter-clump gas. The combination of the available spectral and continuum data and its comparison with the results of



chemical models confirms that the denser clump ( $3 \times 10^6 \text{ cm}^{-3}$ ) of the region is also the more chemically evolved, and it could still undergo further fragmentation (Morata et al. 2012). The inter-clump medium positions are denser than previously expected ( $10^3\text{--}10^4 \text{ cm}^{-3}$ ) and are chemically young, similar to the gas in the lower density clump position, by a factor of 2-3 within the uncertainties. The density contrast between these positions and their general young chemical age seems to support the existence of transient clumps in the lower density material of the core.

## Chemical Abundances in Hot Subdwarf B Stars

Hot sub-dwarf stars, which are found to be helium-main sequence or extended horizontal branch stars of approximately half a solar mass, are the most extreme chemically peculiar stars in our Galaxy. Figure 5 summarizes the measured chemical abundances in hot subdwarf stars relative to solar values. Two helium-rich hot subdwarfs, HE 2359-2844 and HE 1256-2738, show absorption lines due to triply ionized lead which have never previously been detected in any star. The abundance of lead measured using these lines is nearly 10,000 times that measured in the Sun. These heavy-metal stars are a crucial link between bright red giant stars which are thirty or forty times the size of the Sun, and faint blue subdwarf stars which are one fifth the size, but seven times hotter and seventy times brighter than the Sun. A few red giants lose their thick hydrogen skin and shrink to become hot subdwarfs, or nearly-naked helium stars. As they shrink, conditions become favourable for the radiation pressure to act on individual atoms to sort the elements into separate layers, where they are concentrated by a factor of 10,000 or more.

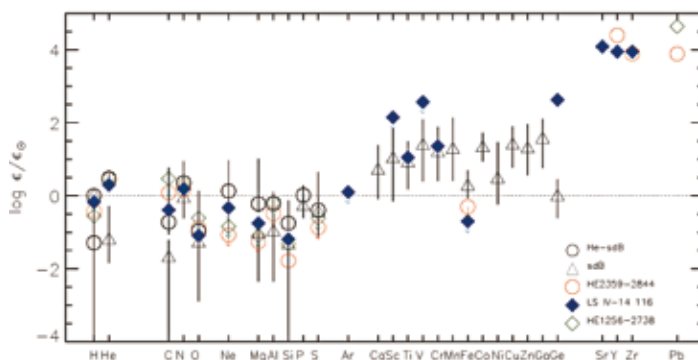


Figure 5. Elemental abundances for hot subdwarf stars relative to solar values. Abundances for helium-rich subdwarfs and helium deficient normal subdwarfs are indicated by a mean (symbol) and range (line). The most heavy metal-rich stars in the Galaxy, HE 2359-2844 and HE 1256-2738 are shown in separate symbols. (Picture Credit: Neelamkodan Naslim)

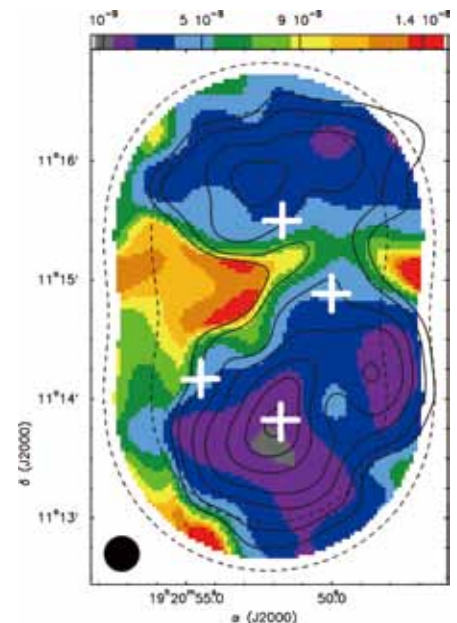


Figure 4. Map of the abundance of the CS molecule from the combined Berkley Illinois Maryland Association (BIMA) interferometer and the Five College Radio Astronomy Observatory (FCRAO) 14 m telescope observations, overlapped with the contour map of the Institut de Radioastronomie Millimétrique (IRAM) 30 m 1.2 mm continuum emission in LDN 673. The angular resolution of both images is  $25''$ . The inner and outer dashed lines show the 0.5 and 0.25 level of the BIMA primary beam response. The white crosses show the four positions observed with the IRAM 30 m telescope, identified as clump and interclump regions.

## Discovery of $C_{60}$ in Galactic Planetary Nebulae

Buckminsterfullerene,  $C_{60}$ , was first discovered in 1985 in the laboratory by Harry Kroto and collaborators, who were performing experiments to mimic interstellar conditions. Despite the expectation that this molecule would form in interstellar space, it took until 2010 when it was actually discovered in a Planetary Nebula (see Figure 6). Planetary Nebulae are the evolutionary end-stages of Solar-type stars, and depending on the initial mass and chemical composition, these stars can develop highly carbon-rich atmospheres. Carbon-rich planetary nebulae show a very interesting chemistry not seen elsewhere

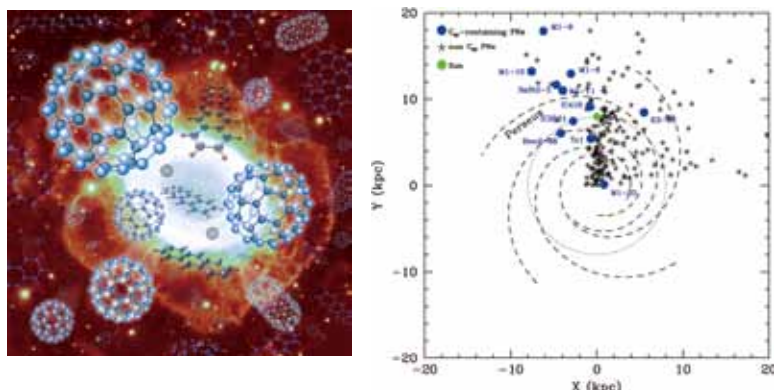


Figure 6. Left panel: Artist impression of fullerenes in front of a planetary nebulae. Recently, these complex molecules ( $C_{60}$ ,  $C_{70}$ , and other species), with a shape similar to soccer balls, have been discovered in space, after their existence was predicted in the 1980s, and current research reveals their presence in more and more environments. Right panel: the location of the  $C_{60}$  containing Planetary Nebulae (blue symbols) in the Milky Way. The location of the Sun is given by a green circle, and the dotted line shows the Solar Circle, e.g. the circle that connects all points with the same distance to the Galactic Centre as the Sun. The dashed lines indicate the approximate location of the spiral arms in the Milky Way. (Picture Credit: NAOJ; Masaaki Otsuka)

in the Universe, and it is in this chemistry that  $C_{60}$  can form. After the initial discovery, several research groups, including the ICSM group at ASIAA, set up to search for this enigmatic molecule in carbon-rich environments. In 2012, a team led by an ASIAA researcher reported the discovery of  $C_{60}$  in M1-11, a very well-characterized Planetary Nebula (Otsuka et al. 2012, ApJ 764, 77), followed by the detection of  $C_{60}$  in a further ten Galactic Planetary Nebulae (Otsuka et al. 2014, MNRAS 437, 2577), predominately located away from the Galactic Center (see Figure 6, right). This discovery should help in gaining understanding how  $C_{60}$ , consisting of 60 carbon atoms and shaped like a soccer ball, should form, and how it is related to other carbonaceous species, such as PAHs and, more speculatively, the building blocks of life.

## Evidence of a Binary-Induced Spiral from an Incomplete Ring Pattern of CIT 6

With the advent of high-resolution high-sensitivity observations, spiral patterns have been revealed around several AGB stars. Such patterns can provide possible evidence for the existence of central binary stars embedded in outflowing circumstellar envelopes. It is suggested that the previously observed incomplete ring-like patterns can be explained with a spiral-shell structure due to the motion of (unknown) binary components viewed at an inclination with respect to the orbital plane. Kim et al. (2013, ApJ, 776, 86) describe a method of extracting such spiral-shells from an incomplete ring-like pattern to place constraints on the characteristics of the central binary stars. The use of gas kinematics is essential in facilitating a detailed modeling for the three-dimensional structure of the circumstellar pattern. It is shown that a hydrodynamic radiative transfer model can reproduce the structure of the  $HC_3N$  molecular line emission of the extreme carbon star, CIT 6 (see Figure 7). This method can be applied to other sources in the AGB phase and to the outer ring-like patterns of pre-planetary nebulae for probing the existence of embedded binary stars. Such structures are highly anticipated with future observations using ALMA.

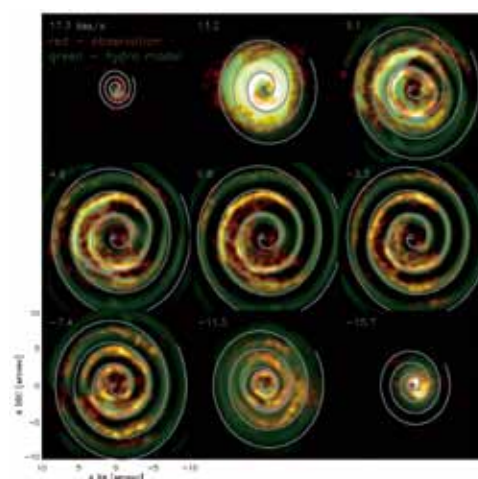


Figure 7. A spiral-shell model due to a binary orbital motion by a hydrodynamic radiative transfer simulation (green; Kim et al. 2013) for an  $HC_3N$  molecular line emission of CIT 6 observed with the Very Large Array (red; Claussen et al. 2011). A simple analytic model is drawn by a gray solid line in each channel.

# High Energy Astrophysics

Current research activities of the group involve studies of the various cosmic phenomena associated with compact objects (i.e., black holes, neutron stars, and white dwarfs). Of interest to many research groups at ASIAA is the nature of flows in the vicinity of black holes in binary star systems and supermassive black holes in the centers of galaxies. As a result, members of the high energy astrophysics group study the nature of flows in an accretion disk, where a fraction of matter is accreted and a fraction of matter is ejected either via a relativistic moving jet of gas or an outflowing wind. Other areas of interest center on the formation of neutron stars and black holes in binary star systems, and the emission mechanisms of high energy radiation from isolated magnetized rotating neutron stars (known as pulsars) and the interaction of pulsar winds with a stellar wind from a companion star in a binary system. Similarly, the nature of high energy emission at gamma-ray and GeV energies, unexpectedly discovered, in recurrent novae and classical novae arising from thermonuclear outbursts from mass accreting white dwarfs in close binary star systems is also under investigation.

Spectral studies of active galactic nuclei (AGN) containing supermassive black holes provide insight into the geometry and nature of accretion flows in these systems. A disk corona evaporation model has been investigated, which provides a physical mechanism for explaining many observational phenomena in low luminosity AGN (LLAGN). In this model, evaporation leads to the formation of an optically thin inner disk and truncation of an optically thick outer disk. Such a model naturally accounts for the soft spectrum at high luminosities and a hard spectrum at low luminosities for high luminosity AGN and LLAGN respectively (for example, see Figure 1). Recently, the disk evaporation model was generalized to include the effect of a magnetic field. The critical transition mass accretion rate for which the disk is truncated is found to be insensitive to magnetic effects, but its inclusion leads to a smaller truncation radius in comparison to a model without its consideration. Based on these results, the truncation radii inferred from spectral fits of LLAGN published in the literature are found to be consistent with the disk evaporation model. The infrared thermal emission arising from the truncated geometrically thin accretion disks may be responsible for the red bump seen in such LLAGN.

Additional theoretical models for accretion disks surrounding black holes are under investigation examining the intrinsic differences between stellar mass black hole X-ray binary systems from the supermassive black holes in AGN. Of particular interest is the thermal state of the gas fueling the black hole. In the stellar context, the gas is cool as it originates from the photosphere of its companion. On the other hand, the gas in the central regions of galaxies can also have a hot component, which leads to the accretion not only of molecular gas, but also of coronal gas. Hence, the ratio of these two components, coupled with the disk evaporation/condensation model, will reveal differences in the spectrum and luminosity profile of such disks.

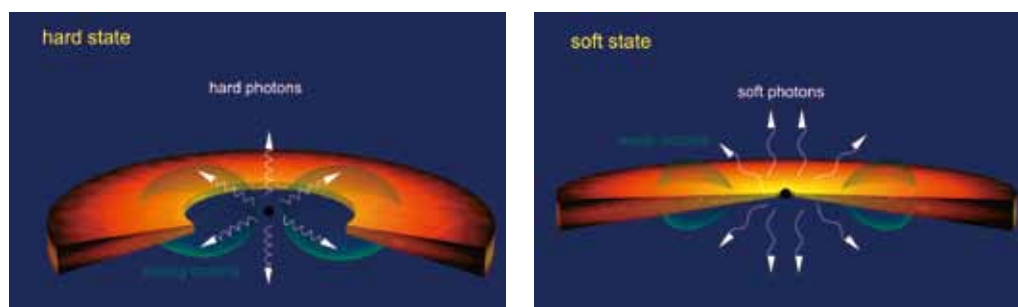


Figure 1. Accretion geometry of disks for LLAGN (left panel) and high luminosity AGN (right panel) corresponding to low and high rates of mass accretion, respectively. (Picture Credit: Ronald Taam & Yin-Chih Tsai)



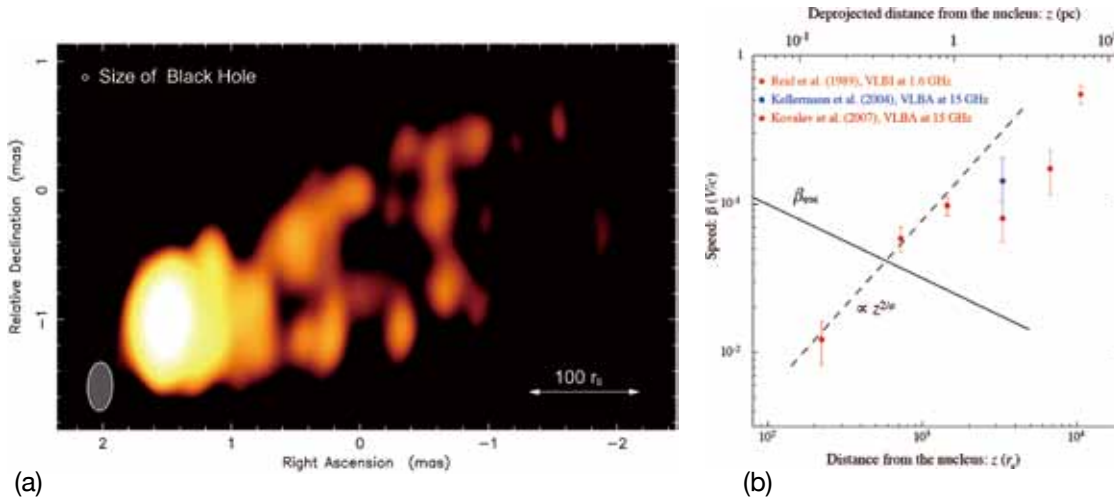


Figure 2. Left panel: VLBA total intensity map of the M87 jet at 43 GHz (2-a), showing the synchrotron radiation of relativistic electrons. A hollow, edge-brightened emission of the jet up to  $\sim 500 r_s$  is clearly seen. A small circle indicates the size of the black hole shadow, which the GLT project is seeking to resolve with future sub-mm VLBI observations. Right panel: Distribution of the bulk velocity relative to the speed of light is shown as a function of the de-projected distance (normalized by  $r_s$ ) from the core of the relativistic jet from M87. The dashed line represents the velocity scaling based on the conservation of energy flux density of the torsional Alfvén waves under the WKB approximation, and the solid line denotes the escape speed along the jet parabolic streamline (Nakamura & Asada 2013, *ApJ*, 775, 118).

It is generally believed that relativistic jets can be emitted close to the event horizon of a black hole. By analyzing observational results at high angular resolution obtained with Very Long Baseline Interferometry (VLBI), the relativistic jet in the nearby AGN, M87, was studied on the scale of 100–1,000 Schwarzschild radius  $r_s$  (Figure 2a). Specifically, an approximate Hugoniot relation for the parabolic magnetohydrodynamic nozzle was derived. This relation is identical to the case of a hydrodynamic solar wind with the thermal pressure substituted by the magnetic pressure. The cross point between the solid and dashed lines (see Figure 2b) corresponds to the fast magnetosonic point. It is suggested that the nature of the trans-fast magnetosonic jet in a parabolic magnetohydrodynamic nozzle, which is powered by torsional Alfvén waves, is similar to the transonic solution of the solar wind. The hoop stress differentially bunches the poloidal magnetic flux toward the central axis so that a rapid expansion of the cross sectional area of the poloidal magnetic flux operates on the hollow parabolic magnetohydrodynamic stream in a manner similar to a de Laval-like diverging nozzle effect in the super fast magnetosonic regime.

Pulsars were discovered more than 45 years ago and are now believed to be rapidly rotating, highly magnetized neutron stars. Within the magnetosphere, electrons and positrons are created and accelerated into ultra-relativistic energies and emit copious radiation from radio to gamma-ray wavelengths, being powered by the spin-down of the neutron star. Until now, over 2,300 rotation-powered pulsars have been listed in the radio band, several pulsars in the optical band, and about 100 in X-rays. In the high-energy gamma-ray domain (between 100 megaelectronvolt and 20 gigaelectronvolt), the Fermi Gamma-ray Space Telescope has detected more than 100 isolated, rotation-powered pulsars. Moreover, in the very-high-energy domain (above 20 gigaelectronvolt), Very Energetic Radiation Imaging Telescope Array System (VERITAS), and Major Atmospheric Gamma-ray Imaging Cherenkov Telescope (MAGIC) ground-based observatories have detected pulsed signals from the Crab pulsar up to 400 GeV. Since interpreting gamma-rays should be less ambiguous compared with reprocessed, lower-energy emissions, the gamma-ray pulsations observed from these objects are particularly important as a direct signature of basic energetic processes, such as the particle acceleration and the resultant photon emissions, that are taking place in pulsar magnetospheres.

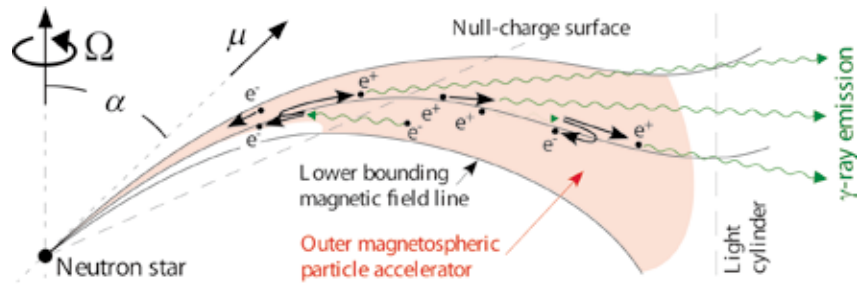


Figure 3. Schematic picture (side view) of a pulsar magnetosphere. The filled circle on the left denotes the neutron star, which rotates along the vertical axis (dash-dotted line). The magnetic dipole axis (short dashed line) is inclined to the rotation axis. The solid curves designate the magnetic field lines. In the convex side of (i.e., above) the lower bounding magnetic field line, a high vacuum is maintained, because charged particles efficiently escape across the light cylinder (vertical long dashed line on the right). As a result, an electric field arises along the local magnetic field lines in the outer gap (red, shaded region), because the high vacuum fails to screen the electric field along the magnetic field line once it arises. In this outer gap, electrons ( $e^-$ ) and positrons ( $e^+$ ) are created by photon-photon collisions and accelerated by the magnetic-field-aligned electric field in the opposite directions along the magnetic field lines. Gamma-rays are emitted mostly outwards by the out-going particles ( $e^+$ ). The gamma-ray luminosity is essentially determined by the trans-magnetic-field (i.e., meridional) thickness of the accelerator, which is, in turn, controlled by the efficiency of the photon-photon collisions that take place within the particle accelerator. (Picture Credit: Kouichi Hirotani)

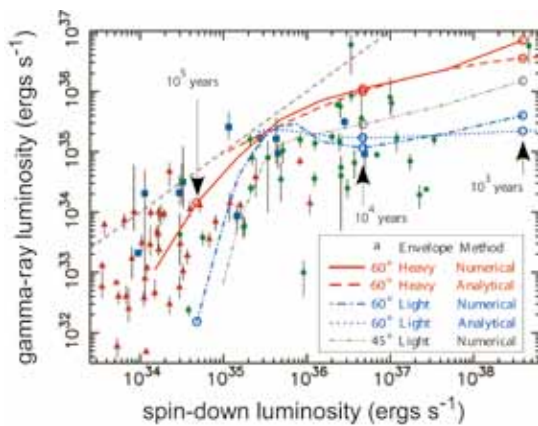


Figure 4. Luminosity evolution of pulsar outer gaps as a function of neutron star spin down luminosity. Two extreme chemical compositions of the neutron star envelopes are considered. The red curves correspond to a heavy element (e.g., Fe, Co, or Ni) envelope, while the blue and black curves correspond to a light element (e.g., H, He, C, N, O) envelope. The actual composition may differ from pulsar to pulsar, and is subject to the amount and the chemical composition of the neutron-star atmosphere. The solid, dash-dotted, and dash-dot-dot-dot curves represent numerical solutions, while dashed and dotted ones represent analytical solutions. The solution evolves from the top right to the bottom left along each curve, as the neutron star spins down (i.e., as the spin-down luminosity reduces). The circles, squares, and triangles designate the pulsars detected by the Fermi satellite: the green filled circles show the radio loud gamma-ray pulsars, while the blue filled squares show the radio quiet ones (Hirotani 2013, ApJ, 766, 98).

The light curves and the spectra obtained from the Crab and other pulsars suggest that the gamma-rays are emitted from the higher altitudes in a rotating magnetosphere, typically a few tens (to more than one hundred times) of neutron-star radius away from the stellar surface. Therefore, the nature of such pulsar emissions has been examined with particular attention focused on the outer-magnetospheric particle-accelerator model, which is also referred to as “the outer-gap model” (see Figure 3). In classic outer-gap models, they have assumed the spatial distribution of the acceleration electric field and the number density of the created, and radiating particles to calculate the pulsar gamma-ray emission properties. Nevertheless, such quantities were solved from the set of basic equations (specifically, one of the Maxwell equations and the Boltzmann equations for particles and photons) in Hirotani (2013, ApJ, 766, 98) for the first time. In this modern outer-gap model, the evolution of the trans-magnetic-field thickness of the accelerator is determined as a function of the pulsar age from the requirement that the outer gap should be self-sustained by photon-photon pair productions. Figure 4 shows how the luminosity of a pulsar evolves as the neutron star spins down. Since the heat conduction is less efficient when the neutron star envelope (within 100 m depth below the surface) contains little light elements (e.g., when the iron envelope contains negligible hydrogen), the surface temperature becomes lower for a heavy element envelope (solid and dashed red curves), compared to a light element one (dash-dotted and dotted blue curves). The observed luminosity scatters around the solutions (i.e., the curves), because the actual composition will reside between the two extreme cases of heavy and light elements, and because our line of sight takes a random viewing angle with respect to the pulsar rotation axis, where the gamma-ray flux in each direction depends on the viewing angle. It follows from Figure 4 that the gamma-ray luminosity is roughly proportional to the square root of the spin down luminosity, the interpretation of which has been a long standing issue in high-energy pulsar astrophysics.

# Cosmology

## Dark Matter Distribution in and around Galaxy Clusters

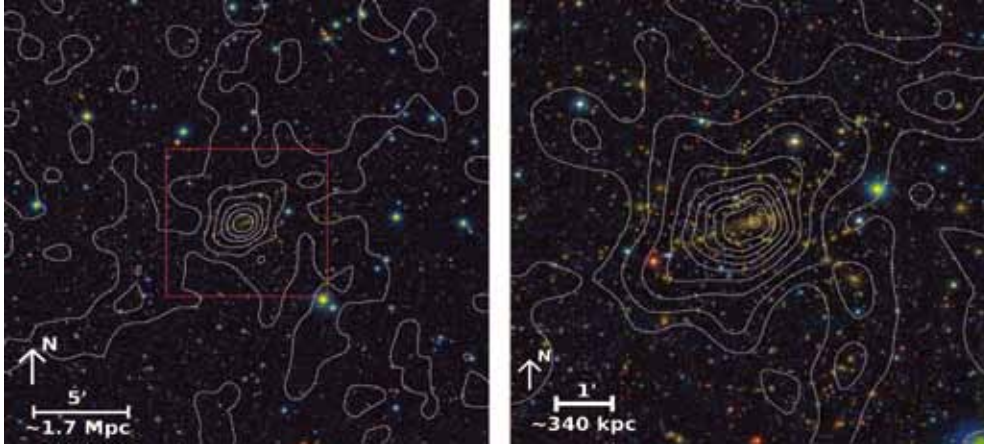


Figure 1. Subaru BVRiz composite color images centered on the galaxy cluster MACS1206, overlaid with mass contours from our joint strong-and-weak lensing analysis of HST and Subaru observations. The image size in the left panel is 24 arcminutes ( $\sim 8$  Mpc) on a side. The cluster is fairly centrally concentrated in projection, and associated with an elongated large scale structure running north-west south-east, both in the projected mass and galaxy distributions (Umetsu et al. 2012, ApJ, 755, 56; Umetsu 2013, ApJ, 769, 13).

The nature of dark matter remains unknown despite much tighter constraints on the traditional thermal relic candidates in the TeV energy scale implied by supersymmetry, an extension to the Standard Model which predicts a symmetry between fermions and bosons. This is puzzling given the need for cold dark matter (CDM) to explain the statistics of large scale structure and of the cosmic microwave background (CMB). Galaxy clusters are the largest self-gravitating systems in the universe, and thus contain a wealth of cosmological information. Clusters, by virtue of their enormous mass, can serve as giant physics laboratories for astronomers to test the role and nature of dark matter that dominates the material universe, physics governing the final state of self-gravitating collisionless systems in an expanding universe, and possible modifications of the law of gravity.

The distribution of dark matter in and around the galaxy cluster MACS J1206.2-0847 (MACS1206) has been mapped by a joint strong-and-weak gravitational lensing analysis with 16-band Hubble Space Telescope and wide-field Subaru imaging observations (Umetsu et al. 2012, ApJ, 755, 56; Umetsu 2013, ApJ, 769, 13). It is found that the filamentary large scale structures are aligned with the cluster and its brightest galaxy shapes (see Figure 1). The mass distribution within the cluster is shown to be consistent with the standard Navarro-Frenk-White form predicted for the family of CDM halos in gravitational equilibrium. The gravitational lensing results, combined with Chandra X-ray gas mass measurements, yield a cumulative gas mass fraction of  $f_{\text{gas}} = 13.7^{+4.5}_{-3.0}\%$  within a cluster radius of 1 Mpc, compared to the cosmic mean baryon fraction of  $f_b \sim 16\%$  deduced from Planck CMB data.

## Cosmology with Gravitational Lens Time Delays

Understanding the nature of dark energy is one of the greatest challenges in modern cosmology. One promising probe of dark energy is gravitational lens time delays. Strong gravitational lensing occurs when two objects are closely aligned along the line of sight so that the light from the background object (the source) is bent by the foreground object (the lens) and forms multiple images. The left panel of Figure 2



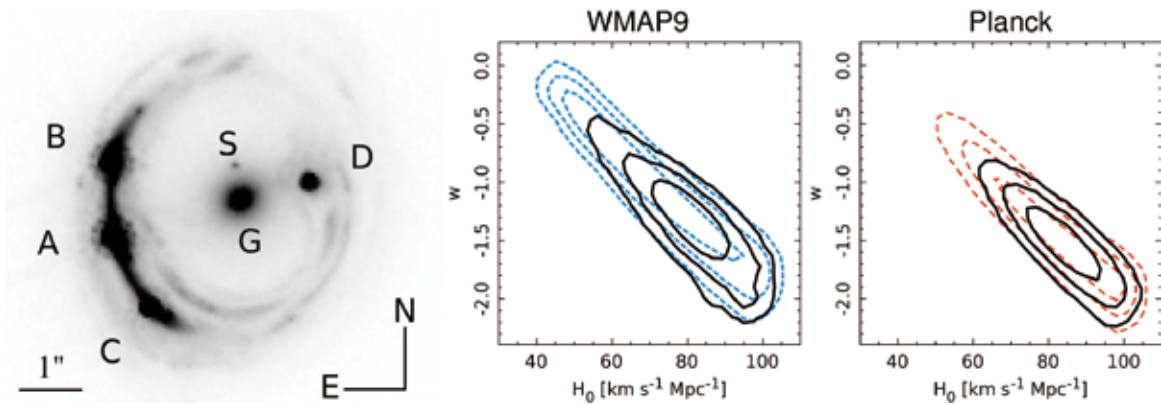


Figure 2. Left: Image of the gravitational lens RXJ1131-1231, taken with the Advanced Camera for Surveys on the Hubble Space Telescope. The lensed AGN images of the spiral source galaxy are marked by A, B, C, and D, and the spiral source galaxy itself forms the spectacular lensed structures. The primary and satellite lens galaxies are indicated by G and S, respectively. Middle and right: Constraints on the dark energy equation of state ( $w$ ) and the Hubble constant ( $H_0$ ). WMAP9/Planck priors are shown as dashed lines, and the combination of RXJ1131-1231 with WMAP9/Planck is in solid. The time-delay distance measurement from RXJ1131-1231, which primarily constrains  $H_0$ , helps break parameter degeneracies in the CMB to determine  $w$ . (Suyu et al. 2014, ApJL, 788, L35)

is an example of a strong gravitational lens system with four images (A, B, C, and D) of the background source galaxy that hosts an active galactic nucleus (AGN). The time it takes the light to travel from the source to us is different for each image due to the different light paths. Any variation in the source intensity with time will therefore manifest itself in the individual images at different times. By measuring the time delays between the multiple images and modeling the mass distribution of the lens galaxy, one can determine the "time-delay distance" to the gravitational lens.

The time-delay distances are useful for constraining cosmological models. The middle and right panels of Figure 2 show that the time-delay distance measurement from RXJ1131-1231 helps to better constrain the dark energy equation of state and the Hubble constant in combination with the Cosmic Microwave Background (CMB) observations from the Wilkinson Microwave Anisotropy Probe (WMAP) and the Planck satellite. (Suyu et al. 2014, ApJL, 788, L35).

## Discovery of the Most Distant Gravitational Lens Galaxy

Gravitational lensing can directly probe the mass distribution of distant galaxies. This allows one to determine the relative contribution of the stars and dark matter in the lensing galaxy and how it varies over cosmic time.

The discovery of the most distant known lens galaxy in the cluster IRC 0218 (Wong et al. 2014, ApJ, 789, L31) provides an opportunity to measure the mass of a galaxy whose light was emitted 9.6 billion years

in the past (Figure 3). The total mass of the galaxy inferred from a lensing analysis implies either a larger amount of dark matter or a different distribution of stars compared to similar galaxies in the local universe, which suggests evolution in one or both of these quantities over cosmic time.

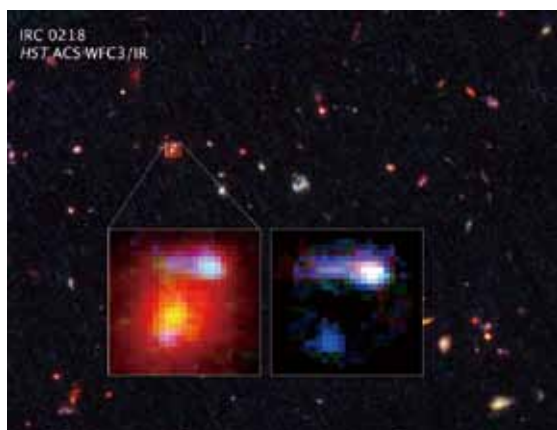


Figure 3. HST image of the gravitational lens system in the galaxy cluster IRC 0218. The left inset shows the red lens galaxy at a redshift of 1.62. The right inset is the same image with the lens galaxy removed, leaving only the blue lensed source (Image credit: STScI).

## Large-scale Inhomogeneity in the Local Universe

The problems in understanding what dark energy is and why it has a particular value have prompted speculation that we might require a paradigm shift. One possibility that has generated considerable interest is the role of inhomogeneity and whether, by removing the assumption of homogeneity in the Cosmological Principle, dark energy would be avoided entirely. In this alternative scenario, “void models” invoke a large local under-density to explain the apparent acceleration of the expansion of the universe. The basic idea in these void models is that if an observer lives near the center of a large under-density, then that observer will witness a local expansion of the universe that is faster than the global expansion. This would provide for a locally measured Hubble constant that is higher than the global value and appear observationally like an accelerating expansion.

As shown in Figure 4, the observed near-infrared luminosity density versus distance relation in the local universe appears to be roughly consistent with void models that seek to explain the apparent acceleration of the expansion of the universe in terms of a large local under-density (Keenan et al. 2013, ApJ, 775, 62). This suggests that, in this age of “precision cosmology”, we may yet have underlying systematics in our measurements that dominate the uncertainties, and which will require more careful consideration.

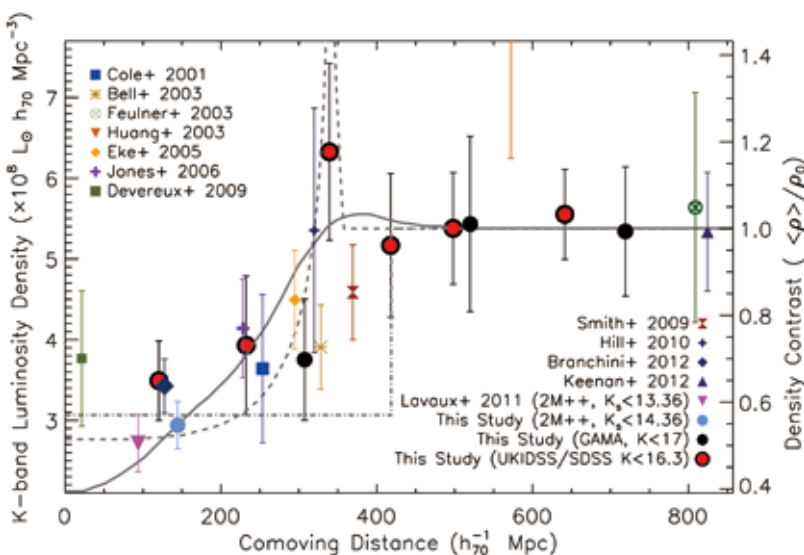


Figure 4. Near-infrared K-band (2.2 micron) luminosity density as a function of comoving distance in the local universe. Data points show measurements from this study and others from the literature. The right hand vertical axis shows total matter density contrast assuming K-band luminosity density is an unbiased tracer of mass density. The curved lines show radial density profiles from two models that invoke a local under-density to fit the type Ia supernovae data without dark energy. The “step function” shows another model that uses a local under-density to reconcile the discrepancy between local measurements of the Hubble constant and those inferred by Planck.

## Asymmetry and Non-random Orientation of the Inflight Beam in the WMAP Data

The anomaly against the Gaussianity in the NASA WMAP data was alleged to be due to “insufficient handling of beam asymmetries”. Asymmetry of the inflight effective beam convolved with the data could distort the image, thus causing systematic errors which can mimic primordial non-Gaussianity.

Figure 5 is an estimation of the inflight effective beam. Due to the scan strategy that the WMAP observes from a Lissajous orbit about the L2 Sun-Earth Lagrange point, and to the fact that the telescope line of sight is around 70 degrees off the WMAP spinning axis, the path swept out on the sky by a given line of sight resembles a Spirograph pattern that reaches from the north to south ecliptic poles. Hence, the inflight beam pattern is closely related to the Ecliptic coordinate. In Figure 5 our estimated inflight effective beam pattern is plotted (Chiang 2014, ApJ, 785, 117).

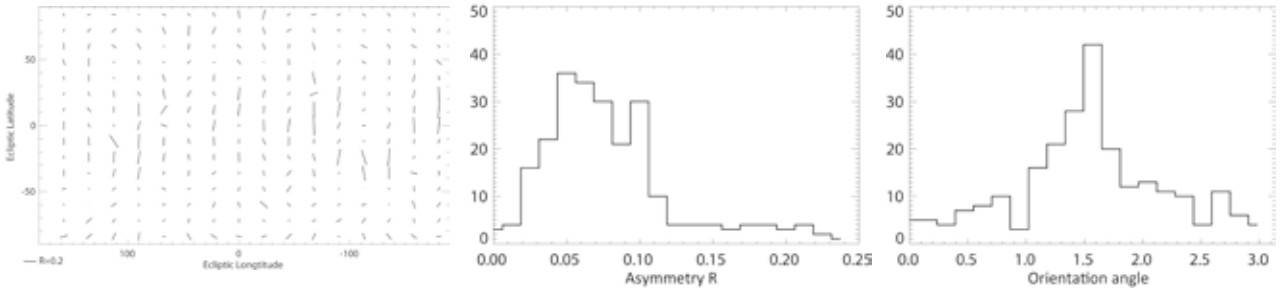


Figure 5. Left panel : Estimation of the effective beam of WMAP Q1 DA in Ecliptic coordinates. The length of the bars indicates the asymmetry  $R = r_{\text{maj}}/r_{\text{min}} - 1$  where  $r_{\text{maj}}$  and  $r_{\text{min}}$  respectively, are the major and minor axes of the elliptical shape of the beam, and the inclination denotes that of the major axis. The middle and right panels show the histogram of the asymmetry  $R$  and the orientation angles. The angle is defined with that between the bar and the Ecliptic Equator.

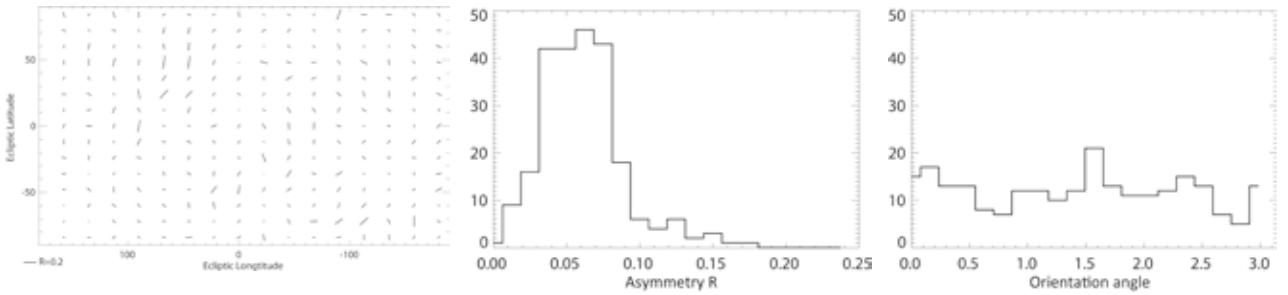


Figure 6. Estimation of the effective beam of WMAP internal linear combination map in Ecliptic coordinate. All the notations are the same as in Figure 5.

The inflight effective beam convolved with the signal is indeed non-symmetric for most of the sky, and it is not randomly oriented. Around the ecliptic poles, however, the asymmetry is smaller due to the averaging effect from different orientations of the beam from the scan strategy. The effective beam with significant asymmetry is oriented in an almost parallel fashion along the lines of Ecliptic longitude.

Figure 6 is a plot that is same for the WMAP foreground-cleaned internal linear combination map. It is shown that the systematic beam alignment is significantly lessened (Chiang 2014, ApJ, 785, 117).

One should note that the lessening of the asymmetry of the effective beam in the ILC map does not guarantee that the ILC map is not without the systematic error from the beam effect. A highly aligned beam with significant asymmetry (as we have shown in Figure 5) scanning through the sky can have an elongated effect on the raw data, which will definitely cause some systematic error in the foreground cleaning process for the CMB if beam asymmetry is not properly treated.



# Planetary Sciences

What was the early environment of the Solar System about 4.5 billion years ago? What were the early environments of other planetary systems several billion years ago when extrasolar planets (“exoplanets”) were still forming and evolving in protoplanetary disks? Most interestingly, how does the climate of other earths possibly evolve in the habitable zone around their parent stars like the Sun? Astronomers at the ASIAA have carried out meteorite studies as well as model calculations, making tremendous progress to answer these extraordinary questions.

## Origins of Short-Lived Radionuclides in the Early Solar System

Calcium-41 (half-life = 0.1 Myr) is a short-lived radionuclide whose former existence was first demonstrated by Srinivasan et al. (1994, 1996) through the detection of excesses of its daughter product  $^{41}\text{K}$  in meteoritic refractory inclusions (CAIs). The initial abundance of  $^{41}\text{Ca}$  in the early solar system, expressed in the form of  $^{41}\text{Ca}/^{40}\text{Ca}$ , was inferred to be  $1.4 \times 10^{-8}$  (Srinivasan et al. 1996). Because of the short lifetime,  $^{41}\text{Ca}$  and its initial abundance have been used as an anchor when discussing the timescale of Solar System formation and the sources of this and other short-lived radionuclides. Recently, reanalysis of K isotopes with an advanced secondary ion mass spectrometer in the meteoritic refractory inclusions where  $^{41}\text{Ca}/^{40}\text{Ca} = 1.4 \times 10^{-8}$  was inferred, revealed a 5-times lower  $^{41}\text{Ca}/^{40}\text{Ca}$  ratio of  $2.6 \times 10^{-9}$  (see Figure 1). This new result could change our current understanding of the origins of short-lived radionuclides, but more data are needed.

A new study (Liu et al. 2012) utilized a state-of-the-art instrument that has enabled better separation between the signal of interest and interferences, which is key in isotopic measurements of such kind. A higher signal to noise ratio obtained on this instrument due to a higher sensitivity compared to the one used in the old study (Srinivasan et al. 1996) also helped to improve the counting statistics of measurements. It is still unclear why there is a factor of 5 difference between the results of Liu et al. (2012) and Srinivasan et al. (1996). Most likely it was because there was some unwanted signal that did not get corrected for in the old study, which was perhaps limited by the instrument used. This new result could change our current understanding of the origins of short-lived radionuclides, but more data are needed.

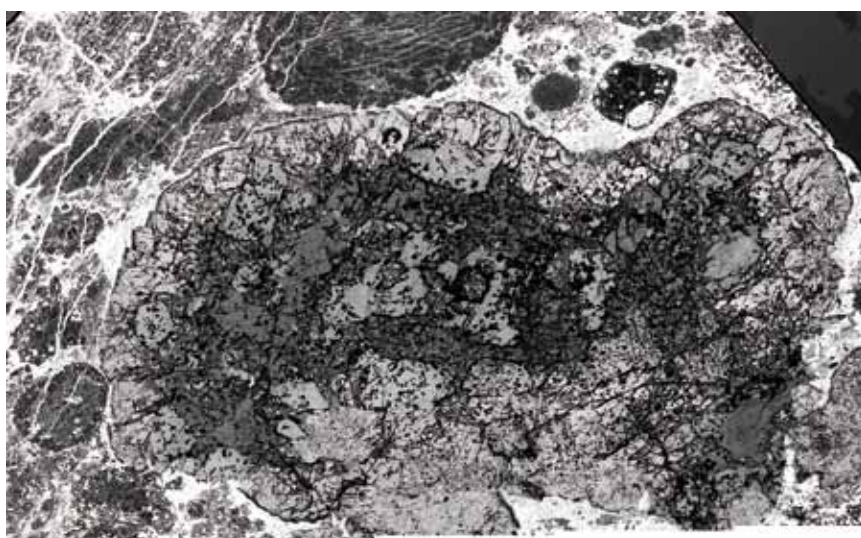


Figure 1. A back-scattered image of the E44 CAI from the CV3 Efremovka chondrite taken on a scanning electron microscope. This CAI is of particular interest because of the first demonstration of the former existence of short-lived  $^{41}\text{Ca}$  ( $t_{1/2} = 0.1$  Myr). Reanalysis of potassium isotopes of this CAI (on the dark-gray minerals, named fassaite) resulted in a lower initial ratio of  $^{41}\text{Ca}/^{40}\text{Ca}$  in the solar system from  $1.4 \times 10^{-8}$  to  $2.6 \times 10^{-9}$ . A factor of 5 difference has an important implication for the origin of  $^{41}\text{Ca}$  and of the solar system. (Picture Credit: Ming-Chang Liu)

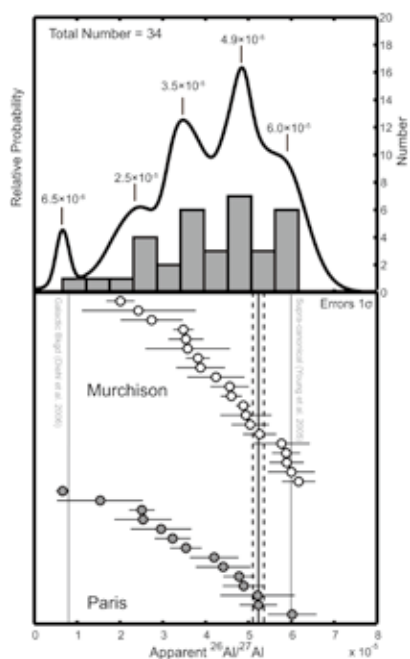


Figure 2. Inferred  $^{26}\text{Al}/^{27}\text{Al}$  ratios for spinel-hibonite spherules (SHIBs) from Murchison and Paris and the probability density plot derived from the data. The overall  $^{26}\text{Al}/^{27}\text{Al}$  range in the two groups of SHIBs is essentially identical, from  $\sim 1 \times 10^{-5}$  up to  $6 \times 10^{-5}$ . Three distinctive peaks can be identified in the probability plot at  $^{26}\text{Al}/^{27}\text{Al} = 4.9 \times 10^{-5}$ ,  $\sim 3.5 \times 10^{-5}$  and  $6.5 \times 10^{-6}$ , respectively. Two barely resolved components at  $6 \times 10^{-5}$  and  $2.5 \times 10^{-5}$  are also revealed (Liu et al. 2012, *Earth and Planetary Science Letters*, 327, 75).

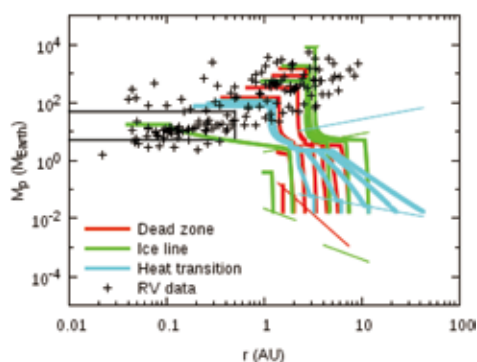


Figure 3. Evolutionary tracks of planet forming at multiple planet traps where the rapid type I planetary migration is halted. Three types of traps are considered: dead zone (red lines), ice line (green lines), and heat transition (blue lines) traps. Five to seven tracks are computed for each planet trap in order to consider planet formation over the entire disk lifetime. The radial velocity observations of exoplanets are shown in the plus signs. The end points of tracks line up well with the observations (Hasegawa & Pudritz 2012, *ApJ*, 760, 117).

At ASIAA, studies of solid debris from stars that predate the solar system are carried out on the NanoSIMS, for a better understanding of the interstellar histories of the dust particles. Besides, materials formed in the beginning of the solar system are also analyzed with the NanoSIMS to constrain the charged particle irradiation environment near the protoSun.

## Different Formation Events of the Oldest Solar-System Minerals

Hibonite ( $\text{CaAl}_2\text{O}_6$ ) is one of the oldest solar system solids and can be categorized into two groups according to its mineralogy. Spinel-hibonite spherules usually contain fossil records of  $^{26}\text{Al}$ , a short-lived radionuclide with a half-life of 0.7 Myr, whereas platy hibonite crystals lack radiogenic excesses of  $^{26}\text{Mg}$ . The literature on  $^{26}\text{Al}$  data in spinel-hibonite spherules showed that this group of hibonite grains are broadly characterized by  $^{26}\text{Al}/^{27}\text{Al} = 5 \times 10^{-5}$ , consistent with the so-called “canonical” ratio found in the majority of meteoritic refractory inclusions. However, the associated analytical uncertainties would also allow for an apparent scatter of  $^{26}\text{Al}/^{27}\text{Al}$  up to  $7 \times 10^{-5}$ . High precision analysis of spinel-hibonite spherules with an advanced secondary ion mass spectrometer revealed, for the first time, that these hibonite grains are characterized by a range of  $^{26}\text{Al}/^{27}\text{Al}$  from  $6.5 \times 10^{-6}$  up to  $6.0 \times 10^{-5}$ . Three distinctive peaks, which could represent three major formation events of hibonite, can be seen in a probability density plot (see Figure 2). Given a more refractory nature of hibonite grains, such a distribution of  $^{26}\text{Al}/^{27}\text{Al}$  could result from early formation before  $^{26}\text{Al}$  was homogenized to  $5 \times 10^{-5}$ .

## Planet Traps and the Population of Exoplanetary Systems

The recent theoretical studies on planet formation in protoplanetary disks have implied that massive planets like Jupiter in our Solar System, are likely to be formed as a consequence of rapid migration of planetary cores into specific trapping sites in protoplanetary disks. The sites are often referred to as planet traps. A new model has been constructed to demonstrate how the combination of planet traps with the standard theory of planet formation, also known as the core accretion scenario, can well reproduce the observations of exoplanets that now amount to more than 900 (the number increases to 4,000 if candidates are included). The time-evolution of planets in mass and semimajor axis is computed under the action of planet traps. The results in Figure 3 show that, when planet traps are coupled with a model of planetary growth, the final distribution of planets in the mass-semimajor axis diagram

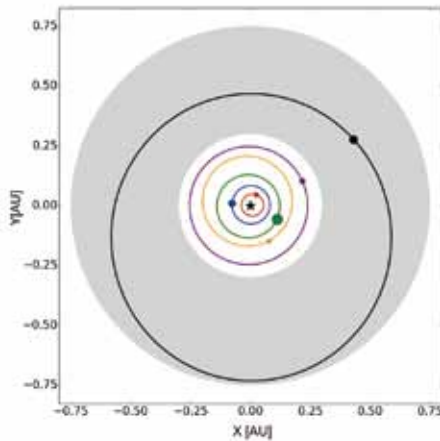


Figure 4. An orbit diagram of the planetary system surrounding the K-dwarf star HD 40307. The grey area indicates the star's habitable zone. Notice that the outermost planet is right in the habitable zone. (Picture Credit: Ramon Brasser)

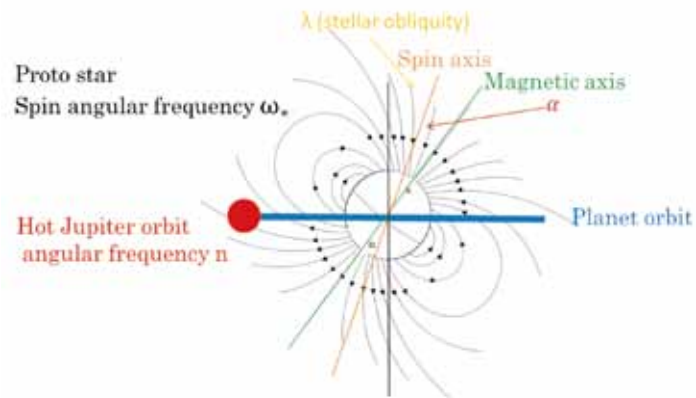


Figure 5. Schematic of the theoretical model showing the dipole magnetic fields of a proto-star that are misaligned with both the stellar spin axis and the orbital plane of a hot Jupiter. Consequently, the young hot Jupiter experiences time-varying stellar fields which induce electric currents, leading to a dissipation torque that can alter the stellar obliquity  $\lambda$ .

is consistent with the radial velocity observations of exoplanets. This arises because planetary cores, that eventually grow to gas giants, are "stored" efficiently around 1–10 AU. Following further growth of protoplanets, this "initial" distribution of the cores ends up with the so-called mass-semimajor axis relation which shows that the upper bound on planetary mass is an increasing function of semimajor axis.

## Habitability of the Super Earth HD 40307 G

One of the most amusing and profound questions from the quest for exoplanets is the probability of life existing in the Universe. The HD 40307 planetary system consists of six super Earth planets, with masses between 4 and 10 Earth masses. The system has five planets very close to the star and one much farther out (see Figure 4). The outermost planet is of interest because it lies in the star's habitable zone (grey area). Simulations indicate that the system is stable and that planet g may undergo frequent ice ages, just like the Earth. There are hundreds of other planets in the habitable zone of other stars that require further study. Here at the ASIAA, astronomers strive to be at the forefront to study how planetary dynamics affect the climate on habitable planets (Brasser, Ida & Kokubo 2014, arXiv1403.5868B).

## Hot Jupiters on Prograde/Retrograde Orbits

The observations of exoplanets based on both radial velocity and transit data suggest that the angle between the stellar spin and the orbital normal of hot Jupiters (i.e. stellar obliquity) may be distributed over a wide range, namely, the orbit can be prograde or retrograde relative to the spin of their parent stars. These observational findings seem contrary to the conventional paradigm in which a planet should orbit in the same direction as the stellar spin as the star and the planets form together in a protoplanetary disk. Nevertheless, it was proposed that before the protoplanetary disk dissipates, the warp torque resulting from the magnetic interactions between the proto-star and the inner part of the disk would move the stellar spin away from the disk angular momentum. At the ASIAA, theoretical work has been conducted to take into account magnetic interactions between the stellar magnetic fields and a hot Jupiter, as illustrated in Figure 5. The result suggests that the stellar obliquity may further evolve after the planet migrates into the magnetospheric cavity of a protoplanetary disk, making the orbit of the young hot Jupiter incline with the disk plane. As a result, a hot Jupiter does not necessarily lie on the same orbital plane with the planets farther out from the central star (Chang et al. 2012, ApJ, 757, 118).



# ***Instrumentation Research***





## Instrumentation Research

As a premier astrophysics research center in the world, ASIAA aspires to be a world leader on the topics of its interest. Instrumentation and facilities are the essential components for such a vision. Our research inspires young students and researchers alike, and the Institute has the capacity and environment to empower those young scientists to pursue their research careers and fulfill their dreams.

ASIAA has concentrated its resources on several important projects. The Submillimeter Array (SMA) project is an excellent example that illustrates how a focused effort directed our major research for the past 10 years. For the SMA project, ASIAA built up the Receiver Laboratory (top-left panel of Figure 1), and set up the Hawaii facilities and our SMA operation team. The Receiver Laboratory and the ASIAA Hawaii staff subsequently led the development and construction of the Array for Microwave Background Anisotropy (AMiBA, Figure 2). The Microwave Device Laboratory (top-right panel of Figure 1) was subsequently built up through the AMiBA project. The SMA project also created an important new component to ASIAA: the Superconducting Device Laboratory (bottom-left panel of Figure 1), which led to the development in Superconductor-Insulator-Superconductor (SIS) mixers and Superconducting Quantum Interference Devices (SQUID). These Laboratories play important roles in supporting the collaborative work in the Atacama Large Millimeter/submillimeter Array (ALMA) project.



Receiver Laboratory



Microwave Device Laboratory



Superconducting Device Laboratory



Optical/Infrared Laboratory

Figure 1. The Laboratories (Picture Credit: ASIAA)



Figure 2. The 13-element, 1.2 meter-dish Yuan T. Lee AMiBA on the Mauna Loa Observatory, Hawaii. The AMiBA project, observing at 3 mm wavelength, was an important initiative for developing our observational cosmology program in a very competitive field of science. This project has met the challenges of several novel technological difficulties, such as the 16-GHz wide-band analog correlator, the unprecedented size of Steward mount, and the 6-meter, detachable, composite-material platform. (Picture Credit: Chih-Chiang Han)

ASIAA has expanded its technical expertise into Optical/Infrared (OIR) wavelengths (bottom-right panel of Figure 1). The team from the TAOS project has been the main driver for the Canada-France-Hawaii Telescope (CFHT)/Wide Field Infrared Camera (WIRCам) programs. Through the WIRCам collaboration, the OIR team has expanded with staff gaining experience in array testing and control electronics. With such expertise, the team continues to work on the advanced instrumentation project of large telescopes, such as SpectroPolarimètre Infra-Rouge (SPIRou) of the CFHT and the Hyper Suprime-Cam (HSC) and Prime Focus Spectrograph (PFS) of the Subaru telescope. Meanwhile, the OIR Laboratory is developing the high-cadence wide-field camera for the TAOS II project. ASIAA also joined the geospace satellite project, the Exploration of energization and Radiation in Geospace (ERG), through collaboration with the National Cheng Kung University and the Japanese space agency JAXA. This will further enhance our capability in space applications. In addition, the OIR Laboratory in ASIAA is also exploring the instrumentation possibility for future thirty-meter class telescopes.

## Receiver Laboratory

Developing forefront technology to drive the next generation astronomical instrumentation is one of the core programs in ASIAA. The SMA was our first major instrumentation achievement, and through its construction the Institute assembled a young technical team specialized in millimeter and submillimeter wavelength technologies. The SMA became the workhorse for the ASIAA science program before ALMA came online. In parallel, our technical program has expanded further into new projects, such as the Yuan T. Lee AMiBA telescope, the various sub-programs for ALMA, the digital correlator upgrade for the SMA, and VLBI in submillimeter wavelengths.

We are continuously upgrading the SMA facility and its observational capability (Figure 3). The SMA observation bandwidth has expanded from 4 GHz to 12 GHz. All the SMA 200 GHz and 300 GHz receivers are capable of wide-band operations (Figures 4, 5). The increase of the bandwidth in the front-end requires the same enhancement in the back-end correlator of the SMA. The development of the new wide-band digital correlator is another collaborative project involving the Smithsonian Astrophysical Observatory (SAO)-ASIAA team. Constructing the digital correlator is part of our effort in developing our own digital instrumentation and signal processing (DSP) capabilities.



The design of digital instrumentation is highly specialized and its development typically consumes a large amount of resources in terms of labor, time and budget. In the past decade or so, there has been a trend toward promoting shared hardware development that include items such as interchangeable digitizers, flexible digital hardware processors, reusable DSP libraries, scalable instrument architectures, and flexible monitor & control and interfaces. Such development benefits the radio astronomy community, especially for those institutes that only support a small group of digital developers. The Collaboration for Astronomy Signal Processing and Electronics Research (CASPER) is one of the major promoters for this effort and has expanded to include several astronomical and engineering institutions around the world. Our contribution to this consortium has been the development of a high-speed analog to digital converter (ADC) board, shown in Figure 6, to be used in conjunction with other hardware available from the CASPER suite.

Our capability for system design and integration has been demonstrated in the AMiBA and ALMA projects. AMiBA is an international endeavor led by ASIAA, in collaboration with various laboratories and experts in the world. On the site of Mauna Loa Observatory, on the big island of Hawaii the AMiBA 7-element array was officially dedicated in Oct. 2006, and the 13-element 1.2 m full array was completed in 2010. The AMiBA project has brought one more important technology into the receiver laboratory, namely the design and integration capabilities for the Monolithic Microwave Integrated Circuit (MMIC). We have applied this technology to the AMiBA and the SMA projects in making front-end amplifiers, mm-wave mixers, and broad-band correlators. This is a collaborative effort involving ASIAA and our partners in the National Taiwan University and the National Central University.

Figure 7 shows the development of a photonic local oscillator (LO) source based on a three-stage Mach-Zehnder modulator (MZM) device for the ALMA project. ALMA utilizes a laser synthesizer based on the beating of a phase-locked slave

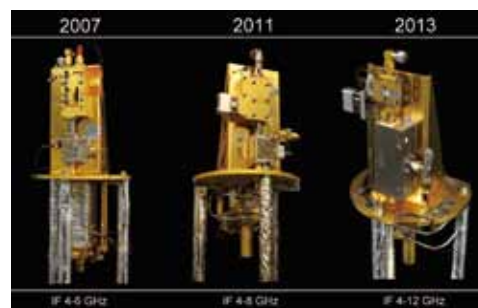


Figure 3. The evolution of the SMA receiver configuration: the low-noise amplifier (LNA) upgrade. In 2007, the LNA bandwidth is only 4–6 GHz for the first generation receiver. By 2011, the amplifier was changed to TTI-CLNA-4080 with a 4–8 GHz bandwidth, manufactured by a Spanish company. Now, we are using the new amplifier, CITCRYO1-12A, made by the California Institute of Technology. This amplifier can realize the bandwidth between 4–12 GHz for SMA receivers. (Picture Credit: Chih-Chiang Han)

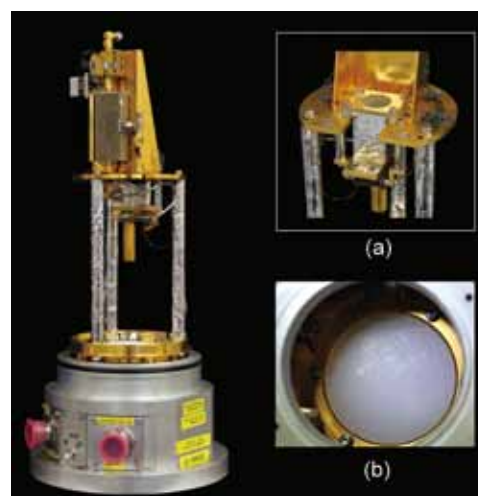


Figure 4. One of the two SMA wideband 300 GHz receiver inserts from ASIAA. This is a new generation receiver with wider IF operation frequency from 4 GHz and 12 GHz. This receiver has shown fairly flat noise temperature performance between 4 to 12 GHz, and the lowest noise contribution of this receiver has approached to 3 times the quantum noise level ( $3 h\nu k^{-1}$ ). Inset (a) shows the area for 4 K heat strip connection on the insert. Inset (b) shows the interior of the IR-quartz filter with low-density polyethylene (LDPE) coating and grid. (Picture Credit: Chih-Chiang Han)

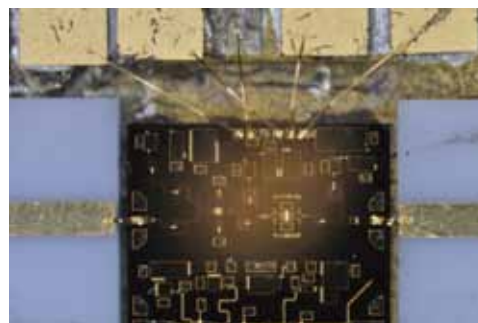


Figure 5. Magnified view of the cryogenic IF amplifier for future wide-IF SIS SMA receiver. The chip size is 2 mm  $\times$  1 mm. It provides more than 20 dB gain when operating at 17.5 K with a power consumption of 20 mW. Circuit design and packaging work were both performed in-house. (Picture Credit: Chau-Ching Chiong)



Figure 6. The 8-bit, 5 Giga Samples/sec ADC developed in ASIAA. This board is the first product from our digital signal processing (DSP) effort in support of the CASPER, an international collaboration of the astronomy DSP community. The CASPER's Reconfigurable Open Architecture for Computing Hardware (ROACH) has combined the flexibility and performance of Field Programmable Gate Wares (FPGAs), and is the most notable outcome from this collaborative community. The ASIAA ADC is enabling the ROACH's capability in handling the need of high-bandwidth DSP needs and operations. Currently, the combination of the ASIAA ADCs and ROACHs are utilized as the core components for the SMA Wide Bandwidth upgrade, and the new generation of the AMiBA correlator. (Picture Credit: Derek Kubo)

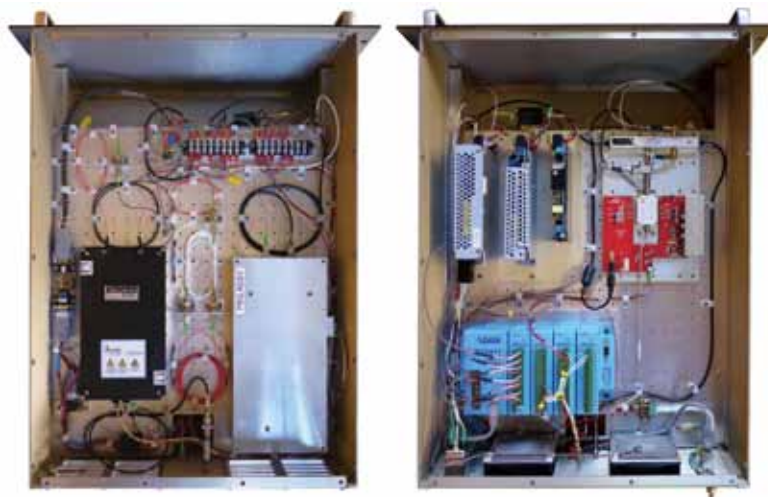


Figure 7. Internal photos of the Laser Synthesizer instrument. Left panel: top view of optical circuitry including Erbium Doped Fiber Amplifier and custom Fiber Bragg Grating filter assembly; right panel: bottom view of RF power amplifier, Mach-Zehnder modulator, DC power supplies (x3), and monitor & control. Developed at the SMA project office by Derek Kubo and Ranjani Srinivasan in collaboration with NAOJ, this instrument was designed to provide a pure optical local oscillator reference for distribution over long distances of optical fiber (Kubo et al. 2013, IEEE T Microw Theory, 61(8), 3005).

laser with a master laser to cover the photonic LO tuning range of 27–34 and 65–122 GHz. To maintain LO coherency, the two lasers must be stable, spectrally pure, have narrow line widths, and be optically phase locked to each other. The practical design challenges in phase locking the slave lasers to the master laser and producing an LO with low phase noise was the impetus for the development of an alternate laser synthesizer based on a MZM device.

The ASIAA receiver group is constantly seeking opportunities to undertake challenging projects. Its role in ASIAA is not only to support the instrumentation effort, but also to stimulate thinking in new research directions, and to motivate scientific members in ASIAA to develop new initiatives in unexplored realms of the Universe.

## Microwave Device Laboratory

The Microwave Device Laboratory is dedicated to the research and development of microwave and millimeter-wave electronic devices and circuits for radio astronomical instrumentations. The present development highlights in the microwave device laboratory are (1) cryogenically cooled RF, microwave, and millimeter-wave broadband low-noise amplifiers for heterodyne receiver front-end, (2) broadband diode and transistor mixers for next-generation astronomical heterodyne receivers, (3) ultra-low-phase-noise broadband voltage-controlled transistor oscillators for local oscillators of next generation astronomical heterodyne receivers, and (4) low-loss broadband passive millimeter-wave planar circuits. The laboratory is also responsible for constructing the Band-1 receiver for ALMA, and upgrading the 700–945 MHz array receiver for the Green Bank Telescope of the National Radio Astronomy Observatory (NRAO).

With few exceptions, radio astronomy applications in millimeter wavelengths require detectors and receivers designed with extraordinary specifications of very wide bandwidth and extra low-noise performance. These instruments are usually cryogenically cooled for performance purposes, and

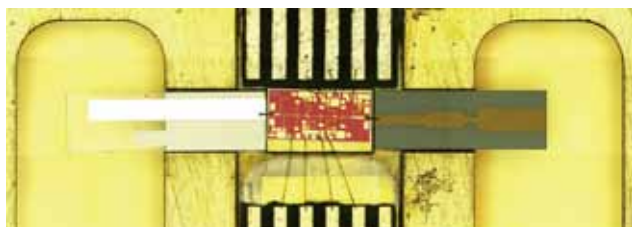


Figure 8. A millimeter-wave amplifier based on mHEMT process. This amplifier is designed through collaborations with our university partners. It covers frequency bandwidth from 30–50 GHz and is suitable for cryogenic operations to reduce its intrinsic noise. This device is fabricated in a Taiwanese semiconductor foundry with an advance technology called monolithic microwave integrated circuit. (Picture Credit: Ching-Chi Chuang & Chau-Ching Chiong)

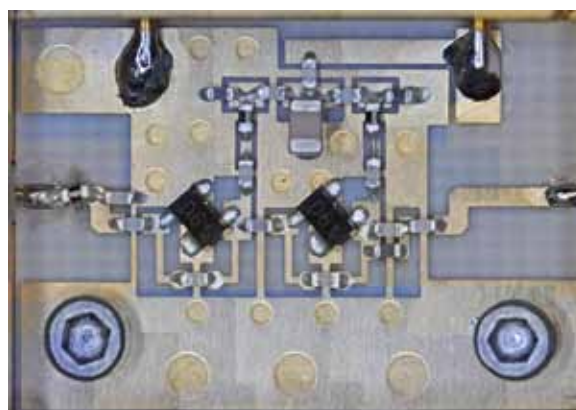


Figure 9. Low-noise amplifier for 700–945 MHz observations. This device is made with commercially available, discrete and packaged SiGe transistors. It can be cooled to a physical temperature of 20 K, and achieve a very low noise performance. (Picture Credit: Ching-Chi Chuang)

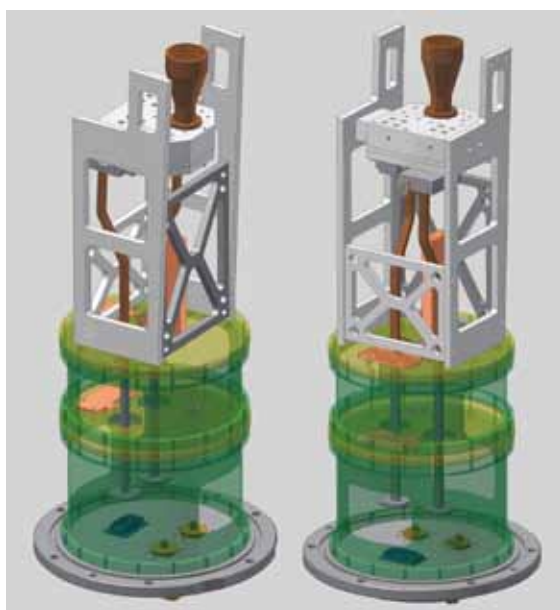


Figure 10. The computer simulated mechanical layout of the ALMA Band-1, cold cartridge assembly (left panel) and warm cartridge assembly (right panel). This model is developed by the Microwave Device Laboratory, in collaboration with colleagues in NRAO, Herzberg Institute of Astrophysics (HIA), University of Chile, and NAOJ. (Picture Credit: Chin-Ting Ho)

their devices are made of special materials and with specific processes. Indium-phosphide (InP), gallium-arsenide, or silicon-germanium are the few types of materials suitable for our purpose, and they are made into “high-electron-mobility” transistors (HEMT), metamorphic high-electron-mobility transistors (mHEMT), or hetero-junction bipolar transistors. Using these devices, we are currently developing amplifiers and mixers to cover the ALMA Band-1 receiver frequency range of 30–50 GHz. (Figures 8 & 9 & 10)



For the voltage-control-oscillator (VCO) MMIC, the phase-lock circuit, integration and optimization of the phase noise performance of the oscillator (Figure 11), the most recent study shows that the measured RMS phase jitter of the optimized phase-locked GaAs HBT varactor (variable capacitor)-tuned VCO can be as low as 54 fsec at 33.5 GHz. To overcome the large variation of the tuning sensitivity of the VCO, a reconfigurable phase-lock circuit with switchable loop filters is now under development.

The 700–945 MHz multi-beam receiver will be installed on the prime focus of the NRAO Green Bank Telescope for use in observing neutral hydrogen line at redshifts  $z = 0.5–1.0$  (Figure 12). The observed results are expected to reveal the baryon distribution over the universe. The microwave device laboratory has designed and built the receiver in collaboration with the National Radio Astronomy Observatory, the University of Wisconsin Madison, and the Carnegie Mellon University.

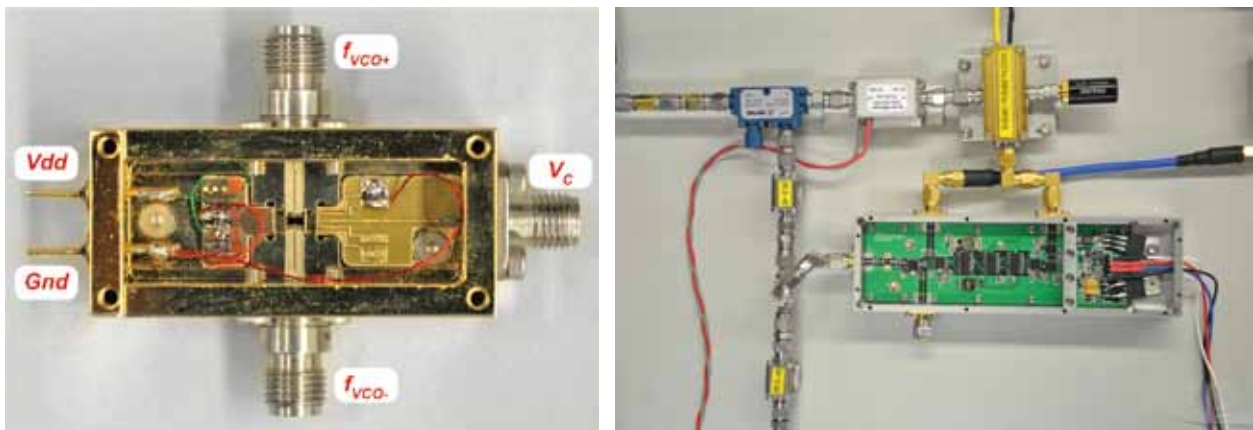


Figure 11. Ultra-low-phase-noise broadband tuning voltage-controlled transistor oscillators. The packaged circuit module (left panel), and the phase-lock circuit module (right panel) are shown. The goal of this development project is to provide a possible miniaturized low-thermal dissipation local oscillator source for the Atacama Large Millimeter/submillimeter Array. This is a collaborative project between ASIAA, National Taiwan University, and the National Radio Astronomy Observatory (USA). (Picture Credits: Chau-Ching Chiong & Yue-Fang Kuo)

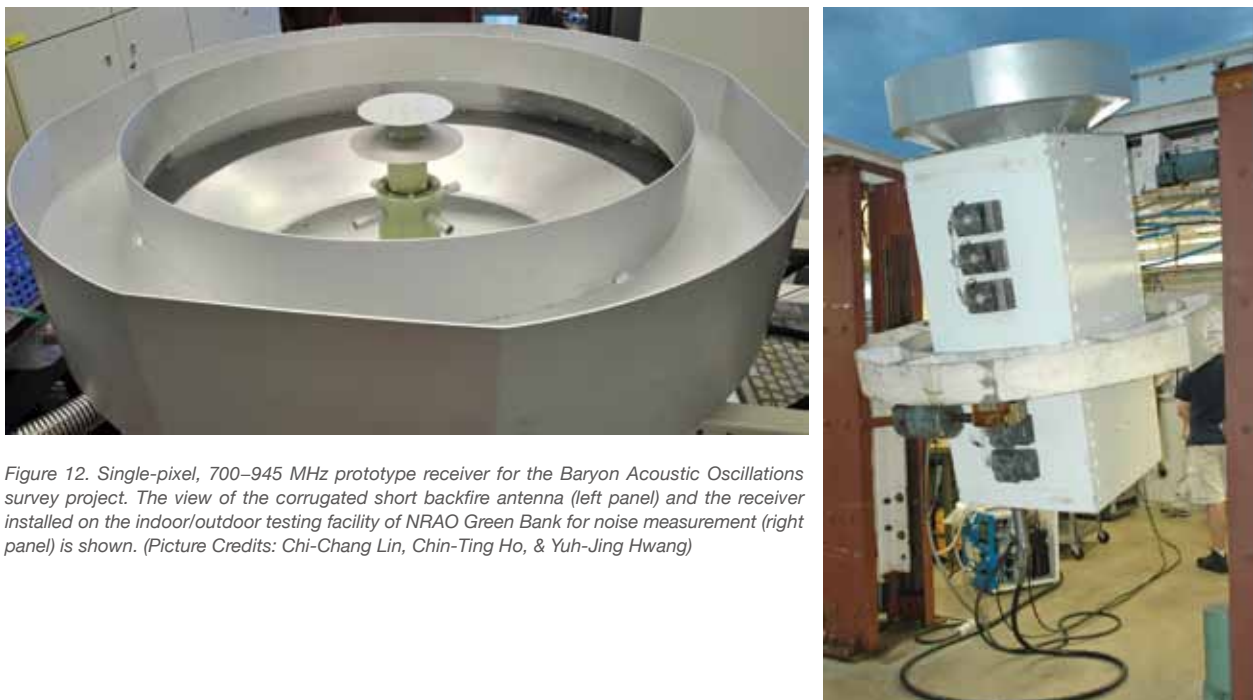


Figure 12. Single-pixel, 700–945 MHz prototype receiver for the Baryon Acoustic Oscillations survey project. The view of the corrugated short backfire antenna (left panel) and the receiver installed on the indoor/outdoor testing facility of NRAO Green Bank for noise measurement (right panel) is shown. (Picture Credits: Chi-Chang Lin, Chin-Ting Ho, & Yuh-Jing Hwang)

## Superconducting Device Laboratory

The Superconducting Device Developing Group was founded in 1994 in collaboration with National Tsing-Hua University (NTHU), Hsin-Chu, Taiwan to provide sensitive superconducting devices for ASIAA's astronomical projects and its worldwide collaborators. The clean-room facilities in NTHU campus were moved to the new clean-room in NTU campus in 2014.



Figure 13. Laboratories in ASIMAB building (NTU campus in Taipei) including clean room, post process (lapping and dicing), and testing systems (Picture Credits: ASIAA)

Our laboratory has had a complete fabricating line for niobium (Nb)-based superconducting devices since 2000. The facilities include metal sputtering systems, mask aligners, insulator deposition systems, metal evaporators, Reactive-Ion Etching (RIE) system, Inductively Coupled Plasma RIE (ICP-RIE) system, ion-milling system, substrate lapping machine, chip dicing system, and wire bonding machine (Figure 13). Our capabilities for superconductor-insulator-superconductor (SIS) mixer devices include: minimum pattern in  $1\mu\text{m}$  size, critical current density from  $300\text{ A cm}^{-2}$  to  $20\text{ kA cm}^{-2}$ , multilayer process, chip thickness of  $30\text{ }\mu\text{m}$ , and an accuracy of chip size to better than  $5\text{ }\mu\text{m}$ . Since 2013, we have used the electron-beam photolithography technology, which enables us to fabricate a superconducting device with nano-structure and ultrathin film. Devices with a minimum feature of  $100\text{ nm}$  and a thickness of  $10\text{ nm}$  can be fabricated. Gradually, we are establishing new processes for fabricating devices with niobium-titanium nitride (NbTiN), niobium nitride (NbN), iron-chalcogenide superconducting nanowire, and graphene.

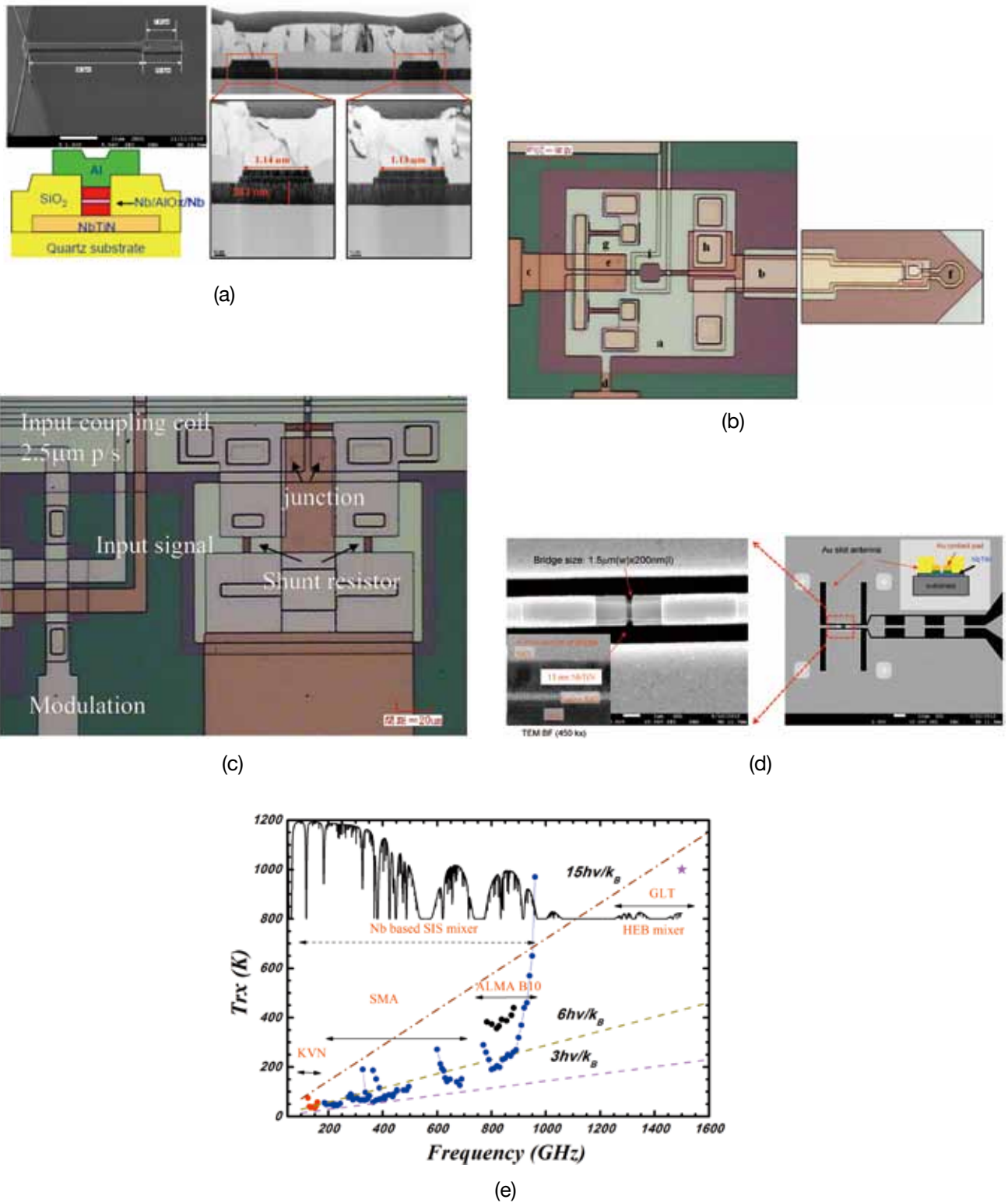


Figure 14. From top to bottom: (a) SIS mixer in top and cross-sectional views, (b) SQUID chips for SSQ system, (c) SQUID chips for SSTM system, (d) HEB mixer in top and cross-sectional views, (e) performance of mixers across the atmospheric windows (Picture Credits: Ming-Jye Wang)



We supply high quality, Nb-based SIS mixers for the 200, 300, 400, and 600-GHz receivers of the SMA. Since 2011, we have also delivered new 200 GHz and 300 GHz mixers with wide intermediate-frequency (IF) bandwidth for the SMA. SIS mixers have also been provided for the Korean VLBI network. In addition, two types of SQUID (Superconducting Quantum Interference Device) have been fabricated and installed in different scanning SQUID systems. Recently, hot-electron-bolometer (HEB) mixers have been successfully developed at 1.4 THz frequency band, as well as integrated dual polarization SIS mixers (Figure 14).

Currently, our group works on the following topics: (1) wide IF bandwidth SIS mixers at 400 GHz and 240 GHz in collaboration with the SAO for the SMA upgrade project, (2) focal-plane, multi-pixel heterodyne receiver system with integrated dual polarization mixers, (3) 7-pixel, HEB, ALMA-type receiver cartridge for the Greenland telescope, (4) wider IF bandwidth for HEB mixers, and (5) THz response of novel materials, such as graphene and iron-chalcogenide superconducting nanowire.

To study these topics, new technologies are under development such as the integration of SIS/isolator/LNA, high quality ultrathin film deposition, novel fabricating process for device using new material, and testing method. Collaborations with many domestic and international institutions are common for the exchange of mutual expertise.

## Optical/Infrared Instrumentation Development

Through collaborations on large international programs, the OIR group focuses on detector technology by working with foreign companies on the advanced sensors and with local companies and groups. In particular, we target on the scientific developments of complementary metal-oxide-semiconductor (CMOS) sensors and infrared detectors.

CMOS sensors have been widely used in many commercial applications. However, in scientific applications, charged-couple devices (CCD) still dominate the market mainly because of their excellent performance characterized by low noise and high quantum efficiency, which are essential for astronomical applications. The major drawback of CCDs is the relatively slow readout speed, which limits the frame rate and minimal exposure time. ASIAA projects such as TAOS II and Subaru/PFS, will require high sampling imaging. For example, the TAOS II camera requires 20 Hz sampling of field stars for occultation detection with typical 15-micron pixels. PFS needs a fast camera with good spatial resolution for the metrology of the fibers to guide the fiber positioner to the targets. Both needs cannot be satisfied with standard scientific CCD chips. Instead, CMOS sensors have shown more potential.

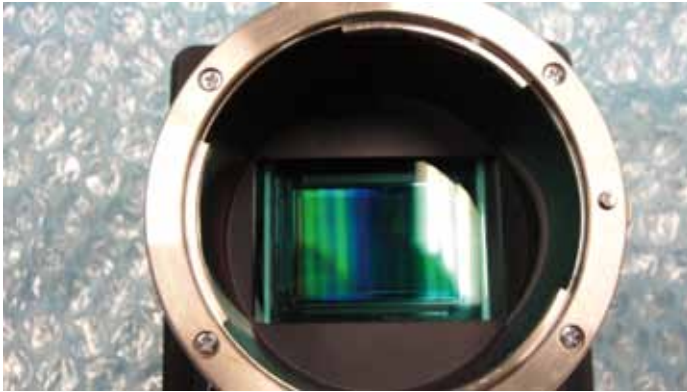


Figure 15. The Canon 50 Mega-pixel camera (Picture Credit: Shiang-Yu Wang)



Figure 16. The interface board and the  $320 \times 256$  InGaAs array for the characterization system (Picture Credit: Shiang-Yu Wang)

Thanks to recent developments on scientific CMOS sensors, the issue of low quantum efficiency has been solved with a backside illumination and a deep depletion structure. The quantum efficiency for CMOS is now similar to that of back-thinned CCDs. A smaller format device has been successfully developed. For TAOS II, the OIR group is now working with e2v ([www.e2v.com](http://www.e2v.com)) on a large format CMOS with  $4.5k \times 2k$  pixels. With 10 such devices closely packed to form an array, the CMOS sensors can cover the useful telescope field of view. The sampling rate of 20 Hz with a readout noise lower than  $5e^-$  has been successfully achieved.

For the PFS metrology camera, we collaborate with Canon on CMOS development. Canon is the leading producer of CMOS sensors for commercial applications. The metrology camera requires a large number of pixels, each with a small size to provide sufficient spatial resolution for the accurate centroid calculation. The PFS metrology camera uses a 50 Mega-pixel CMOS sensor from Canon (Figure 15). The camera shows a low readout noise at room temperature and a high pixel readout rate with the test facility in ASIAA. Although it is a front side illuminated device, the micro lenses help to enhance the peak quantum efficiency to higher than 40%. With the readout noise at about  $5e^-$ , it will generate a good signal-to-noise ratio for the fiber images of the PFS.

Large and high-quality image arrays are at the hearts of infrared astronomical instruments. Up to now, advanced infrared arrays have been mainly produced in the US. Locally in Taiwan, the Advanced Technology Research Laboratory of Chunghwa Telecom (ATR Laboratory) has been working on developing alternative infrared arrays. The OIR group in ASIAA has experience in developing imaging arrays and is working with the ATR Laboratory to test the cryogenic characteristics of the InGaAs arrays as shown in Figure 16. We are hoping to develop a useful infrared array for astronomical purposes. Unlike the commonly

used HgCdTe sensors, InGaAs technology is much more mature and better accessible economically. The drawback is the short cutoff wavelength, above which the material stops absorbing photons. The current array that the ATR Laboratory provides has a cutoff wavelength around  $1.7\ \mu\text{m}$  with a format of  $640 \times 480$  pixels. The size of the array is about 1/16 of that of a normal 1 M pixel CCD camera. Since we use the readout IC for normal environment applications, the array has a relatively high gain and large full well capacity. However, it is not sensitive enough for astronomical observations, which usually deliver lower background and signal level. Initial test results show relatively high dark current and strain pattern at 77 K. Some improvement has been made for lower dark current and better material strength at cryogenic temperatures. We plan to combine the development of CMOS sensor with InGaAs arrays as the low noise CMOS sensor will be very suitable for the readout circuit of InGaAs array with low background environment and cryogenic temperatures.

Infrared detectors made with semiconductor quantum dots (QDs) technology have been predicted to have the advantage of low cost and high operating temperature. Many efforts have been concentrated on improving the performance of quantum dot infrared photodetectors (QDIPs) based on the self-assembled QDs. One of the major drawbacks of QDIPs is the lower quantum efficiency due to the limited density of QD and the wavefunction distribution. A new QDIPs structure called confinement enhanced structure was proposed by us in collaboration with National Chiao Tung University. A high band gap material is added on top of the QDs to increase the confinement of the electronic wavefunctions in QDs. The result shows a dramatic increase of device efficiency in the conventional dot-in-a-well QDIPs. With this idea, the operation temperature and device performance is greatly enhanced after a preliminary optimizing process. The blackbody signal can be detected even for the device operating at a temperature of 220 K. At 8 micron, the device detectivity at 77 K is higher than  $4 \times 10^{10}$  Jones. The detectivity is similar to the existing quantum well infrared photodetector (QWIP) performance and the device can provide the capability to be operated at higher temperature. The group is developing a focal plane array based on the optimized structure to demonstrate the performance of this new structure.



A full-page artistic illustration of a cosmic scene. Two figures, seen from behind, are sitting on a dark, rocky surface in the foreground, looking out at a vast, colorful nebula. The nebula features swirling clouds of gas in shades of blue, purple, and orange, with numerous bright stars scattered throughout. The overall atmosphere is one of wonder and exploration.

# ***Education and Public Outreach***

Letter from the Director

Introduction

Projects

Science Highlights

Instrumentation Research

Education and Public Outreach



## Education and Public Outreach

The expansion of the Education and Public Outreach (EPO) activities at the ASIAA is in direct response to the recommendation by the Academia Sinica 5-year review panel in 2009. EPO covers outreach, the web, brochures, and library services. The EPO group members handle the daily tasks on publication, public relations, the World Wide Web, educational activities and collaborations.

### Publication

Publication involves producing and maintaining the ASIAA research brochure and project pamphlets. Starting from 2010, we also produce the ASIAA Quarterly (IAAQ) to promote our facility, projects and current research topics, introduce our research staff, and raise awareness of the many contributions from astronomy. It usually includes a poster-size illustration or high-resolution celestial photographs. It is our standard platform for introducing ASIAA and current astronomical topics to the general public. The IAAQ printing was changed from double-sided to single-sided in 2015. In collaboration with publishing companies, libraries, and the Taipei Astronomical Museum, each issue is now sent to more than 100 schools in Taiwan, and available for pickup at astronomical meetings and outreach events (see Figure 1). The IAAQ has also been archived online for public access worldwide.



Figure 1. The double-sided IAAQ 2014 Spring issue (upper panels); IAAQ promotional poster for the distribution in the 2013 ASROC Annual Meeting in Penghu (lower left panel), and Quarterly distribution in the 2013 AS Open House Day (lower right panel).

We also produced a set of 4 specially designed project leaflets (ALMA, SMA, TAOS and VLBI) in the form of paper folders to introduce our telescope projects, and a series of plastic folders to illustrate the scientific information of 7 deep sky images and 1 telescope site. (Figure 2)

We have also published articles to introduce the SMA, AMiBA, TAOS, and ALMA in magazines, e.g. Taipei Astronomical Museum Magazine, Science Monthly, and Physics Bimonthly. In addition, articles are written for an astronomical columns in Merit Times and the latest astronomical news for Physics Bimonthly magazine.

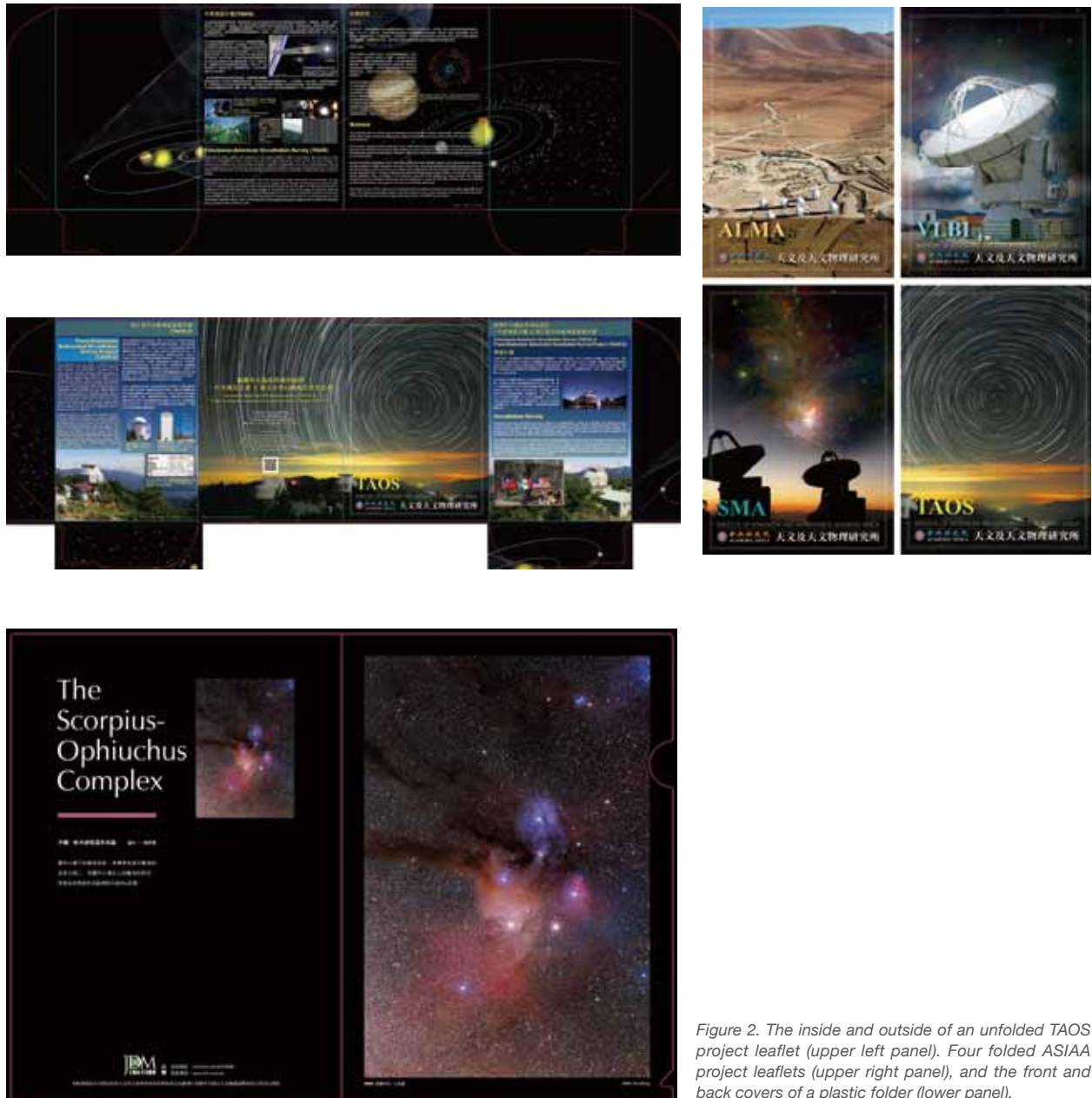


Figure 2. The inside and outside of an unfolded TAOS project leaflet (upper left panel). Four folded ASIAA project leaflets (upper right panel), and the front and back covers of a plastic folder (lower panel).



## Public Relations

Public relations at ASIAA deals with news releases and press conferences. We hold press conferences whenever there are significant findings led by ASIAA personnel. We have good relations with journalists and occasionally invite them to interview our researchers about ASIAA projects. We have strong collaborations with various television groups in order to present stories and films on visits to our observatories. The National Geographic Channel (NGC) has reported ASIAA's endeavor on frontier research in astronomy, in particular our involvement in the ALMA project. The Taiwan Television Enterprise (TTV) has had some in-depth one-hour reports on ASIAA projects and sciences, and our assistance in science content and accuracy helped the program to win a nomination for the annual Golden Bell Award in 2013. Our projects in Hawaii were even reported in a popular program on travel and culture, "Focus Series", by the Eastern Television (ETTV). We are recently awarded a grant from the Ministry of Science and Technology to produce a documentary film on our Greenland Telescope.

## World Wide Web

We maintain a Chinese-language website dedicated to the latest astronomical discoveries. This portal provides a venue for the general public to learn the latest and the most interesting findings in astronomy. We have posted news articles covering a wide range of interesting topics in contemporary astronomy. Our staff also translates NASA educational videos and produces the ASIAA collection of short videos. More than 30 videos have been put on our EPO ASIAA YouTube channel. ASIAA is also on Facebook where we upload the most updated information and photos.

## Educational Activity

One of the major educational activity events is the annual Academia Sinica Open House held in Nangang every autumn (Figure 3). ASIAA takes advantage of these opportunities to present to the public our astronomical researches in a very lively way. Apart from giving public lectures and displaying posters and exhibits of our research results, we have hands-on activities such as the big-bang balloon or simple DIY spectrometers for students to understand astronomy. We also demonstrate remote controls of



Figure 3. AS Open House: ASIAA staff is explaining ASIAA projects to students (left panel); ASIAA staff is explaining expansion of the Universe with "big-bang balloon" (right panel).

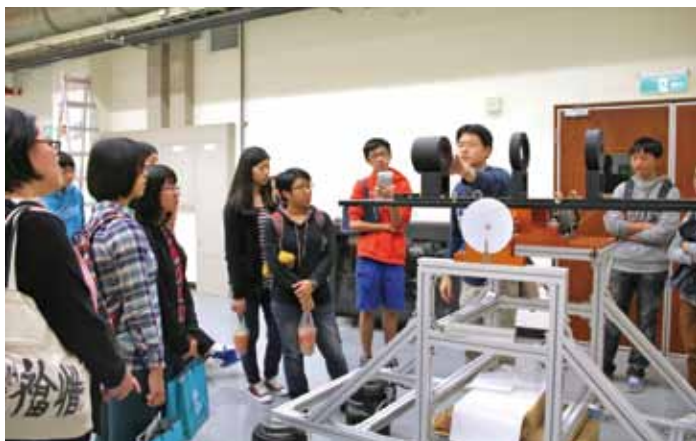


Figure 4. NTU Azalea Festival: ASIAA staff is introducing the Optical Testing Lab to students and the public.

telescopes in Hawaii and on the summit of Lulin Mountain. To introduce the culture of Hawaii where the ASIAA radio telescopes are located, we have invited the Hula Angel club to perform the traditional Hula dance. Owing to the collaboration on TAOS II with Universidad Nacional Aut3noma de M3xico (UNAM), in 2011 we invited Mexican musicians and a chef to introduce their culture. At 2014 Open House more than 3,000 people visited ASIAA's activities and exhibitions. Since 2013, ASIAA also participates in the NTU Azalea Festival (open house day of the National Taiwan University) every spring in order to engage young university and high school students in astronomy (Figure 4).

“Explore IAA”, which was held regularly at the ASIAA building in 2011, has been transformed to “Ask an Astronomer” on the Academia Sinica Open House Day (Figure 5) since 2012 and at the NTU Azalea Festival since 2013. This educational activity is conducted through lively, fun and engaging discussions for small groups of students with our researchers. Students are free to ask any questions related to astronomy and astrophysics.

Since 2013, ASIAA has been collaborating with the Zooniverse, an internationally renowned web-based citizen science platform, to translate their projects into Chinese. With over 20 live projects, the Zooniverse turns hundreds of millions of classifications into real science papers (68 publications as of June 2014). Through five localized websites, school lectures, and teachers' workshops, the ASIAA outreach staff have officially become Zooniverse ambassadors bridging science and public in the Chinese world.



Figure 5. Our astronomers are in face to face discussion with students at the Ask an Astronomer events at the 2012 (left) and the 2013 (right) AS Open House Day.



Figure 6. The World's biggest astronomy class of 834 took place in June 2014 in Miaoli Taiwan (left panel); the Guinness Record adjudicator, John Garland, Dr. Richard Chou and Ms Sun, the event organizer (right panel from left to right).

In June 2014, ASIAA participated in "the largest Astronomy Lesson" Guinness World Record Challenge event by lecturing to a class as large as 834 students, and re-wrote the record previously set by NASA (Figure 6). Interactively engaging school students from a dozen cities all over Taiwan, our researcher vividly showed the enormous size of our universe and enthusiastically outlined the latest scientific and instrumental achievements of ASIAA.

## Collaboration with High Schools, Local Astronomical Societies and Museums

Since 2010, we have actively participated in and co-sponsored the annual Star Party at Tsuei-Feng in central Taiwan (Figure 7). This Star Party is an annual gathering of more than 2,000 astronomy enthusiasts, which is organized by the Astronomy Association of Taichung. Among the registered participants, roughly half of them are college and high school students. Since 2013, we have also participated in the Southern Cross Star Party in Kenting, which is held by Pingtung County government. In both star parties, apart from handing out IAAQs and souvenirs, we have given several lectures on ASIAA projects, frontier research led by ASIAA, and other popular topics such as exoplanets and black holes.

We are also closely collaborating with the Taipei Astronomical Museum, giving lectures at high schools, hosting visiting teacher and student groups, and supervising high-school student projects. In order to introduce radio astronomy, 4 activities were held at the "Radio Telescope DIY" project during 2008 and 2010 in cooperation with the Taipei Municipal Jianguo Senior High School. More than 100 senior high school students and teachers participated in this project, and they built radio telescopes with commercial satellite dishes (12 GHz). Family Star Club, an organization of parents who are interested in astronomy and assisted by the Taipei Astronomy Society, held a monthly event in ASMAB 1F auditorium during the 2011 and 2012 school semesters, in which we provided lectures and talks. In March 2011 we collaborated with National Music Hall in sponsoring "Sun Rings" by the well-known Kronos Quartet commissioned by NASA Art Program.





Figure 7. ASIAA information desk at 2013 Star Party

There are additional personal efforts on publishing popular-science books, writing articles for magazines, and assisting schools in educational projects. Several astronomers are supervising astronomy projects for promising high-school students.

## Summer Student Program

ASIAA officially started the summer student program in 1998. The goal of the summer student program is to provide an opportunity for students to study selected topics on astronomy, astrophysics, and astronomical instrumentation to compensate for the lack of undergraduate astronomy programs in Taiwanese universities. The students admitted are potentially capable and interested in carrying out research or engineering projects in astronomy or astrophysics for their future academic careers. The projects provided by the supervisors in ASIAA cover theoretical astrophysics, numerical simulations on astrophysical problems, radio astronomical observation and data analysis, optical/infrared astronomical observations, observational cosmology, radio astronomical instruments, and even the fabrication and measurement of superconductor devices. From 1998 to 2014, the ASIAA summer student program has trained more than 240 undergraduate students. Among those students, two of them have been appointed as assistant research fellows (Drs. Ming-Chang Liu and Yen-Ting Lin), and several have been appointed as postdoctoral fellows of our institute (Drs. Mei-Yin Chou, Li-Jin Huang, Cheng-Yu Kuo, Chueh-Yi Chou, Hung-Yi Pu, Ya-Wen Tang, and Hsi-Wei Yen).

## Future Plan

Aside from continuing the above outreach efforts, our next goal is to promote multimedia presentations. We plan to “animate” ASIAA projects by producing an animation movie for each project (to appear on YouTube and ASIAA Facebook page), and introduce our latest news and development in monthly broadcasts. With the advance of technology, apps on mobile devices are a revolutionary medium in receiving information. Our long-term goal is to devise an ASIAA free app that includes all outreach material: articles, images, sound, movies, lecture videos, and activity schedule.

Through proactive outward approaches in the past years, ASIAA has got in touch with several outreach groups and formed various partnerships, such as TAM, Family Star Club, Kavli Institute for Cosmological Physics at the University of Chicago, ALMA Chile, etc. Working together has enabled ASIAA and our friends to share resources and extend to a bigger audience. With accumulated experience, and maintaining the driving force, we plan to increase public awareness of astronomy and attract more young people to science in the future.



中央研究院  
天文及天文物理研究所

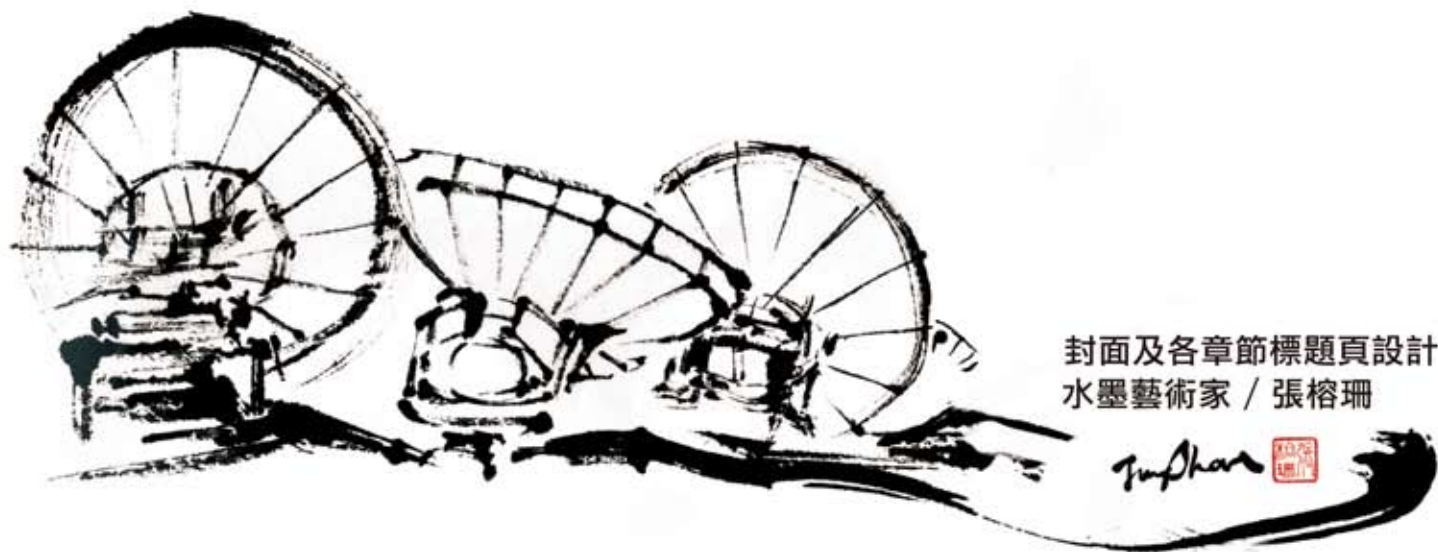
ACADEMIA SINICA

Institute of Astronomy and Astrophysics

11F of Astronomy-Mathematics Building, AS/NTU

No.1, Sec. 4, Roosevelt Rd, Taipei 10617, Taiwan, R.O.C.

TEL: 886-2-3365-2200 FAX: 886-2-2367-7849



封面及各章節標題頁設計  
水墨藝術家 / 張榕珊

*Zhang Rongshan*



中央研究院  
天文及天文物理研究所  
ACADEMIA SINICA  
Institute of Astronomy and Astrophysics